ANKARA YILDIRIM BEYAZIT UNIVERSITY

GRADUATE SCHOOL OF NATURAL AND APPLIED SCIENCES



DESIGN AND ANALYSIS OF MULTIBAND COMPACT ANTENNAS FOR FUTURE 5G APPLICATIONS

M.Sc. Thesis by

Abdullah ALSAQABI

Department of Electrical and Electronics Engineering

August, 2021

ANKARA

DESIGN AND ANALYSIS OF MULTIBAND COMPACT ANTENNAS FOR FUTURE 5G APPLICATIONS

A Thesis Submitted to

The Graduate School of Natural and Applied Sciences of

Ankara Yıldırım Beyazıt University

In Partial Fulfillment of the Requirements for the Degree of Master of Science in Electrical and Electronics Engineering, Department of Electrical and Electronics Engineering

by

Abdullah ALSAQABI

August, 2021

ANKARA

M.Sc. THESIS EXAMINATION RESULT FORM

We have read the thesis entitled **"DESIGN AND ANALYSIS OF MULTIBAND COMPACT ANTENNAS FOR FUTURE 5G APPLICATIONS"** completed by **ABDULLAH ALSAQABI** under the supervision of **PROF. DR. HÜSEYİN CANBOLAT** and we certify that in our opinion it is fully adequate, in scope and in quality, as a thesis for the degree of Master of Science.

Prof. Dr. Hüseyin CANBOLAT

Supervisor

Doç. Dr. Thamer Almashadani

Jury Member

Prof. Dr. H. Haldun GÖKTAŞ

Jury Member

Prof. Dr. Sadettin ORHAN

Director

Graduate School of Natural and Applied Sciences

ETHICAL DECLARATION

I hereby declare that, in this thesis which has been prepared in accordance with the Thesis Writing Manual of Graduate School of Natural and Applied Sciences,

- All data, information and documents are obtained in the framework of academic and ethical rules,
- All information, documents and assessments are presented in accordance with scientific ethics and morals,
- All the materials that have been utilized are fully cited and referenced,
- No change has been made on the utilized materials,
- All the works presented are original,

and in any contrary case of above statements, I accept to renounce all my legal rights.

Date: 6.08.2021 **Signature: ……**

Name & Surname: Abdullah ALSAQABI

ACKNOWLEDGMENTS

Making and writing this thesis was one of the most difficult things that I got through, but at the same time, it was a very good challenge for me. I was getting upset sometimes but I was remembering my beloved parents, sisters and my friends who were making me feeling better.

My supervisor, Prof. Dr. Hüseyin CANBOLAT, thank you for your infinite support, advices, discussions and feedback. Prof. Dr. Alaa El-Rouby, I really appreciate all the help you gave to me, your precious time and information.

Thank you, my father, and my mother, for your unlimited support, for your beautiful words and for your pretty smiles you were sending to me. Thank you, my brothers and lonely sister who were motivating me all the time. My friends who are living with me, and all over the world, thank you from the bottom of my heart for being beside me all the time.

I have a lot of friends to thank, but I can't mention all of them, they are inside the university and outside it. They know already how much I respect and love them, they were so good with me and were helping me with all the available ways. I really appreciate your help and I hope the best for all of you, may Allah help you and be with you always. And of course, Thank you Allah for giving me the strength, the well, the patience, the health and being besides me all the time.

Finally, I would like to thank you for reading and studying my thesis, and I hope you can get the benefit from it.

2021, August **Abdullah ALSAQABI**

DESIGN AND ANALYSIS OF MULTIBAND COMPACT ANTENNAS FOR FUTURE 5G APPLICATIONS

ABSTRACT

This thesis introduces new versions of multi-band compact antennas design and analysis as candidates for future 5G applications in communication systems. This work approach has mainly depended on the triple-band microstrip patch antenna as a reference antenna by size miniaturizing and slots removing. The antenna structures have been composed of patches with various shapes of slots to enhance the behavior of the proposed antennas and direct feeding methods such as inset microstrip transmission line feeding to get good bandwidth impedance matching.

In this regard, the proposed antennas' dual-band approach obtain through the modifications on various antenna structures with the assistance of electrical current behavior inside the patch. It found that the changing of patch and ground plate dimensions have highly effective for achieving this purpose. The dual-band antennas build to have a suitable dual-band response as well as acceptable radiation and gain properties.

This thesis aims to introduce three proposed multiband micro-strip compact antennas and new slots with different etches for removal of undesired frequencies and generate the main dual-band resonance frequencies required.

All proposed multi-band antennas build on the same substrate, which is (Roger RT5880 Duroid) with (0.508) mm thickness, and (2.2) relative permittivity as well as connected with 50 Ohm microstrip inset feeding. The performance of these antennas has been studied, analyzed, and evaluated through various parameters of the proposed antennas.

The antenna modelling and evaluation performance accomplish by using one of the most important commercially available EM simulators, the Computer Simulation Technology Microwave Studio suite (CST MWS).

These antennas have a miniaturized size compared with previous works and the adopted reference antenna in this work, with patch dimensions of (12.72 × 7.475 mm^2), (11.585 × 8.88 mm^2) and (11.585 × 8.98 mm^2) for the first, second and third proposed antenna, respectively. All suggested designs operate at 10 GHz of X-band and 30 GHz of Ka-band for future 5G mobile communication systems.

Keywords: High gain, 5G, Fork-shaped, Inset feeding, Dual-band, X-band, Partial ground plane, Ka-band, Microstrip patch antennas, Slotted-patch.

GELECEKTEKİ 5G UYGULAMALARI İÇİN ÇOK BANTLI KOMPAKT ANTEN TASARIMI VE ANALİZİ

ÖZ

Haberleşme sistemlerinde ileride çıkabilecek 5G uygulamalarında kullanılabilecek çok bantlı kompakt antenlerin yeni modellerinin tasarım ve analizi bu çalışmada sunulmaktadır. Bu çalışmadaki ana yaklaşım ölçek küçültme ve yarık (slot) azaltma işlemlerine altyapı sağladığından üç bantlı mikro-şerit yama anten yapısına dayalıdır. Önerilen antenin özelliklerini ve eklenmiş mikro şerit iletim hattı besleyicisi gibi doğrudan besleme yöntemini iyileştirmeyi hedefleyen çeşitli biçimlerde yarıkları olan yamalardan oluşmuş anten yapıları iyi bir bant genişliği empedans uyumlaması elde etmek için kullanılmıştır.

Bu bağlamda, anten dizaynında kullanılan çift bant yaklaşımı yama içindeki elektrik akım davranışı yardımıyla çeşitli anten yapılarında değişiklik yaparak elde edilebilir. Bu hedefe erişmek konusunda yamanın ve toprak plakasının boyutlarını değiştirme işleminin çok etkili olduğu bulunmuştur. Çift bantlı antenler Kabul edilebilir bir yayınım ve kazanç özelliği yanında amaca uygun bir çift bant çıkışı almak için çift bantlı antenler imal edildi.

Bu tezde, gerekli çift bant rezonans frekanslarını üretmek ve istenmeyen frekansları söndürmek için farklı şekillerde oyulmuş yeni yarıklar eklenmiş üç tane çok bantlı mikro şerit kompakt anten önerilmektedir.

Önerilen çok bantlı antenlerin hepsi 50 Ohmluk içeriye beslemeye bağlanmış 0,508 mm kalınlıkta 2,2 bağıl geçirgenlikli Roger RT5880 Duroid altlığı üzerine yerleştirilmiştir. Bu antenlerin performansları incelenmiş, analiz edilmiş ve çeşitli parametreler açısından değerlendirilmiştir.

Antenlerin modelleme ve performans değerlendirme işleri en yaygın EM simülatörlerinden biri olan Computer Simulation Technology Microwave Studio (CST MWS) program paketi ile yapılmıştır.

Bu antenler daha önceki araştırmalarda tasarlanan antenlere ve bu çalışmada ele alınan referans antene (8,98 mm^2) göre daha küçük ölçeklerdedir. Önerilen bütün tasarımlar 10 GHz X-band ve 30 GHz Ka-bantta çalışabilir.

Anahtar Kelimeler: Yüksek kazanç, 5G, çatal biçimli, içe doğru besleme, çift bant, X-bandı, kısmi toprak düzlemi, Ka-bandı, mikro şerit yama antenler, yarıklı yama.

CONTENTS

M.Sc. THESIS EXAMINATION RESULT FORM ii
ETHICAL DECLARATION iii
ACKNOWLEDGMENTS iv
ABSTRACT v
ÖZ vii
CONTENTS ix
NOMENCLATURE xii
LIST OF TABLES xv
LIST OF FIGURES xvi

CHAPTER 1 - INTRODUCTION 1
1.2 Printed Antenna Design Categories 2
1.3 Literature Review 3
1.4 Thesis Objective 7
1.5 Thesis Organization 8

CHAPTER 2 - BACKGROUND AND COMPACT ANTENNA THEORY WITH FEED METHODS 9
2.1 Introduction 9
2.2 Antenna Parameters 9
2.2.1 Directivity 10
2.2.2 Radiation Pattern 10
2.2.3 Bandwidth 11
2.2.4 VSWR 12
2.2.5 Gain 12
2.2.6 Efficiency 13
2.2.7 Complex Impedance 13
2.2.8 Polarization 14
2.3 Antenna Definition 15
2.4 Types of Antennas 15
2.4.1 Wire Antenna / Half-Wavelength Dipole 15

2.4.2 Monopole Antenna/ Image Theory 16
2.4.3 Loop Antenna 17
2.4.4 Spiral / Helical Antenna 18
2.4.5 Horn Antenna 19
2.5 Transmission Line Modeling 19
2.5.1 Microstrip Transmission Line Building 20
2.5.2 Parameters Computation for Microstrip 21
2.5.3 Types of Conducting and Dielectric Materials 23
2.5.3.1 Dielectric Material Properties 23
2.5.3.2 Conductor Material Properties 24
2.6 Micro-strip Antenna Feeding Methods and Techniques 24
2.6.1 Direct Method: Microstrip Line Feeding 25
2.6.2 Direct Method: Probe Feeding 26
2.6.3 Indirect Method: Aperture Coupled Feeding 27
2.6.4 Indirect Method: Proximity Coupled Feeding 27
2.6.5 Indirect Method: Coplanar Waveguide Feeding 28
2.7 Analyzing Techniques 30
2.7.1 Full Wave Model Technique 30
2.7.2 Cavity Model Technique 31
2.8 Miniaturization Methods of Antenna 33
2.8.1 Changing The Antenna Structure 33
2.8.1.1 Slots Etching 34
2.8.1.2 Dielectric Material with High Permittivity 34
2.8.1.3 Inductive and Capacitve Element Loading 35
2.8.1.4 Metallic Pins Loading 36
2.8.2 Fractal Geometry Technique 37
2.8.3 Meander Line Technique 39
2.8.4 Improving of Geometry Shapes 41
2.9 Frequency Band with Antenna Selection 41
2.10 CST MWS 41

CHAPTER 3 - DESIGN AND SIMULATION OF INSET FEED MULTI-BAND COMPACT ANTENNAS 43

3.1 Introduction 43

3.2 Reference High Gain Compact Printed Antenna 44
3.3 First Proposed of Multi-Band Compact Antenna Design 46
3.3.1 Antenna Size Modification 46
3.3.2 Inserting Slots within Patch Element 50
3.4 Second Proposed of Multi-Band Compact Antenna Design 58
3.4.1 Antenna Size Modification 58
3.4.2 Inserting Slots within Patch Element 61
3.5 Final Proposed of Multi-Band Compact Antenna Design 71
3.5.1 Modification of Inset Feed Line and Patch Length 71
3.5.2 Inserting Slots within Patch Element 73
3.6 Comparison Between Proposed Antennas with Other Designs 83

CHAPTER 4 - CONCLUSIONS AND FUTURE WORK 87
4.1 Conclusions 87
4.2 Future Work 88

REFERENCES 89

CURRICULUM VITAE 100

NOMENCLATURE

A_e	Effective aperture
c	Velocity of EMW in free space ($c = 3 \times 10^8$ $^m/_S$)
e_t	Total efficiency
e_r	Radiation efficiency
e_c	Conduction efficiency
e_d	Dielectric efficiency
f	Frequency
v_p	Phase velocity
G	Gain
tan δ	Loss tangent
Γ	Reflection Coefficient
ε_r	Dielectric constant
ε_{eff}	Effective dielectric constant
α_d	Attenuation due to dielectric loss
α_c	Attenuation due to conductor loss
Z_{in}	Input impedance
Z_o	Characteristic impedance
P_{in}	Power input
λ	Wavelength
ω	Angular frequency
σ	Metal conducting
μ_o	Permeability
h	Substrate thickness
t	Thickness of Copper Material
W_p	Patch width
L_p	Patch length
W_s	Substrate width
L_s	Substrate length
W_f	Feeding width

L_f	Feeding length
W_g	Ground plane width
L_g	Ground plane length
g	Width of inset feed
Y_o	Length of inset feed
$\frac{W}{h}$	Width to height ratio
GaAs	Gallium arsenide
Ta	Tantalum
NiCr	Nickel Chromium Alloy
Si3N4	Silicon Nitride
Sio2	Silicon dioxide
mmWave	Millimeter wave
BW	Bandwidth
CST	Computer Simulation Technology
FR-4	Flame retardant 4
GPS	Global Positioning System
SHF	Super High Frequency
RF	Radio Frequency
VSWR	Voltage Standing Wave Ratio
T.L	Transmission line
EMW	Electromagnetic Wave
1G	First Generation
2G	Second Generation
GSM	Global system for mobile communications
3G	Third Generation
4G	Fourth Generation
LTE	Long Term Evolution
5G	Fifth Generation
T/R modules	Transmit/Receive modules
SATCOM	Vehicular Satellite Communication Terminal
SAR	Synthetic Aperture Radar

Tx	Transmitter
Rx	Receiver
MIMO	Multiple-Input Multiple-Output
DGS	Defected Ground Structure
ZVA	Vector Network Analyzer
HFSS	High-Frequency Structure Simulator
FBW	Fractional Bandwidth
AC	Alternating Current
HF	High Frequency
VHF	Very-High Frequency
UHF	Ultra-High Frequency
2D	Two dimensional
AM	Amplitude Modulation
TEM	Transverse Electromagnetic Mode
CPW	Coplanar waveguide
EFIE	Electric-Field Integral Equation
MFIE	Magnetic-Field Integral Equation
PEC	Perfect Electric Conductor
PMC	Perfect Magnetic Conductor
3D	Three dimensional

LIST OF TABLES

Table 3.1 Shows the overall dimensions of a reference antenna..... 43

Table 3.2 The comparison between values of first modified and a reference antenna. 47

Table 3.3 Depicts the final dimensions of first multi-band microstrip patch antenna. 51

Table 3.4 The comparison between values of first modified and a reference antenna. 59

Table 3.5 Depicts the final dimensions of second multi-band microstrip patch antenna. 64

Table 3.6 The comparison between measurements of present modified and previous proposed antenna..... 71

Table 3.7 Depicts final dimensions of third multi-band microstrip patch antenna ... 76

Table 3.8 Depicts comparison between proposed antennas and former works..... 81

LIST OF FIGURES

Figure 2.1 General of radiation pattern plot of antenna 11

Figure 2.2 Exhibited Voltage Standing Wave Ratio 12

Figure 2.3 Illustrated the linear, circular and elliptical polarization 15

Figure 2.4 Shows the basis strucutre of half wave dipole antenna..... 16

Figure 2.5 Depicts the concept work of monopole antenna 17

Figure 2.6 Shows the different shapes of loop antenna strucutre..... 18

Figure 2.7 Illustrates the basic form of spiral antenna 19

Figure 2.8 Shows the different types of horn antennas 19

Figure 2.9 Shows the T.L structure 21

Figure 2.10 The electric and magnetic field of microstrip T.L 21

Figure 2.11 Various methods of transmission line feeding..... 25

Figure 2.12 Shows (a) 3D-dimensions of patch antenna with fixed point of feed, and (b) how to install the parts of coaxial feeding with patch antenna..... 26

Figure 2.13 Antenna structure with aperture feed method..... 27

Figure 2.14 Illustrates proximity coupled feeding mechanism 28

Figure 2.15 Shows the CPW feeding with various shapes..... 29

Figure 2.16 Depicts the basic functions such as (a) rectangular pulse function [66], and (b) triangular pulse function 31

Figure 2.17 Depicts the behavior positive and negative charges in compact antenna 32

Figure 2.18 Shows cavity model structure with PMC and PEC plates 33

Figure 2.19 Shows the simple example of slot patch antenna..... 34

Figure 2.20 Simple instance of compact antenna with capacitive element..... 36

Figure 2.21 Shows shorting-pin loaded with circular patch and ground plane..... 36

Figure 2.22 Shows iteration stages of Koch monopole antenna 38

Figure 2.23 Illustrates the basic shape of meander line antenna 39

Figure 2.24 Shows the equivalent circuit of meander line 40

Figure 3.1 Depicts 2D of a reference patch antenna 44

Figure 3.2 Displays the reflection coefficients of a reference antenna for each resonance frequency 46

Figure 3.3 Depicts the return losses values due to the change in the patch antenna dimensions..... 47

Figure 3.4 Depicts modifications of ground plane and patch dimensions without change substrate 48

Figure 3.5 Illustrates the effect of changing ground plane dimensions on return losses values..... 48

Figure 3.6 Illustrates final dimensions of slots for first proposed design to generate dual-band resonance frequency 50

Figure 3.7 Depicts the advancement steps of dual-band proposed first design 51

Figure 3.8 Depicts reflection coefficients for each stage of first proposed antenna . 52

Figure 3.9 Shows final measurements of first proposed multi-band compact patch antenna 52

Figure 3.10 Depicts return losses and bandwidth of first proposed microstrip patch antenna 54

Figure 3.11 Illustrates radiation efficiency of first proposed microstrip patch antenna 55

Figure 3.12 Shows gain results of first proposed microstrip patch antenna..... 55

Figure 3.13 Depicts 2D-radiation pattern of first proposed multi-band microstrip antenna for (a-b) at 10 GHz and (c-d) at 30 GHz..... 56

Figure 3.14 Illustrated 3D radiation pattern at (a) 10 GHz and at (b) 30 GHz 57

Figure 3.15 Demonstrates current distributions of dual-band first proposed microstrip patch antenna for each resonance frequency at (a) 10 GHz and (b) 30 GHz..... 57

Figure 3.16 Illustrates different results for all steps of modified patch antenna 59

Figure 3.17 Shows return loss values after modified of ground plate and substrate Roger RT-5880..... 59

Figure 3.18 Describes the final dimensions of a reference antenna modified without slots..... 60

Figure 3.19 Illustrates final dimensions of slots for second proposed design to generate dual-band resonance frequency..... 62

Figure 3.20(a) Shows first three-stages of dual-band second proposed design 62

Figure 3.20(b) Shows final three-stages of dual-band second proposed design..... 63

Figure 3.21 Describes reflection coefficients for each stage of second proposed antenna 64

Figure 3.22 Shows final dimensions of second proposed multi-band compact patch antenna 65

Figure 3.23 Shows return losses and bandwidth of second proposed compact patch antenna 67

Figure 3.24 Illustrates radiation efficiency of second proposed microstrip patch antenna 67

Figure 3.25 Shows gain results of second proposed microstrip patch antenna..... 68

Figure 3.26 Depicts 2D-radiation pattern of second proposed multi-band microstrip antenna for (a-b) at 10 GHz and (c-d) at 30 GHz..... 69

Figure 3.27 Illustrated 3D radiation pattern at (a) 10 GHz and at (b) 30 GHz 70

Figure 3.28 Demonstrates current distributions of dual-band second proposed microstrip patch antenna for each resonance frequency at (a) 10 GHz and (b) 30 GHz 70

Figure 3.29 Illustrates return loss values of all modification steps of patch length and feed line..... 72

Figure 3.30 Shows the conventional third proposed antenna design dimensions..... 72

Figure 3.31 Demonstrates final measurements of slots for third proposed design to generate dual-band resonance frequency. 74

Figure 3.32(a) Shows first three-stages of dual-band third proposed antenna design 74

Figure 3.32(b) Shows final three-stages of dual-band third proposed antenna design 75

Figure 3.33 Describes reflection coefficients for each stage of third proposed antenna 76

Figure 3.34 Shows final dimensions of third proposed multi-band compact patch antenna 77

Figure 3.35 Shows return losses and bandwidth of third proposed compact patch antenna 79

Figure 3.36 Illustrates radiation efficiency of third proposed microstrip patch antenna 80

Figure 3.37 Shows gain results of third proposed microstrip patch antenna 80

Figure 3.38 Depicts 2D-radiation pattern of third proposed multi-band microstrip antenna for (a-b) at 10 GHz and (c-d) at 30 GHz..... 81

Figure 3.39 Illustrates 3D-radiation pattern at (a) 10 GHz and at (b) 30 GHz 82

Figure 3.40 Demonstrates current distributions of dual-band third proposed microstrip patch antenna for each resonance frequency at (a) 10 GHz and (b) 30 GHz..... 83

CHAPTER 1

INTRODUCTION

1.1 A History of Wireless Technology

The mobile and wireless industry has evolved from 1G to the digital 2G (GSM), and then to the 3G, 3.5G, and to the systems which are high data rate cellular networks like 4G (LTE) in the last ten years ago [1]. Development of technology from 1G to 4G respectively led to growing interest in achieving high data rates in present wireless communication systems. However, the 4G cannot approach the requirements of the next generation because it failed to solve the main communication problems such as crowded users, low quality, unreliable connection, and flexibility [2]. Furthermore, the work on modern techniques of wireless systems is ongoing yet, for tackling those problems and is expected to be initiated by the end of 2025 [3, 4].

Fifth-generation technology has a significant influence on wireless communication systems because it provides large bandwidth and higher resolution for a cell as well as it can support modern interactive multimedia technology like Self-automotive driving and virtual reality [5, 6]. The 5G frequencies range includes two bands (greater than 6 GHz and within 100 GHz).

Compact antennas play a significant role in modern wireless communications systems. Modern wireless communication system requires printed antennas with specific features like compact, conformal, low cost, and easy to fabricate to keep pace with the evolution of the 5G system that will use higher frequency bands like a millimeter-wave band.

Because of microstrip antenna versatile in terms of various possible geometries and its small size that makes them suitable to printed in devices and using at many different future applications.

For that, three different shapes of microstrip patch antennas with inset feed technique have been presented and working at the SHF bands (Super High Frequency), especially at X and Ka-band.

The printed antennas suffer from some drawbacks despite those advantages mentioned above, such as narrow bandwidth of the operating frequency, low efficiency, and low gain [7]. So, many techniques have been recommended to beat some drawbacks, like using the inset feed technique to get high impedance matching between line feeding and the patch and using slots with various shapes to cancel unwanted frequencies and create resonance frequencies required [8,9]. The fast development of wireless communication systems indicates that there is a requirement for multi-band antennas. There are a few techniques presently available to attain multi-band work with microstrip patch antennas [10].

1.2 Printed Antenna Design Categories

The techniques types of printed antenna design can divide into three sections as follow: The first type is a basic general patch design; this design type is treated in easily fabricated and is generally used in multi-band compact antennas. There are two types of single patch design; the first type depends on the two dimensions of the rectangular patch to generate the resonance frequency from the bare dimensions patch [11]. The frequency proportion, in this case, will be roughly equal compared with the dimensions of the patch. So, the two different frequencies agitate two orthogonal polarizations and considered clear conditions in this way. Although the polarization stipulations are not urgent in this design type, this method is helpful in low-expense close-range applications.

The second type of design consisting of adding passive components such as capacitors to a single patch as well as other components like varactors [12], notches [13], pin diode [14], stubs [15], and slots that may be outward or installed into the patch [16-20]. For above, using a reactive-loading technique leads to the radiation pattern of the top-order mode could be comparable to that of the primary mode. So, we can vary the resonance manner of the patch by using this approach. So, this style of design stands for the most famous technique for generation a multi-band frequency demeanor.

When using two [21] or more [22] patches on the same dielectric material, a dual-frequency band can be achieved because of a piece of them supporting high currents and emission at the resonance frequencies.

This classification also contains multi-patches on multi dielectric materials [23] that can use radiating elements of different shapes. Those microstrip antennas work with a dual-polarization and the same polarization at the two frequencies. Some structures can be used to widen the bandwidth of a single band antenna, such as multilayer structures when the two frequencies are compulsory to be nearly spaced. At all working frequency bands, the Radiation patterns can be harmonious.

These techniques above are suitable for short-link T/R modules or SATCOM (Vehicular Satellite Communication Terminal). Synthetic Aperture Radar (SAR), scatterometers, and some applications demand large segregation between the bands, also the double-resonator structure must contain patches of quite different dimensions [24, 25].

The standard of radical separation of the compact antenna combined with each band can be approved. The standard of radical separation of the compact antenna combined with each band can be approved for high separation between bands. For instance, the patches and the related feed networks for the two bands can be piled on two various dielectric materials; for this reason, getting two approximately freelance antennas.

The last type of design depends on using the space-filling geometry to generate dual-band frequencies and because its properties allow the multi-band operation to be reached with fractals forms. Fractal geometry design has advantages; it enhances the response of multi-band patch antenna, impedance matching and Voltage Standing Wave Ratio (VSWR) and makes it have a smaller size [26]. Despite the application of the space-filling technique being more complex when related to antenna design and has limited profit for the first iteration levels, the fractal antennas have advantages such as facilitating circuit design of Tx and Rx communication systems [27].

The multi-band proposed printed antennas systems in this work used electric current distribution analysis as a new procedure to get the multi-band resonance demeanor,

and it will offer appropriate radiation efficiency and gain values. Furthermore, the anticipated reflection and correlation coefficient features are suitable for 5G smartphones and future applications.

1.3 Literature Review

Recently, researchers have done many works to keep pace with the progress in wireless communication systems that need a new patch antenna design, especially in dual-band printed antennas with different feed techniques, shapes, slots, and features.

In the following, some works mentioned by researchers are very closely related to the subject of this thesis in the last few years:

- **Othman et. al.** [28] in 2014, presented a new shape of a printed antenna as a spanner to generate 10 GHz resonance frequency for radar and bio detecting systems (medical industry) applications after treating a circular patch with many features like the low profile and cost, and easy manufacturing. In this work, the FR4 dielectric material used with 1.6 thickness that has been considered is not enough for high frequencies, and mm-Wave uses that need substrate with low dielectric constant. Also, the parametric study has done by increasing the length of the feed line has affected the Value of Return loss and VSWR. This antenna achieved the results required for wireless communication technology with lower than -10 dB return loss and VSWR lower than 2, as well as a 4.123 dB gain.

- **Ullah et. al.** [29] in 2017, introduced a dual-band microstrip patch antenna with a different structure as a spiral shape that consists of two arms started from the center of the feed line, and each one responsible for creating resonance frequency. The left-arm produces the lower frequency, and the right arm controls the upper frequency. Roger RT/ Duroid 5880 has been used with 0.254 mm thickness and 2.2 dielectric constants. Also, the researcher used an 8-element array antenna to increase the value of gain that will be greater than 10 dB. Furthermore, the bandwidth and efficiency have enhanced and, it was higher than 6 GHz and 90 % for both 28 GHz and 38 GHz operating frequencies.

Finally, this antenna has a large narrow beam-with around 12º for each frequency resonance. After the design, this antenna becomes ready to use for future 5G communication mobile phones.

- **Marzouk et. al.** [30] **in** 2019, has designed three different types of multiband microstrip MIMO antennas operating at 28 GHz and 38 GHz for fifth-generation mobile communication and smartphone applications and the DGS technique used in this work. The first design consists of an inset feed traditional compact patch antenna with 2-radiator. However, the second design comprises mirror multiband 2-radiator multi-input multi-output I-shape slotted compact antenna also relevant with inset feed technique. The last one includes a 4-element MIMO antenna also with I-shape slotted. Noticed, the data rates and channel capacity enhanced with more antenna elements to the system. These antennas are fabricated and built on dielectric material with a low dielectric constant such as Roger RT 5880 with 0.508 mm thickness. These antennas were simulated by used CST and constructed and measured by used ZVA 67 Vector Network Analyzer. Although there are differences between reflection with transmission coefficient, there is a remarkable similarity between simulation and measurement results, either because of the natural work of substrate used or the mismatching between the patch and the feed line.

- **Ahmed Abdelaziz and Ehab K. I. Hamad** [31] in 2019, proposed a tri-band microstrip patch antenna with an inverted T-shape slotted symmetrically vertical around the inset feed line to get triple resonance frequency working at 10 GHz, 28 GHz, and 38 GHz by using Roger RT 5880 with 2.2 low dielectric material and 0.508 mm thickness. The measured and simulated results proved that the difference between them is insufficient because of the circumstances. The process of compact antenna passed through three stages. The first stage, design a conventional microstrip patch antenna with a specific dimension, depends on the standard design formulas. However, in this stage, some of the ripple waves with some resonance frequency required appeared. In the last two stages, inverted T-shape slots are etched on the traditional patch to cancel unwanted frequency bands and improve bandwidth and return loss levels.

The final results of gain, reflection coefficient, VSWR, bandwidth, and efficiency become good enough to make this antenna is suitable for 5G wireless devices, devices with space constraints and point to point wireless communication.

- **Almashhdany et. al.** [32] in 2020, presented a new shape multi-band printed antenna operated at 28 GHz and 38 GHz center frequencies of mm-Wave bands for future 5G mobile network and smartphone applications. The compact antenna was fabricated and built on FR-4 dielectric material with a 4.4 dielectric constant and 0.245 mm thickness. The top left and right corners of the rectangular patch antenna have been cut with a length and width of 1.5×3 mm^2 for each side. Then, Cross-slot was inscribed in the middle patch and partially used the ground of copper technique. After simulated this antenna at CST, the results appeared as expected in the case of all parameters. 1 GHz bandwidth for the first two resonance frequencies in order and 3GHz for the last one. Also, the gain improved with 4.73 dBi for 28 GHz and 32.5 GHz and 5.13 dBi for 38 GHz. Finally, bandwidth enhancement leads to using this antenna in high rates 5G networks to keep up the development.

- **Ali et. al.** [33] in 2016, introduced a coplanar waveguide slot multiband printed directive patch antenna that worked at 28 GHz and 38 GHz and has been used in future 5G mobile networks, short-range communication, sensor and imaging systems applications. This antenna has been manufactured on Roger RT/Duroid 5880 substrate with 2.2 relative permittivity and a thickness of 0.254 mm. The antenna has been analyzed by using HFSS and CST. After simulated, return loss was less than -21 dB at each resonance frequency for both software. The same applies for gain was maximum at both center frequencies, and it equals 5.6 dB at 28 GHz and 6.6 dB at 38 GHz.

- **Verma et. al.** [34] in 2016, applied a compact structure printed antenna with dimensions of 20×20×1.6 mm^3 operating at 10.15 GHz resonance frequency, and it is appropriate for fixed wireless access, handheld devices and Telemedicine applications. The required antenna was fabricated on FR-4 dielectric with 4.4 dielectric constants with a height of 1.6 mm in addition to a small rectangular slot etched directly above the feed line to reject the undesired frequencies.

The outcomes turned up using HFSS software, which indicates that -18.27 dB return loss around the center frequency and the bandwidth of 400 MHz. Finally, the suggested compact antenna works with a gain of 4.46 dB and a good radiation pattern. These features have qualified it to use in 5G future systems.

1.4 Thesis Objective

This work will suggest new versions of multiband compact antennas design and analysis as candidates for future 5G applications in communication systems. The antenna structures will be patches and feeding by direct feeding (microstrip transmission line) to get good bandwidth impedance matching. They are inserting new different slots in the patches to enhance the behavior of the proposed Antennas. This work aims to achieve a design operated at resonance frequencies required for future 5G communication networks.

The compact printed patch antennas have designed will have features and specifications as follows:

- Printed antennas designed have new different slot shapes and are suitable for future 5G applications.
- Partially copper ground plane techniques have been used in one of the designs to study its effects on the other parameters.
- Each design has a specific characteristic that sets it apart from others, such as high gain rates, directivity, reflection coefficients, and high levels of total and radiation efficiency, taking into account other parameters.
- The compact antennas have been fabricated on low-cost Rogers RT/Duroid 5880, which is used for high frequencies and mm-Wave band because they have a low dielectric constant of around 2.2 and are available commercially in abundance.
- The proposed antennas size has been minimized as much as possible to work at SHF bands and become appropriate for satellite links, microwave relay links, 5G mobile, radar, TV, WIFI, subscriber radio, and remote sensing, aircraft navigation and medical diathermy applications.

- All suggested compact antennas have very good total and radiation efficiencies above 70%.

1.5 Thesis Organization

Chapter One: Presents a history of wireless technology development from 1G to 5G and printed compact antenna sections with its types and discusses the previous works of the researchers and the purpose of this thesis.

Chapter Two: Provides the theoretical formulas of Microstrip compact antenna and studies the parameters required and steps of the design with styles of feed techniques alongside types of substrates and their dimensions to analyze the efficiency work of slotted antennas.

Chapter Three: Introduced three printed antenna designs simulated by using CST-MWS that operated at 10 GHz and 30 GHz resonance frequency with different slots like the shape of rectangle rings, T-character, Fork and small squares, as well as using inset feed technique to transfer maximum power from feed line to the patch. Besides, it gives a comparison between the work of this thesis and the others.

Chapter Four: Contains the conclusions of thesis results and future motivation work to keep up the fifth-generation communication systems and devices.

CHAPTER 2

BACKGROUND AND COMPACT ANTENNA THEORY WITH FEED METHODS

2.1 Introduction

Because of the fast development that happens in modern wireless communication applications and the entry of the fifth-generation technology for the first time to work in some East Asian countries and European Union as well as America, the need to design newly printed patch antennas become urgent with various shapes, size, techniques, and cost to keep up with the modern era of telecommunications engineering.

They add the pins diode or capacitor and varactor in the middle, between patch antenna and ground plane. These elements have adaptability with a pattern, polarization, and resonance frequency to invent and open new horizons in compact antennas fabrication. Microstrip antenna suffers from fringing fields. To obtain high performance of antenna with excellent specifications operated in Super High-Frequency bands, especially in the X-band and Ka-band, thick dielectric material with low permittivity used, to get better radiation, bandwidth, and efficiency [35].

This chapter describes the parameters and theory of patch antenna design and its types, size, and suitable feed method techniques to avoid mismatching and power loss between the feed line and compact antenna.

2.2 Antenna Parameters

These measurements mention checking the antenna with all types to guarantee that it meets with specifications required. The most general significant parameters necessary to testing any antenna are gain, bandwidth, radiation pattern, efficiency, and directivity.

For instance, the reflection coefficient must be lower than -10 dB to prevent back the high amount of reflected wave from the antenna as well, as the antenna's efficiency must be greater than 50% and so on. These parameters will determine if the antenna is work efficient or not based on their outcomes.

2.2.1 Directivity

Directivity is known as the capability of the radiating element to make its energy emits from it in a specific direction in sending case or to collect the best amount of energy with a better-specific direction in receiving [36]. The unit of measurement for directivity is decibel or dB. Despite the antenna's ability to orients the radiation in the desired direction in the case of static, there is no sender and receiver fixed. For that, the antenna which has directivity equal to one is called an omnidirectional antenna [37].

$$D = \frac{U}{U_o} = \frac{4\pi U}{P_{rad}} \qquad \textbf{(2.1)}$$

Where:

D : Directivity

U : Maximum radiation intensity

U_o : Average radiation intensity

P_{rad}: Radiated power

2.2.2 Radiation Pattern

The radiation pattern is known as the antenna's ability to receive power into space as a function of radial distance and angular position from the antenna, and it can be represented as a plot. The radiation pattern has two primary types: The elevation plane, E-plane and theta-plane, and the Azimuth plane or H-plane and Phi-plane. The pattern plot comprises the main lobe with sides and back lobe. The side lobes and back lobe consider unwanted exclude dipoles and monopoles, although it can be gained with all types of the antenna because of a significant role in losing energy and noise sources for transmitting and receiving antennas.

The shape of the radiation pattern in figure 2.1 illustrated the parts and types of radiations that appear when antenna operation to study and discussed the performance, efficiency, and direction of the antenna and to know its suitability for respective applications or not.

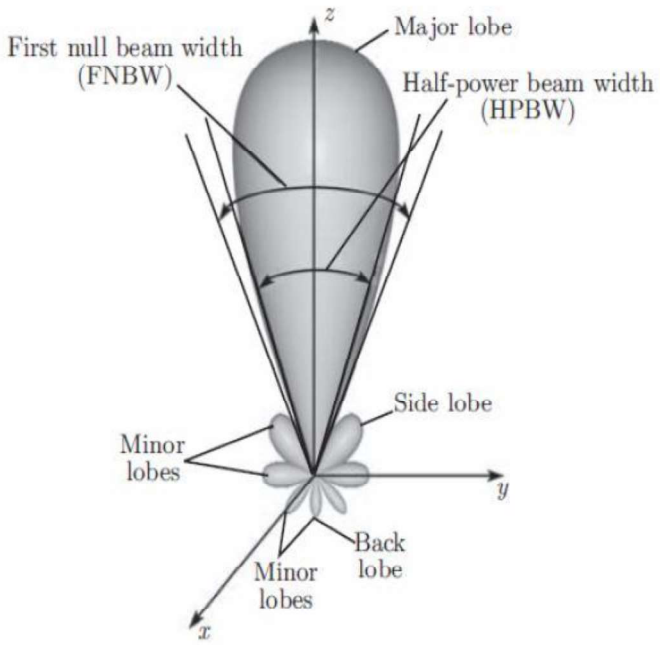

Figure 2.1 General of radiation pattern plot of antenna [36]

2.2.3 Bandwidth

Bandwidth describes the range of frequencies that the antenna provides in case of either transmitting or receiving. Bandwidth considers a main parameter of the antenna, and to know the resonance frequency that the antenna operated and taking into account the primary conditions which the antenna depends on for purpose its work rightly [38]. It is including VSWR and return loss that must be less than 2 and -10 dB, respectively. The basic formula of bandwidth is called the fractional bandwidth (FBW) is as follow:

$$FBW = \left(\frac{f_{High} - f_{Low}}{f_C}\right) \times 100\ \% \qquad \textbf{(2.2)}$$

Where:

FBW : Fractional bandwidth

f_{High} : Represent the highest frequency on the curve

f_{Low} : Represent the lowest frequency on the curve

f_C : Represent the center frequency on the curve

2.2.4 VSWR

The parameter VSWR or Voltage Standing Wave Ratio is called. It represents how efficiently an antenna operated, and through it, it can transfer the most significant power to space with the lowest possible power reflected from the antenna. The VSWR describes the relationship between the incident wave to the transmitter and the reflected wave to the AC voltage source. If the reflected wave were more significant than the incident wave, the breakdown would happen in the system, and the sender cannot radiate and vice versa. The VSWR is considered a prime element for matching the patch and feed line and must have a minimum justifiable value equal to or less than 2. Figure 2.2 depicts the simple idea about VSWR, and its formula can be stated as following [39]:

$$VSWR = \frac{V_{max}}{V_{min}} = \frac{1+|\Gamma|}{1-|\Gamma|} \qquad \textbf{(2.3)}$$

Where:

V_{max}: Maximum peak voltage

V_{min} : Minimum peak voltage

Γ : Reflection coefficient

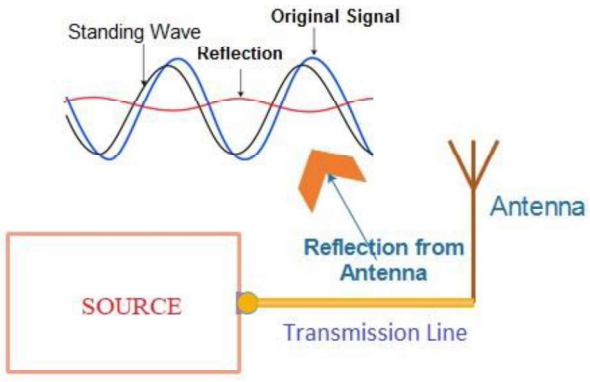

Figure 2.2 Exhibited Voltage Standing Wave Ratio

2.2.5 Gain

The gain is a non-dimensional ratio and not a physical quantity like Ohm and Watt, and it has given relative to the most prevalent reference antenna such as half-wave dipole and isotropic antenna. There is no found antenna radiated perfect in all directions like isotropic, but can use and compare it with real antennas manufactured to know its performances and specifications [40]. Any antenna can generate sufficient energy in a specific directive, and it is low in others. The gain equation can be expressed as below [36]:

$$G = \frac{U}{P_{in}/_{4\pi}} \qquad \textbf{(2.4)}$$

2.2.6 Efficiency

Antenna efficiency measures how much power arrived at the antenna compared with its radiated power [39]. In real work-life, the antenna that radiates 50-60 % power of all power delivered is considered a good antenna.

The total efficiency of the antenna depends on three types of efficiency that affect a radiated element. The first and second efficiencies are conduction and dielectric efficiency of material used as well as a reflected efficiency that can be written as below:

$$e_t = e_c e_d e_r \qquad \textbf{(2.5)}$$

Where:

e_t: Total efficiency

e_c: Conduction efficiency

e_d: Dielectric efficiency

e_r: Reflected efficiency

2.2.7 Complex Impedance

It is a significant parameter of antenna and input impedance that can read on the Smith Chart. Complex impedance appears at load terminals and consists of the real part on the X-axis and the imaginary part on the Y-axis.

The power indeed radiated by the antenna is connected with emission impedance, but the power lost as heat has called dissipated power because of conducting and dielectric material losses [40].

The unit its measurement is Ohm. The complex or input impedance formulas can be illustrated as below:

$$Z_{in} = R_{in} + jX_{in} \qquad \textbf{(2.6)}$$

Where:

Z_{in}: Complex or input impedance

R_{in}: Real part and represents the antenna resistance

X_{in}: Imaginary part and represents the antenna reactance

2.2.8 Polarization

A Polarization is the oscillation of the electric field of an electromagnetic wave with its types with various shapes. The polarization of waves can be found by comparing the electric field's direction and position with the ground or our planet's surface [35]. We can depict the polarization commonly by three types: linear, circular, and elliptical, as illustrated below in figure 2.3.

Linear polarization: E-filed has represented as vertical or horizontal of a single plane.

Circular polarization: E-field has two transversal components equal in their amplitude, and the phase difference is 90 degrees constant.

Elliptical polarization: E-field has transversal components that are not equal in their amplitude, and the phase difference is not 90 degrees not fixed.

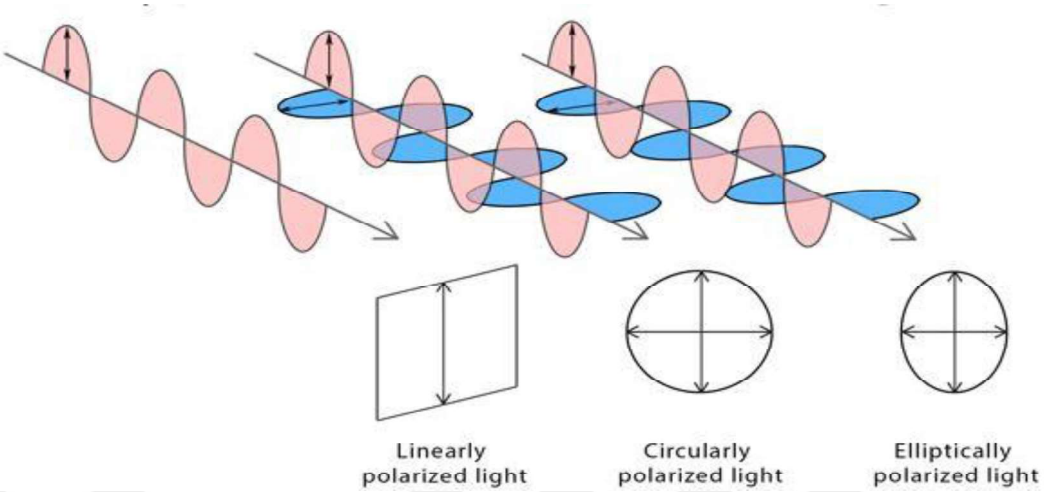

Figure 2.3 Illustrated the linear, circular and elliptical polarization

2.3 Antenna Definition

The antenna is a significant part of a wireless communication system that converted the Radio-frequency signal flowing in the conductor to electromagnetic waves radiated in free space or vice versa in working as a signal receiver; this is known as reciprocity. All types of antennas operated sufficiently in a specific narrow resonance frequency band [35].

The antenna must be appropriately fitted in proportion to the radio frequencies systems it will be operated. The antenna will radiate electromagnetic waves in a specific direction in free space after receiving a signal [40].

2.4 Types of Antennas

Antennas have various forms and sizes extensively that outfit with all kinds of wireless communication applications. Its size, form, and the type of metallic material used for its fabrication; will specify the properties and features of the antenna required. Some of the generally used antennas have explained below and divided into:

2.4.1 Wire Antenna / Half-Wavelength Dipole

Half-wave dipole antenna considers so widely used by researchers due to its radiation impedance have between 50 and 75-ohm characteristic impedance that leads to easy and perfect matching between a transmission line and antenna [35]. Figure 2.4 illustrated a simple half-wave dipole antenna structure.

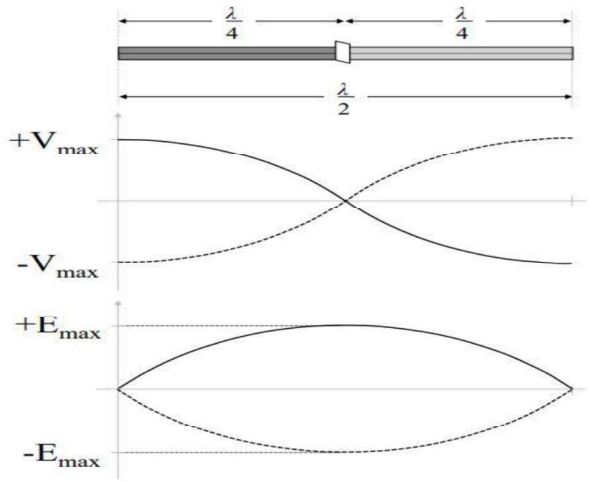

Figure 2.4 Shows the basis structure of half-wave dipole antenna [41]

Two conductors can create this antenna addressed vertically and then bending one of them reverse another with quarter wavelength for each and left the gap between them. The currents and voltages have different behavior in the half-wave dipole antenna; the current will be maximum in the center and zero at the terminal's ends and vice versa for voltage.

2.4.2 Monopole Antenna/ Image Theory

Monopole antenna is a quarter-wavelength dipole antenna; its design is based on applying image theory to dipole by placing the ground plane under the individual element with length L/2. The composition of single elements and their image works similarly to dipole with length L, but the emission happens just in free space upper the ground plate [42].

This type of antenna is suitable for mobile communication where the conducting plate will take different forms, such as outer car surface or phone handheld box. The directivity will be doubled, but the radiation resistance will reduce to half relative to the dipole. The gain of this antenna is 2-8 dB with radiation resistance equal to 50% of the half-wave dipole antenna [43]. Figure 2.5 illustrated the structure of the quarter-wavelength dipole antenna and the effect of image theory on the antenna's performance.

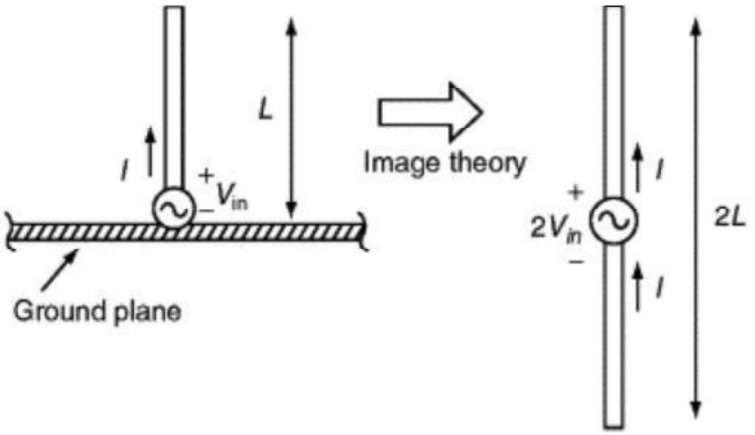

Figure 2.5 Depicts the concept work of monopole antenna [44]

2.4.3 Loop Antenna

This antenna is constructed by curving the metallic conductor and can make it, same as a square, square, ellipse, and many other forms with a gap in the middle-below of the conductor to connect the terminals [43]. The circular loop antenna takes the most attention because of its ease of fabrication. This antenna has divided into two types in case of electrical behavior. A large loop antenna has a perimeter equal to the free space wavelength ($C \sim \lambda$), but the small loop antenna has a perimeter equal to ($C < {}^{\lambda}/_{10}$). The loop antenna is used in many applications that operate in HF, VHF, and UHF bands and are near the microwave band [35].

When filled the loop antenna with ferrite, its performance will enhance, leading to an increase in the radiation resistance. As mentioned before, the perimeter of the loop antenna is equal to the wavelength, then it is known as significant electrically, and its radiation pattern is different from an electrically small loop antenna. This antenna commonly has gained around 5 dB from -2 to 3 dB and 10% of bandwidth [43]. The loop antenna receivers create in the shape of a small loop, but the single and multi-loop antenna is used in pagers and AM receivers, respectively, as seen in figure 2.6.

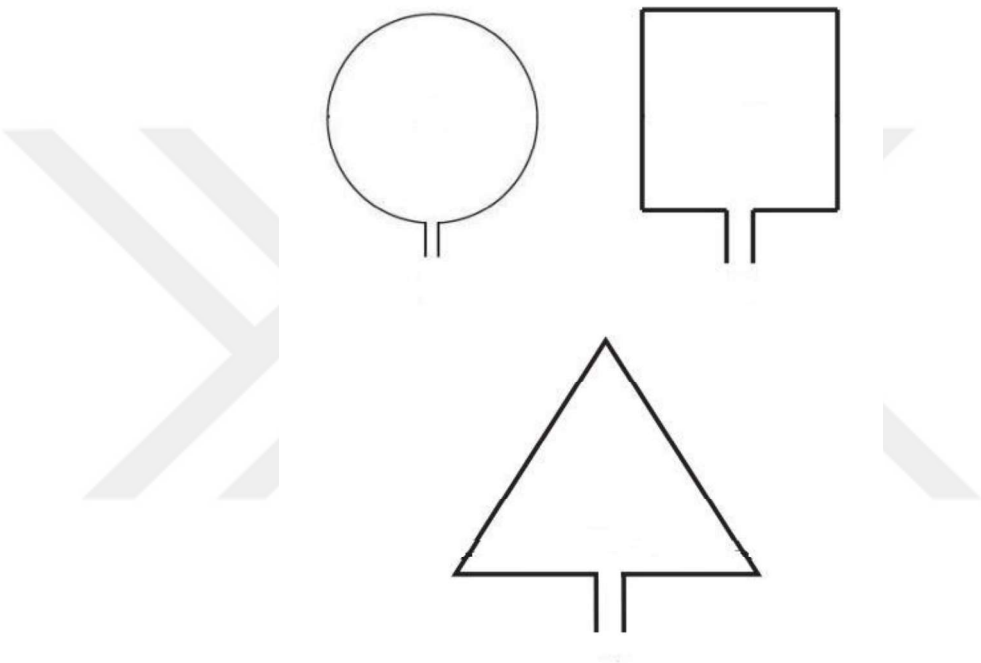

Figure 2.6 Shows the different shapes of loop antenna structure [45]

2.4.4 Spiral / Helical Antenna

A spiral antenna, known as a helix antenna, consists of a single conductor warps form of spiral up vertically and connected to the ground plane as shown in figure 2.7. This situation of the antenna will generate high gain and bandwidth relative to the normal working mode. The spiral antenna has two modes which are the broadside and end-fire radiation [43].

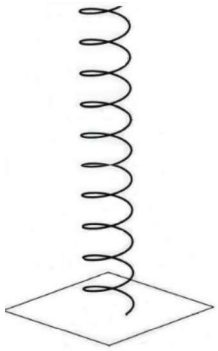

Figure 2.7 Illustrates the basic form of spiral antenna [46]

2.4.5 Horn Antenna

The Horn antenna is considered one of the most significant radiated elements used in microwave antennas, satellite tracking, and communication dishes, as wells as in reflectors [35]. The horn antenna has more advantages such as ease in manufacturing, high performance, and gain. The horn shape of the antenna consists of a cavity, and it can take different shapes depending on required applications, as seen in figure 2.8.

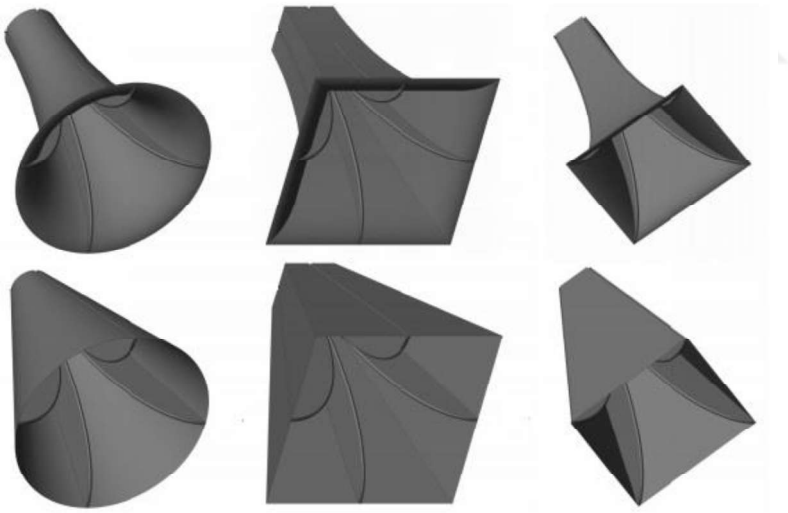

Figure 2.8 Shows the different types of horn antennas [47]

2.5 Transmission Line Modeling

It is a metallic conductor or another material such as copper or aluminum generally used for transmitting signals from point to point or used for feeding load by the generator.

There are many transmission lines, but the microstrip is the most frequent because of its easily manufactured and integrated with modern microwave and wireless devices [39]. It consists of a strip line of metal placed on dielectric material with a specific thickness and relative permittivity for each application used, and it is generating magnetic and electric fields that are perpendicular to each other. There are mainly three types of the transmission line as follow [39]:

- Multi conductor lines: includes microstrip, slot, coplanar, strip and coaxial.
- Single conductor waveguides: includes rectangular, circular, elliptical, single and double ridged.
- Open boundary: includes open waveguides and dielectric rods.

2.5.1 Microstrip Transmission Line Building

The evolution that has taken place in modern nanotechnology led to a reduction in the size of devices used in daily life. There was becoming an urgent need to invent a micro-transmission building that was reconcilable with present-day circuit fabrication to supply efficient signals during finite distance. It has been achieved by placing a small single conducting with width W and height t on a particular dielectric material of constant relative permittivity ε_r with depth h. The dielectric material places into the center between two conductors. The dielectric material separates the microstrip line above it, and the ground plane placed below it. It preferably uses a low-loss substrate for SHF and mm-Wave applications. The Micro-strip line cannot back the pure transverse electromagnetic (TEM) mode because it is surrounding by two regions, the insulating material below it and the air above it. There are differences between the TEM phase velocity calculation of dielectric and air, as clarified in the 2.7 and 2.8 equations below [48].

$$v_{p1} = \frac{v}{\sqrt{\varepsilon_r}} \qquad \textbf{(2.7)}$$

$$v_{p2} = v \qquad \textbf{(2.8)}$$

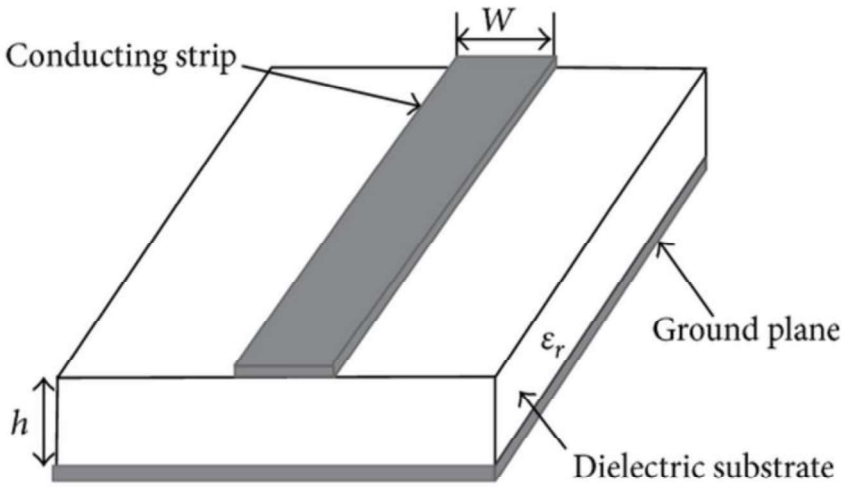

Figure 2.9 Shows the T.L structure [49]

Where:

v_{p1} : Represents the phase velocity in dielectric.

v_{p2} : Represents the phase velocity in air.

ε_r : Represent the relative permittivity of dielectric material.

v : Represent velocity of wave in medium.

Figure 2.9 illustrates the primarily elements of tiny transmission line and the figure 2.10 below states process spread of magnetic and electric field started from T.L to through air into the dielectric material.

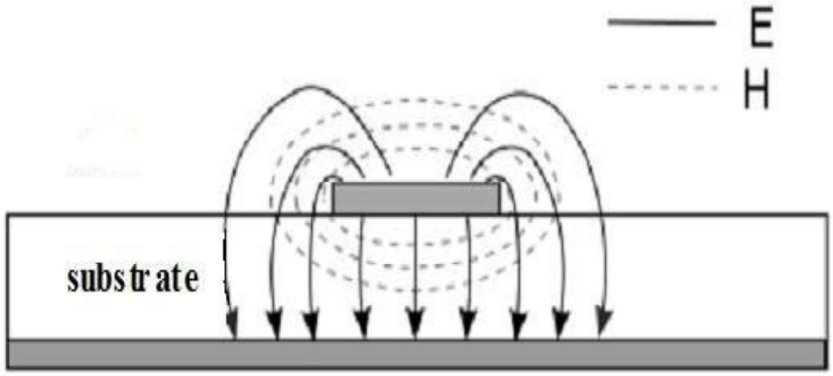

Figure 2.10 The electric and magnetic field of microstrip T.L [50]

2.5.2 Parameters Computation for Microstrip

In this section, we will compute the effective dielectric constant for quasi transverse electromagnetic mode (TEM) [40]:

$$\varepsilon_{eff} = \frac{\varepsilon_r+1}{2} + \left[\frac{\varepsilon_r-1}{2}\frac{1}{\sqrt{1+\left(12\frac{h}{W}\right)}}\right] \qquad \textbf{(2.9)}$$

There are two methods to compute the characteristic impedance Z_o by compared the width W of microstrip to the thickness h of substrate as follow:

If $\frac{W}{h} \leq 1$:

$$Z_o = \frac{60}{\varepsilon_{eff}} \ln\left[\frac{8h}{W} + \frac{W}{4h}\right] \qquad \textbf{(2.10)}$$

Then $\frac{W}{h} > 1$:

$$Z_o = \frac{120\pi}{\sqrt{\varepsilon_{eff}\left[\frac{W}{h}+1.393+0.667\ln\left(\frac{W}{h}+1.444\right)\right]}} \qquad \textbf{(2.11)}$$

After characteristic impedance calculation, we must find the value of $\frac{W}{h}$ in two methods depending on the its ratio:

If $\frac{W}{h} < 2$:

$$\frac{W}{h} = \frac{8e^A}{e^{2A}-2} \qquad \textbf{(2.12)}$$

Then $\frac{W}{h} > 2$:

$$\frac{W}{h} = \frac{\pi}{2}\left[B - 1 - \ln(2B-1) + \frac{\varepsilon_r - 1}{2\varepsilon_r}\left[\ln(B-1) + 0.39 - \frac{0.61}{\varepsilon_r}\right]\right] \qquad \textbf{(2.13)}$$

We can find *A* and *B* as equations below:

$$A = \frac{Z_o}{60}\sqrt{\frac{\varepsilon_r+1}{2} + \frac{\varepsilon_r+1}{\varepsilon_r+1}\left[0.23 + \frac{0.11}{\varepsilon_r}\right]}, \; B = \frac{377\pi}{2Z_o\sqrt{\varepsilon_r}}$$

The attenuation that happens because of the conductor and dielectric losses and can be found as formulas below:

$$\alpha_c = \frac{R_s}{Z_o W} \qquad \left({}^{N_p}/_{m}\right) \qquad \textbf{(2.14)}$$

$$\alpha_d = \frac{k_o \varepsilon_r (\varepsilon_{eff} - 1) tan\delta}{2\sqrt{\varepsilon_{eff}}(\varepsilon_r - 1)} \qquad \left({}^{N_p}/_{m}\right) \qquad \textbf{(2.15)}$$

Where the tanδ represents the loss tangent of the dielectric material, $k_o = \frac{\omega}{v}$ and R_s represents the skin resistance of the conductor, and the conductivity of metal conducting is σ as well as ω and μ_o are constituting the angular frequency and permeability of free space respectively.

$$R_s = \sqrt{\frac{\omega\mu_o}{2\sigma}} \qquad \textbf{(2.16)}$$

2.5.3 Types of Conducting and Dielectric Materials

Four types of materials are used in microwave and printed circuits depending on the capability of conducting or isolating each of them. For instance, the conducting material that microstrip has been consisted of, such as silver, aluminum, copper, and gold, has the highest conductivity that is almost perfect. The second type includes the substrates placed between the conductors as in antenna fabrications such as silicon, FR-4, and Rogers that have low permittivity, and it is recommended to use them in high frequency and mmWave applications. The last two types are resistive and dielectric films like *Ta*, *GaAs*, *NiCr* and *Si*3*N*4, *Sio*2, respectively. We will enough to study the first two types of materials regards to studying in this thesis.

2.5.3.1 Dielectric Material Properties

The overall characteristics of substrates used in High-frequency bands are as follow below:

- It should be available in the markets at a low price.
- All impedance and frequency bands would be determined by choosing the dielectric constant and the highest of the substrate.
- For reducing the dielectric loss of material used, the loss tangent must be low.

The dielectric material will determine the specifications of the antenna designed and the desired frequency required according to their permittivity and dimensions. It considers one of miniaturizing techniques used in microstrip antennas design. Roger RT/ Duroid is used in this thesis because it has a low dielectric constant, which leads to quickly getting the high resonance frequencies for SHF and mmWave applications [51].

2.5.3.2 Conductor Material Properties

The characteristics and types of Printed Circuit board and Microwave circuit and also the type of conductor used. As mentioned previously, it will determine the system's features required whether it is convenient in high or low-frequency applications. The printed circuit board can be fabrication with various kinds like multi-layer and single or double-sided [52]. The electrical losses of printed circuit boards lead to an efficiency decreasing of the antenna and transmission line operation. For instance, the antenna will suffer from lower sent power, reduced gain, thermal issues, thermal problems, and lower supplied power to the load in a transmission line. The roughness of the conductor surface plays an essential role of effect in the transmission line and antenna [53]. There are significant points that must behold into consideration. For example, when the copper roughness increase, its resistivity will go up from 10% to 50% [53]. For that, the frequency will increase when the surface conductor roughness increased. Finally, the conductor material used in the printed circuit board must have specific properties; to ensure the saving highest rate of current density in the conductor, such as low temperature, high conductivity, and quick weldability [48].

2.6 Micro-strip Antenna Feeding Methods and Techniques

The Microstrip compact antenna needs to feed it by different techniques, and also every method has benefits and disadvantages that differ from others. There are two general classifications as follow;

Firstly, the power can generate and arrive at the patch antenna directly through a small microstrip transmission line or coaxial feed [54].

Secondly, the power can be generated and transferred to the patch indirectly; with the coupling process between transmission line feed and patch antenna through the apertures has placed in the substrates such as aperture-coupled and some other techniques like proximity-coupled feed and Co-planar waveguide feed [54].

2.6.1 Direct Method: Microstrip Line Feeding

This feed technique considers simple and easy to fabricate and can provide maximum power transfer from transmission line feed to the radiated patch without impedance mismatching issues. In this method, the feeding connects directly with the antenna without any additional elements needed to help it match [35]. The transmission line is placed in the same dielectric material as the antenna, and it has a small width relative to the radiated patch. There are several various shapes of this technique, as illustrated in figure 2.11. For example, typically, an offset edge-feed and quarter-wave transformer and inset feed technique [54].

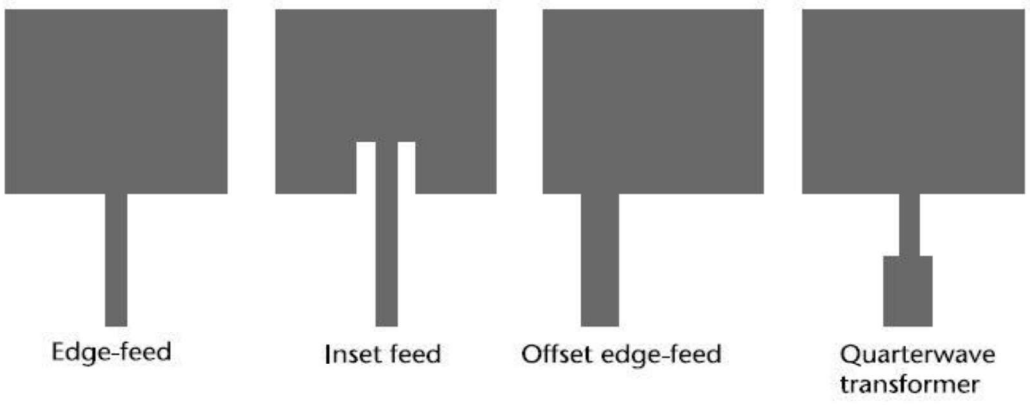

Figure 2.11 Various methods of transmission line feeding [54]

Every technique mentioned previously is used in a specific environment, but inset feeding considers the best in the case of impedance matching since it starts from a certain point located inside the patch to match the T.L and radiated element fully.

2.6.2 Direct Method: Probe Feeding

This feed technique is known as a probe or coaxial feed. Also, it considers highly generally used for compact patch radiated antennas because of having some advantages such as simple fabrication, a low level of spurious emitted, and can be situated at any wanted position to reach maximum input impedance. The probe feeding consists of two parts; the first one connects with radiated patch element via the insulating material, and it is an inner conductor called [35]. The second part links with the ground plane and knows as the outer conductor [35].

This feed technique has several minor drawbacks, such as difficult substrate drilling that makes the inner conductor pass through it, and narrow bandwidth has resulted [55]. It is advised not to increase the insulating material's thickness because that results in making the input impedance more inductive [56]. Figure 2.12 below will illustrate the coaxial feed when joining with a microstrip antenna.

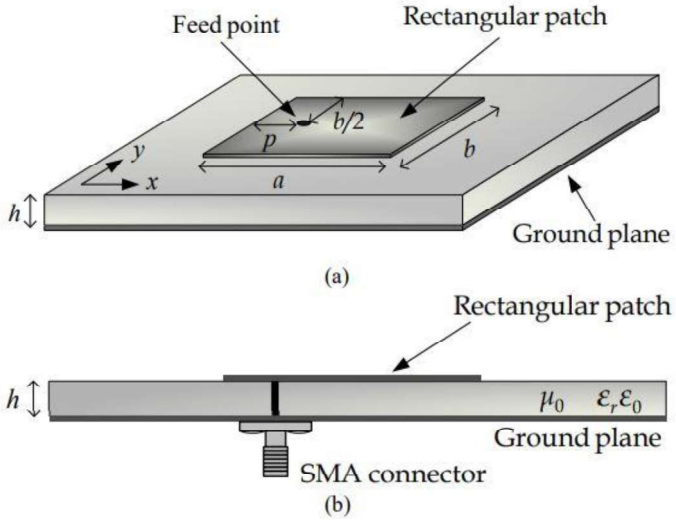

Figure 2.12 Shows (a) 3D-dimensions of patch antenna with fixed point of feed, and (b) how to install the parts of coaxial feeding with patch antenna [57]

2.6.3 Indirect Method: Aperture Coupled Feeding

When designing an antenna with a wide bandwidth of resonance frequency, the aperture coupled feed considers the best way to get these results. This feed technique includes two dielectric materials with two different relative permittivity's [58]. One of these substrates is placed below the patch antenna and the other above the transmission line. The central part is the ground plane that will isolate between the two substrates. The ground plane contains an aperture with various shapes and sizes. The electromagnetic wave will transfer from the strapline feed via aperture to the compact patch antenna. The thick dielectric material with low relative permittivity will use for the patch's substrate, but the thin dielectric material with a high dielectric constant will use for the strapline feed's substrate [56]. Aperture coupled has a drawback of fabrication difficulty because it increases the compact microstrip antenna thickness [35]. Figure 2.13 depicts the aperture coupled feed with antenna structure.

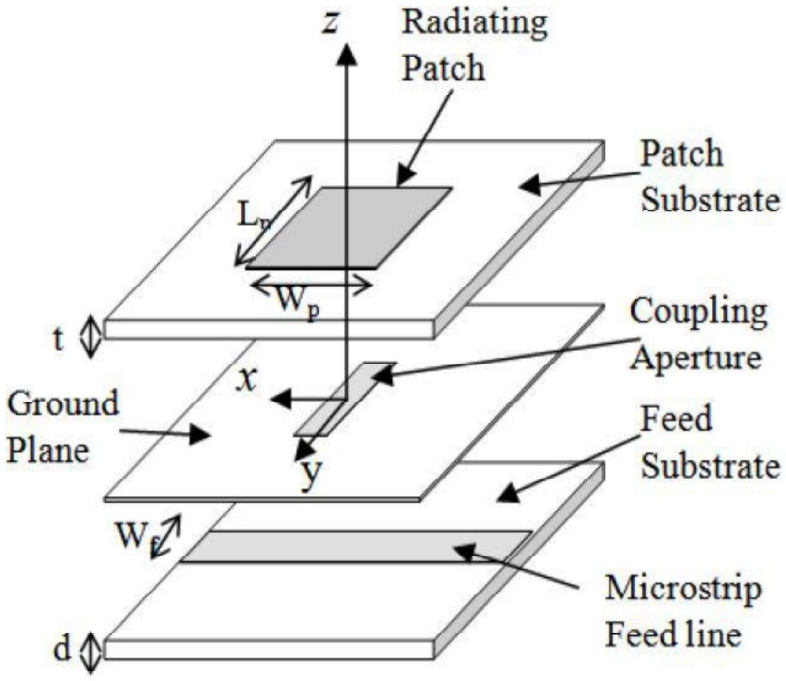

Figure 2.13 Antenna structure with aperture feed method [53]

2.6.4 Indirect Method: Proximity Coupled Feeding

This feed method is also known as electromagnetic coupled feeding, and it is using for enhancing or increasing bandwidth to 14% [54].

The proximity coupled techniques consist of two substrates, such as the aperture coupled feeding technique, but there are differences in materials location without aperture etched. Moreover, the two substrates are taken with different relative permittivity [60]. The whole microstrip antenna composition includes a transmission line between dielectric materials, one substrate for the patch and another for the ground plane. The impedance matching can be attainment with dimensions changed of the T.L feed compared with the compact patch antenna width.

Microstrip antenna with coupled technique is challenging to fabricate because of double layers dielectric materials that increase the total antenna size and need accurate alignment [54]. Figure 2.14 shows proximity coupled feeding.

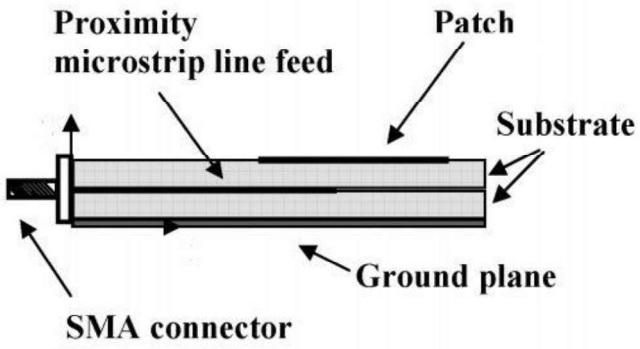

Figure 2.14 Illustrates proximity coupled feeding mechanism [61]

2.6.5 Indirect Method: Coplanar Waveguide Feeding

The last feed technique is coplanar waveguide feeding (CPW) called, and it consists of three conductors printed with the same dielectric material. The center conductor has separated by a small gap with another two reverse conductors [62]. The small gap has unvaried widths. Most time, the reverse conductors expand to unlimited distance. The structure types of coplanar waveguide feeding can be exhibited in figure 2.15. CPW uses for feeding patch antenna because of having advantages as follow:

- The active devices (semiconductor devices) such as transistors, amplifiers, and diodes can be installed above the microstrip patch antenna.
- The linking with Co-planar does not require any interruption in parasitical; it can supply the antenna with the high frequency desired more than 100 GHz.
- Co-planar waveguide feeding is suitable for miniaturization, wide-band, and dual-band microstrip antenna design, and it can achieve maximum impedance matching between the patch element and the feed line [65].
- The antenna will have low emission losses and less dispersion.
- This feed technique property provides comfortable in system integration that is mainly used for mmWave applications.
- It used in high-insulation wireless switches to provide more than 60 dB insulation.

As well the advantages mentioned above, the drawbacks of CPW can be summarized as follow [64]:

- It is considered more expensive than other types of feeding techniques in fabrication processes.
- Coplanar waveguide feeding requires a thick dielectric material that results in badly heat wasting.
- Some concepts about CPW are not clear yet within the microwave design society.

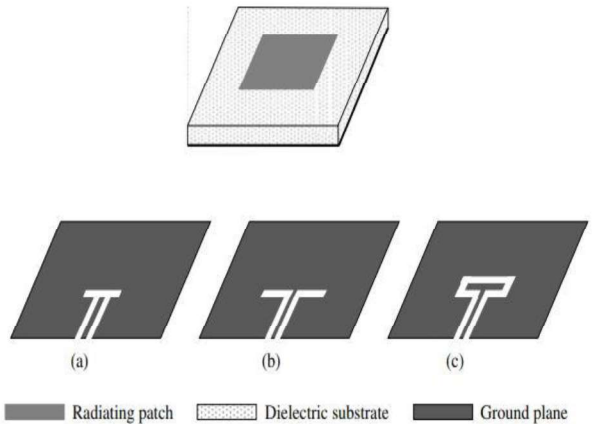

Figure 2.15 Shows the CPW feeding with various shapes [63]

The coupling represents capacitive and inductive, between patch antenna and co-planar waveguide feeding in figure 2.15 (a, and b), and also the figure 2.15 (c) used for removing undesired back emission [63].

2.7 Analyzing Techniques

Three prevalent methods to analyze compact patch antennas rely upon main factors: vision, correctness, and accuracy. The cavity model, full-wave, and T.L model represent the practical techniques to check microstrip antenna. Besides, these techniques have benefits and drawbacks that make them very suitable for various circumstances. These models with their features and disadvantages have been illustrated as follow:

First: The transmission line model considers one of the most accessible techniques used, and a compact antenna is checked the same as T.L shaped, and its emission performance is obtained analytically. This method provides high vision with low accuracy.

Second: The full-wave model evaluates field integral formulas and is considers more complex in analyzing.

Third: The cavity model analyzes the compact antenna as insulation-loaded hollow and increases the accuracy and vision.

The full-wave and cavity model have been discussed in detail below.

2.7.1 Full Wave Model Technique

This technique is a digital procedure used to check and analyze compact patch antennas. This method is modeled the surface plate of the patch and size in dielectric material with meshes to use the current domain per mesh point [54]. The approximation accuracy relies on the functions used to determine the currents and fields.

The EFIE and MFIE are integral equations with various shapes according to issues and used to represent the relationships between emitted fields and supply, along with

considering so complex when using analytical equations. For that reason, the robust approach will be used and known as a numerical system that leads to unclear interaction between supply and load [54].

The main objective of this method is to create an advanced mathematical equation find a solution of the specified formula below:

$$Lf(x) = g(x) \qquad \textbf{(2.17)}$$

For getting the value of f, the undefined f value will be as a linear equation with N known as total meshes as follow:

$$f = \sum_{n=1}^{N} a_n f_n = a_1 f_1 + a_2 f_1 + \ldots\ldots\ldots\ldots + a_N f_N \qquad \textbf{(2.18)}$$

Where:

L : Represents linear operator defined

g : Excitation function

f : Represents of currents and fields of unknown function.

a_n: Undefined coefficient

f_n : Basic function

N : Number of meshes in conducting surface

The primary functions and the number of meshes will affect the accuracy of this method, as well as there are different forms of basis function as illustrated in figure 2.16.

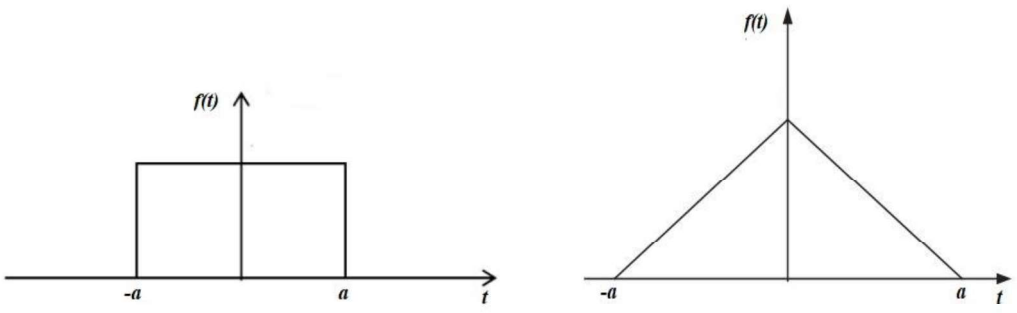

Figure 2.16 Depicts the basic functions such as (a) rectangular pulse function [66], and (b) triangular pulse function [67]

2.7.2 Cavity Model Technique

The prime concept of the technique depends on making the patch antenna as an insulation-loaded cavity by using an analytical technique. Therefore, the patch antenna with a fragile insulation material can be supposed as a cavity enclosed by ideal electrical plaques and magnetic [54]. Field values will slightly change within a thin insulation material plate in the usual orienting of the ground plane. The currents values establish by the cavity area that fields constrictive within itself to obtain a good radiation performance of the compact antenna [54]. Figure 2.17 illustrated a random rectangular patch antenna with charges movement and distribution as negative and positive charges that transfer from the lower right side to the top of the patch and continue to move to another side [68]. The patch will supply by power relative to the thickness value of dielectric material because of the repulsion of similar charges found on the patch and ground plane as well as the contrary charges appear as attractive or pull power [68].

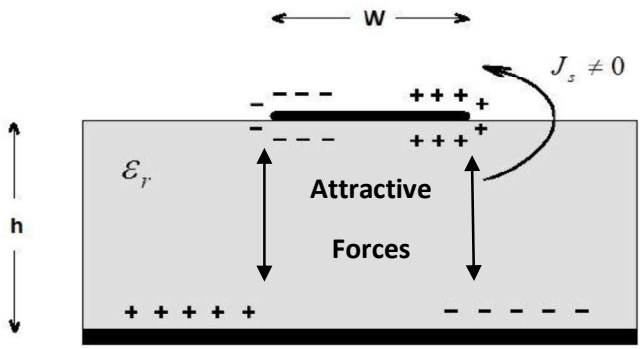

Figure 2.17 Depicts the behavior positive and negative charges in compact antenna [69]

The concept of charge movement will start to change when decreasing the thickness of the substrate as much as possible to make the microstrip antenna near the ground plate, and the attractive forces become very strong between the ground and printed patch [54]. For this reason, the current on the compact antenna surface will drop sharply and prevent appearing the magnetic fields at the edges of the compact antenna due to the boundary conditions. Lastly, to address the issue that the printed antenna sides do not support magnetic fields, these walls can be supposed to be perfect Electric

Conductor PEC as well as the four sides between the top and bottom PEC layers will be Perfect Magnetic Conductor PMC as illustrated in figure 2.18 below [69]:

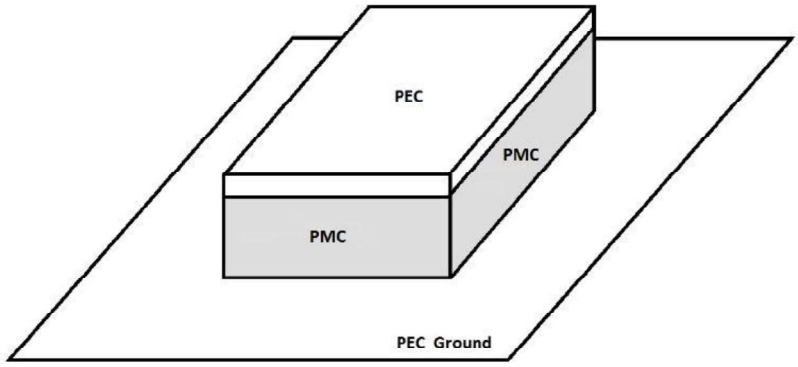

Figure 2.18 Shows cavity model structure with PMC and PEC plates [69]

A perfect cavity model works as a resonator, and it cannot emit energy the same as dielectric material and loss-free conductors. The calculation of the losses became compulsory because all amount of the energy reaching to patch will be ultimately returned to the source.

2.8 Miniaturization Methods of Antenna

The modern future 5G wireless devices and technologies demand new and high-frequencies operated at SHF and mm-Wave bands, especially in 10 GHz and 30 GHz. It is also known from the basic mathematical formulas of the microstrip antenna. When increasing the resonance frequency required for main applications, the antenna's dimensions have minimized.

Public and private technology companies have benefited from miniaturizing techniques to fix the issues of the radiated element in radar, satellites, and mobile applications. These methods have been represented using slots etched with different shapes and fractal antenna geometries [71]. The purpose of utilizing this technique is to diminish the size of the patch antenna as much as possible with improving antenna efficiency and bandwidth [70].

2.8.1 Changing The Antenna Structure

Antenna structure manipulating and adding components within it considers one of miniaturizing techniques and also other methods used in modern microstrip patch antenna which divided into:

2.8.1.1 Slots Etching

This technique is commonly used for compact patch antenna to generate dual-band desired resonance frequency or broadband made it. There are no standard equations that can be used for analyzing it, just which in design the primary structure of the antenna. Every Slot emits electromagnetic waves, same as dipole antennas and using in devices that need high control of radiation patterns. Making slots in radiated elements depend on their positions, shapes, and sizes. According to needed applications, it can take different forms such as E, S, C, star, square, polygon, and triangle [73]. The impedance matching and current distribution determine antenna performance. Furthermore, do not forget the disadvantages of this method, which decreases efficiency and bandwidth.

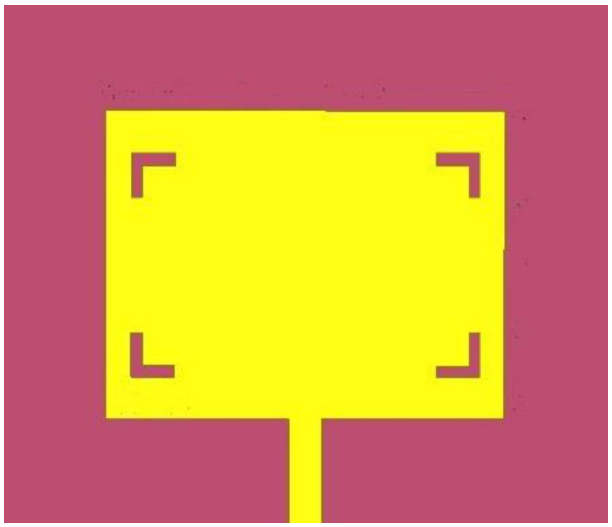

Figure 2.19 Shows the simple example of slot patch antenna [72]

2.8.1.2 Dielectric Material with High Permittivity

This method has been studied by using a substrate with high permittivity, and it considers a simple way to minimize the physical size of a microstrip antenna.

If the value of the dielectric constant increases, then the capacitance and the number of the charge stored between layers will increase. The resonance frequency required can calculate in equation (2.19); this formula shows that frequency is inverse proportional with capacitance. This technique is suitable for the multiband antenna. Despite these advantages of the method, there are more drawbacks such as low gain, bandwidth, and radiation pattern [74]. The equations below depicted that:

$$F = \frac{1}{2\pi\sqrt{LC}} = \frac{c}{2L\sqrt{\varepsilon_r}} \qquad \textbf{(2.19)}$$

$$\lambda = \frac{\lambda_o}{\sqrt{\varepsilon_r \mu_r}} \qquad \textbf{(2.20)}$$

Where:

F : Represents resonance frequency

L : Inductance

C : Capacitance

ε_r: Relative permittivity

μ_r: Relative permeability

c : Speed of light in free space ($3\text{x}10^8$ $^m/_{sec}$)

2.8.1.3 Inductive and Capacitve Element Loading

All researchers work in the field of microwave and wireless systems, especially in compact antennas design. They consider this technique the easiest and fast way and use it to make the antenna operate in frequency minor than the actual frequency for microstrip antenna. The technique's concept is that any radiated element lower than five-unit will have high input impedance. This impedance can be made up by adding lumped components such as capacitance and inductance, which minimizes the antenna dimensions. If the lumped element has low loss, then the antenna bandwidth will decrease, and if it has a high loss, then the performance of radiated antenna will decrease [75].

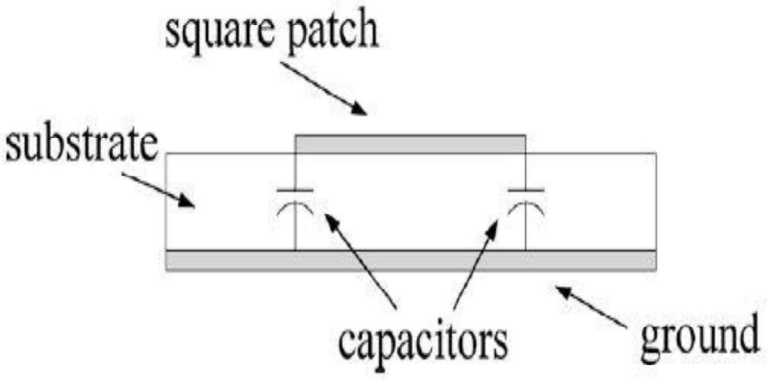

Figure 2.20 Simple instance of compact antenna with capacitive element [76]

2.8.1.4 Metallic Pins Loading

This method aimed to join the ground plate with a microstrip patch antenna as a short circuit to increase the electric current flux that leads to more minimizing antenna size [79]. Despite the antenna size being minimized, The other parameters such as directivity and gain will also decrease. The shorting pin can change the compact antenna's resonance frequency by modifying its position between the patch and ground plane [78]. It can place more than one pin between two conductors, and it can use it with various feeders such as transmission lines or coaxial cables. Figure 2.21 describes the structure of a compact antenna with a coaxial feed technique.

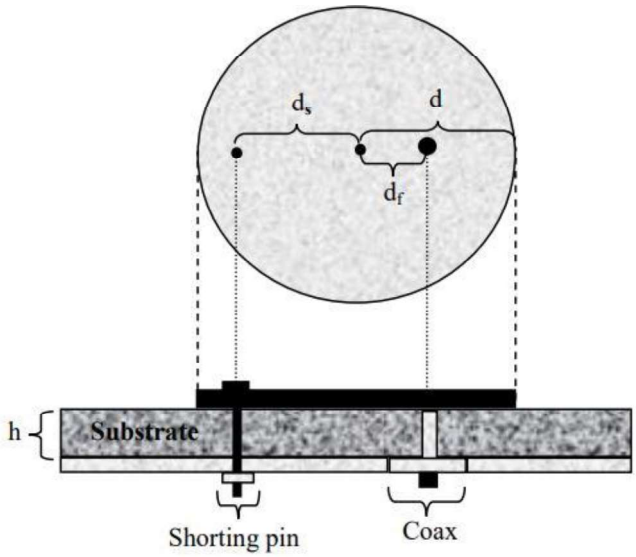

Figure 2.21 Shows shorting-pin loaded with circular patch and ground plane [77]

2.8.2 Fractal Geometry Technique

Space-filling geometry, known as fractal geometry, was invented for the first time in 1975 by Benoit Mandelbrot [83]. In 1988, Dr.Nathan had designed the basic fractal radiated element and followed that his first fractal antenna design in 1995; it has been used in military and trading applications [80]. He also considers a well-known designer in the area of fractal antenna. It satisfied all parameter properties of the customer concerning size, price, fabrication, and bandwidth [84].

The word fractal is derivative from the ancient Greek language, which stands for fractured or erratic parts [82]. A repetitious geometry alludes to the method of partition a shape into a tiny duplicate of itself. The conventional antenna works at only one resonance frequency which a wider region is required to two antennas or more [85].

The fractal antenna has distinct characteristics, as illustrated below:

- Radiated element has the same form but repeated itself with decreasing in length sequentially.
- Hilbert curve is used to reduce the antenna's physical size because of the space-filling characteristic that makes electrical current flows in long paths into compressing space; this property is known as space-filling.

Fractal antenna fixes two constraints of the conventional radiated element [81]:

- The antenna parameters such as input impedance, gain, and radiation pattern determine the antenna work's performance.
- Modern military and wireless communication techniques depend on increasing the fractal antenna's length to minimize the antenna volume.

Fractal antenna geometry can be exegesis and created by the repetitious method that provides to self closeness structure. The fractal antenna can be divided into [86]:

- Deterministic fractal can be represented by numerous dimension down and round copies such as von Koch snowflake and Sierpinski gaskets.

- Random fractal appears a regular event happens in the life same as thunderbolt and dendrites.

These configurations prove and describe construction in nature that was hard to implement by traditional geometry [87].

Advantages of fractal antenna are [85]:

- Small in size.
- Using one antenna is enough rather than more.
- Suitable for dual-band antenna design.
- Maximum power transfer from feeder to the patch.
- Enhancement of bandwidth.

Disadvantages of fractal antenna [87]:

- Lossing of gain.
- Antennas' design is complex.
- Numerical constraints.
- The benefit starts to reduce after the first repetitous.

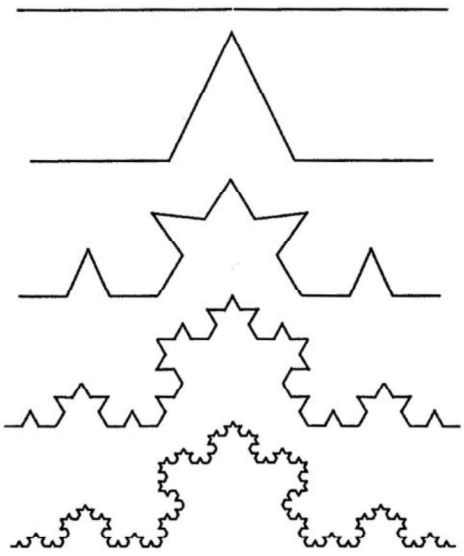

Figure 2.22 Shows iteration stages of Koch monopole antenna [88]

2.8.3 Meander Line Technique

This technique assumes making a patch the same as the shape of snake's movement that leads to an increased path of current flow and antenna will radiate with lower desired frequency than the actual length of the patch. The meander line is a group of lines places vertically and horizontally to form the snake's movement. Designers have used this method to keep the space and bend the metallic conductors forward and backward to minimize the patch size as much as possible [89]. The drawback of this technique is represented by decreasing values of bandwidth and efficiency of the antenna.

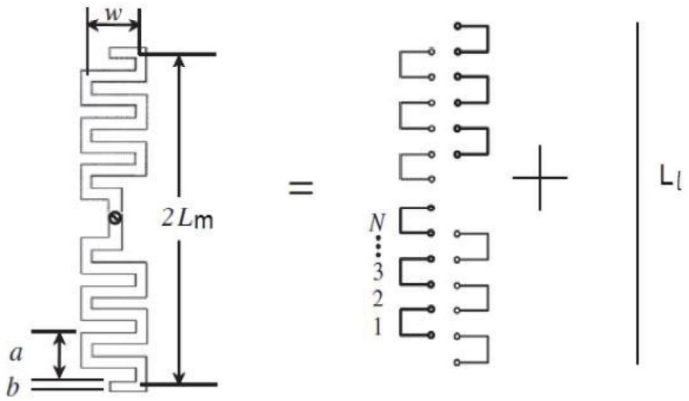

Figure 2.23 Illustrates the basic shape of meander line antenna [90]

The meander antenna radiated electromagnetic waves that have phase velocity as follow:

$$v_{p=}\frac{L_l}{L_m}c \qquad \textbf{(2.21)}$$

Where:

v_p : Phase velocity of electromagnetic wave

L_m : Meander line length

L_l : Linear line length

c : Speed of light in free space (3x10^8 $^m/_{sec}$)

The meander line operated as a circuit consists of capacitance located as vertical lines and inductance located as horizontal lines. The length of the patch with the total length of the meandering line as well as characteristic impedance can be computed as following [43, 91]:

$$NXS = \frac{\lambda}{10} \qquad \textbf{(2.22)}$$

$$L_p = \frac{c}{2f\sqrt{\varepsilon_{eff}}} \qquad \textbf{(2.23)}$$

$$Z_o = 276\log\frac{2S}{d} \qquad \textbf{(2.24)}$$

Where:

N : Represents number of turns

S : Represents number of spacing between turns

λ : Wavelength of resonance frequency

L_p: Represents the patch length

f : Resonance frequency

Z_o: Characteristic impedance of line

d : Diameter of wire antenna

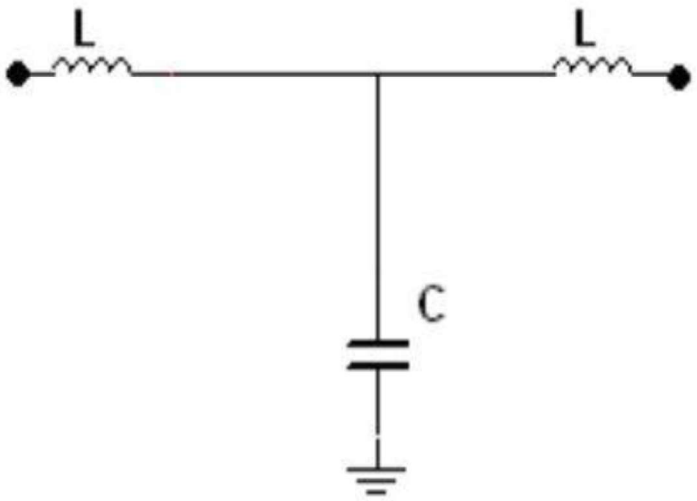

Figure 2.24 Shows the equivalent circuit of meander line [91]

2.8.4 Improving of Geometry Shapes

This method is the simple way to minimize the physical size of the microstrip antenna by edit its shape and dimensions. L-inverted antenna considers a good instance by curving of monopole antenna. The drawbacks of this technique are low bandwidth and gain and generating highly ohmic losses [92].

2.9 Frequency Band with Antenna Selection

In this thesis, we will focus on the SHF band (Super High frequency) that operated from 3 GHz to 30 GHz, and it is also known as the centimeter band or centimeter wave [93]. SHF bandwidth assigned from 30 MHz to 300 MHz will allow fast digital communication above 1 Giga per second [89]. Super High-frequency bands will be affected by solid atmospheric attenuation and rainfall dispersion losses and high penetration losses during Radio wave propagation via the outside walls of buildings. Some applications to SHF bands include microwave relay links, radar senders, satellite communication, and wireless LANs [94].

Various microstrip patch antennas will be designed with different slots shapes to measure the parameters such as gain, directivity, VSWR, efficiency, and return loss at each desired frequency. These antennas will be dual-band at 10 GHz, and 30 GHz operated at X and Ka bands specifically and connected by a direct inset feed transmission line for maximum power transfer from the feeder to the patch. This work suggested keeping up future 5G wireless devices and applications.

2.10 CST MWS

Electromagnetic waves play an important role nowadays, which led to the development of technology industries remarkably. It has entered into various industries such as manufacturing vehicles, medical devices, and aerospace significantly [95]. Simulation made designers can check with an elementary model of the first steps of designing; to optimize the component functions. The simulation process also leads to a decreased number of models needed and time to improve it with their cost [95]. CST Studio Suite is one of the most significant simulation applications used to analyze and evaluate the

performance of electromagnetic devices and systems by designers. CST software provides more tools and parameters that support the engineers; to simulate the virtual models in the computer by designing closer to reality [96]. This software is used for microstrip antenna designing by calculating their parameters such as return loss, VSWR, directivity, gain, impedance matching, and current distribution [96]. In this thesis, new versions of dual-band microstrip antennas will design by using the Computer Simulation Technology (CST) version of 2018.

CHAPTER 3

DESIGN AND SIMULATION OF INSET FEED MULTI-BAND COMPACT ANTENNAS

3.1 Introduction

Three compact patch antennas are suggested and designed in this chapter with various shapes of etched slots to check the performance of radiated elements through the evaluation of parameters such as return loss, VSWR, gain, and efficiency.

These printed antennas will be designed by one of the most critical simulation software, CST ver.2018. All three printed antennas will be dual-band and work at X-band and Ka-band for 10 GHz and 30 GHz, respectively. These patch antennas can be illustrated as below:

- **First Design:** Multi-band microstrip patch antenna with slots in the shapes of big rectangle rings and small rectangles in their middle and partially ground technique used.
- **Second Design:** Multi-band microstrip patch antenna with T-shaped slots horizontally placed and two slots in the form of small rectangles.
- **Third Design:** Multi-band microstrip patch antenna with slots in the shapes of Fork and small squares.

In this chapter, the design principle of the proposed antennas is based on fundamental equations in Balanis's book [35]. These antennas will be designed and analyzed step-by-step using one of the antennas miniaturizing techniques, etching slots within a compact radiated element. These slots have been created in different shapes and sizes; to study the effect of these inscribed slots on behavior and performance for three antennas.

Besides, this work will be compared with a reference antenna designed chosen; for improving suggested antennas by reducing their size, inset feed dimensions changed, and place the slots in suitable locations for resonance frequencies required.

3.2 Reference High Gain Compact Printed Antenna

Because of the fast progress in the world of wireless systems, until the 5G in the world of communication, this has led to the need to invent modernized antennas to keep pace with this technical revolution.

Researchers also produced several good enough designs that work in the satellite and microwave bands. A Tri-band Microstrip compact antenna was taken as a guide because of these works' limitations, as illustrated in figure 3.1 [31]. The reference antenna built-in CST and HFSS were elected because of its small size, which allows for some improvements and makes it ready for future wireless devices.

The reference patch antenna is made up of a rectangular copper plane with two inverted T-slots on either side of an inset feed line to produce the appropriate resonance frequencies, as well as a partially copper ground technique used in this work to reduce the patch antenna's back-lobe emission [31, 97].

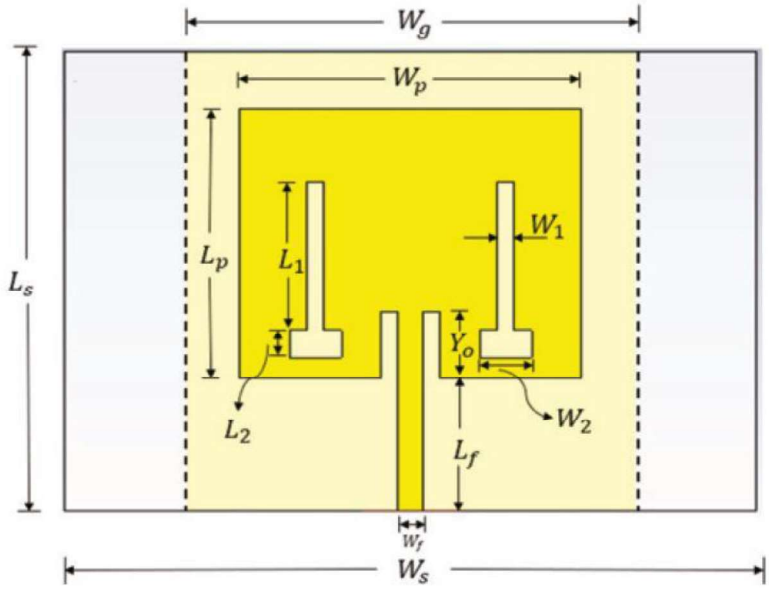

Figure 3.1 Depicts 2D of a reference patch antenna [31]

The compact antenna is built on Roger RT5880 Duroid, which has a dielectric constant of 2.2, a height of h = 0.508 mm, and dimensions of $W_s \times L_s$ mm^2 [31].

The inset feed method is used in a reference antenna to provide full power to a patch with $W_f \times L_f$ dimensions [31]. Table 3.1 depicts all of the values of a reference antenna in (mm).

Table 3.1 Shows the overall dimensions of a reference antenna [31]

Parameter	Value (mm)	Description
W_g	13	Width of ground plate
L_g	16.5	Length of ground plate
W_S	20	Width of Roger RT5880
L_S	16.5	Length of Roger RT5880
W_P	9.9	Width of copper patch
L_P	9.7	Length of copper patch
W_f	0.7	Width of feeder
L_f	4.75	Length of feeder
W_1	0.5	Width of slot 1
L_1	5.3	Length of slot 1
W_2	1.5	Width of slot 2
L_2	0.5	Length of slot 2
Y_o	2.4	Length of gap inside patch

This antenna operated at three different frequencies: 10 GHz, 28 GHz, and 38 GHz, with bandwidths of 343 MHz, 761 MHz, and 1.5 GHz, respectively [31]. Furthermore, a reference antenna has a return loss of -25.8 dB at 10GHz, -25.9 dB at 28 GHz, and -23.9 dB at 38 GHz, as illustrated in Figure 3.2 [31]. This small printed antenna has a radiation efficiency of more than 70% and gains of more than 5 dB for all necessary frequencies [31]. The only difference between CST and HFSS results is in the bandwidth and reflection coefficient at 38 GHz, which is due to the different environments of each software.

This guide antenna is regarded as the best reference for modifying it, such as changing its size and slot shapes and improving its parameters to make it run in Dual-band rather than Tri-band.

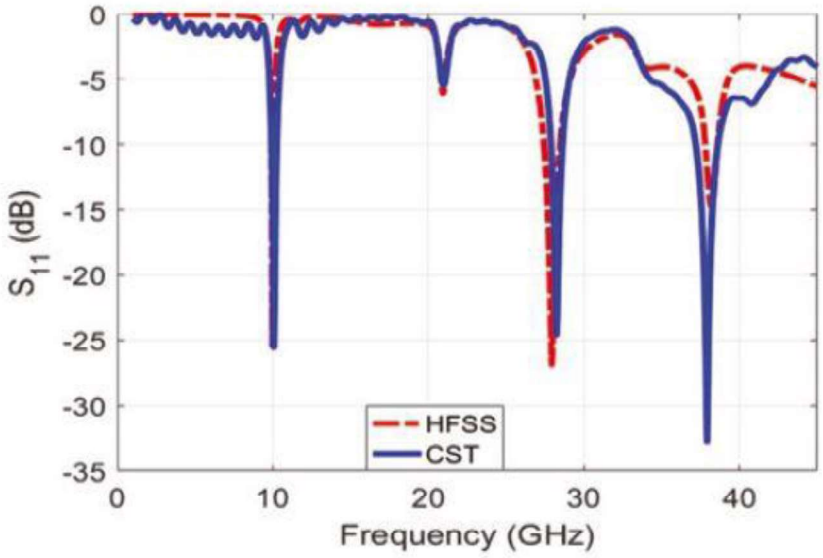

Figure 3.2 Displays the reflection coefficients of a reference antenna for each resonance frequency [31]

Some changes must be made to a reference printed antenna to reduce antenna dimensions and make it suitable for multi-band potential 5G applications. The following sections explain the three built antennas, their modifications, and their effect on antenna parameters and improvement suit for the applications needed.

3.3 First Proposed of Multi-Band Compact Antenna Design

This section proposes a dual-band microstrip patch antenna with slots in the form of a rectangle ring and two slots in the center of it, this inset feed microstrip antenna worked at 10 GHz and 30 GHz after minimized reference antenna sized. Also, this radiated element will be suitable for 5G future wireless and devices and operated at Satellite and Microwave systems.

3.3.1 Antenna Size Modification

Firstly, a copper patch of a reference antenna was taken, and its T-inverted slots were removed to make it act as a conventional printed antenna, and then modifications were

made to its standard dimensions $W_p \times L_p$ mm^2 while keeping all other values constant. Figure 3.3 shows the return losses of changeable patch dimensions in (mm).

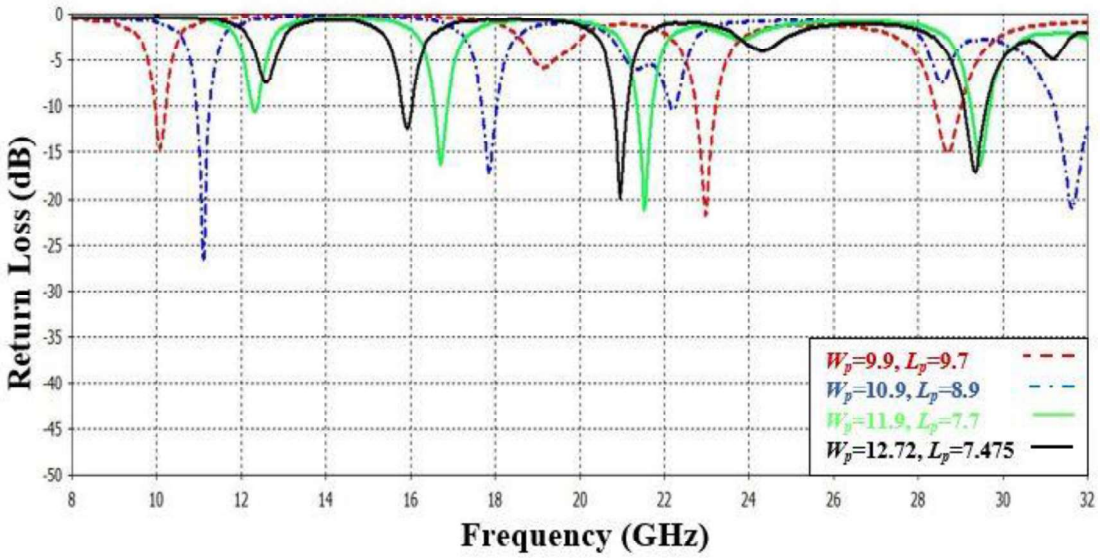

Figure 3.3 Depicts the return losses values due to the change in the patch antenna dimensions

Increasing the patch width W_p and decreasing the length L_p affected on shifting frequencies towards the highest, with unwanted bands emerging between 12 GHz and 24 GHz, and these changes in dimensions of radiated element resulted in low impedance matching between the patch and line feeding Furthermore, none of the other parameters had sufficient values to make the antenna function without getting the required results efficiently.

Some antenna parameters, such as efficiency, bandwidth, and desired frequency, are influenced by ground plane dimensions. In addition, the width of the feed line and the dimensions of the ground plane influence the amount of power supplied to the radiated element for matching.

Following a general patch size adjustment to W_p= 12.72 mm and L_p =7.475 mm, the width of the feed line W_f was increased to 1.52 mm while its length L_f was decreased to 1.24 mm for impedance matching, as well as several changes to the size of the ground plane while retaining the area covering patch from bottom as shown in figure 3.4.

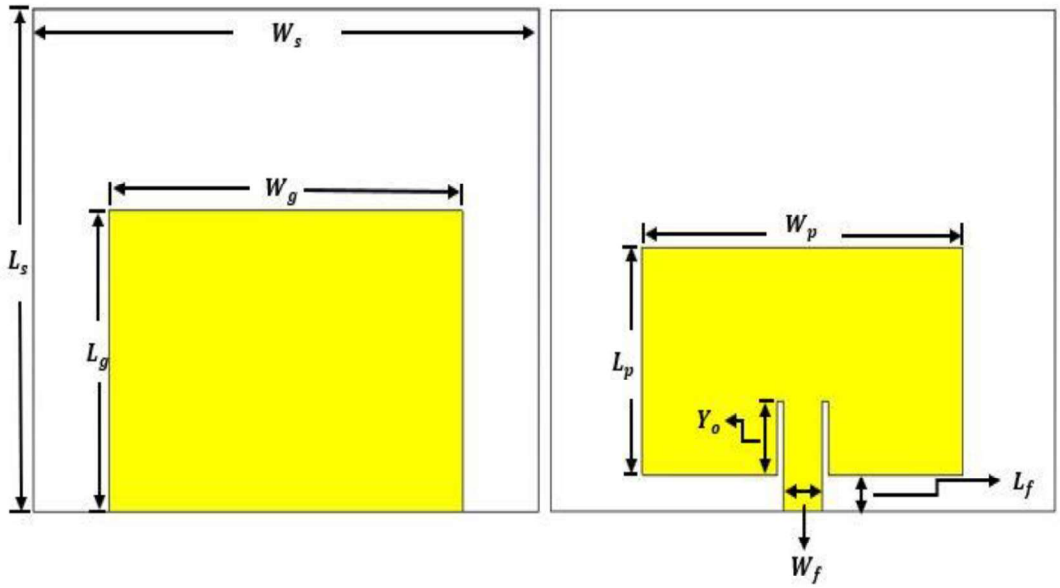

Figure 3.4 Depicts modifications of ground plane and patch dimensions without change substrate

After reducing the ground plane size to W_g= 14 mm and L_g= 9.9 mm, the radiation efficiency increased from 61 percent to 65 percent at 10 GHz, and some unnecessary frequencies were removed, leaving one frequency at 21.55 GHz, as shown in figure 3.5.

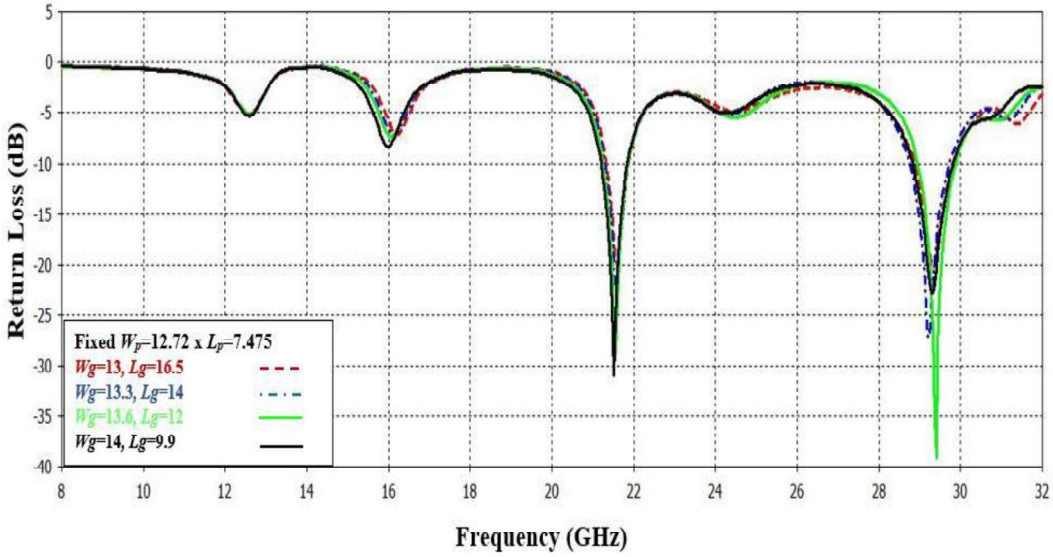

Figure 3.5 Illustrates the effect of changing ground plane dimensions on return losses values

Because of the low losses in the surface wave of the patch antenna, the modification on the ground plane resulted in increased radiation efficiency, allowing electrical fields

to disperse more readily in free space as shown in figure 3.4, the dimensions of the substrate appear to be very high compared to the reduced size of the ground plane and patch antenna.

As a result, the substrate dimensions of the Roger RT 5880 must be minimized in order to obtain a suitable size. The dielectric dimensions were modified as follows: the width W_s was reduced from 20 mm to 15 mm, and the length $L_s$was reduced from 16.5 mm to 11.5 mm.

Despite the changes in substrate size, the values of reflection coefficients and other parameters remain unchanged. The difference between the reference antenna measurements and the antenna after adjustment is shown in table 3.2.

Table 3.2 The comparison between values of first modified and a reference antenna

Parameter	Reference Antenna Value (mm)	Modified Antenna Value (mm)	Description
W_g	13	14	Width of ground plate
L_g	16.5	9.9	Length of ground plate
W_S	20	15	Width of Roger RT5880 substrate
L_S	16.5	11.5	Length of Roger RT5880 substrate
W_P	9.9	12.72	Width of copper patch
L_P	9.7	7.475	Length of copper patch
W_f	0.7	1.52	Width of feeder
L_f	4.75	1.24	Length of feeder
W_1	0.5	Removed	Width of slot 1
L_1	5.3	Removed	Length of slot 1
W_2	1.5	Removed	Width of slot 2
L_2	0.5	Removed	Length of slot 2
Y_o	2.4	2.4	Length of gap inside patch

3.3.2 Inserting Slots within Patch Element

Because of the benefits of etching slots in conductor patches, these slots enable patch antennas to operate at several frequencies or more, and it creates two distinct pathways for radio frequency signals to generate new high or low desired frequencies. In addition, slots were added to the patch antenna to address input impedance, reflection coefficient issues, and increased bandwidth.

After modification total size of antenna, as described in the previous section. Slots in the shape of a complete rectangle and two slots in the middle of it have been added to the patch to produce the appropriate dual-band frequency at 10 GHz and 30 GHz.

The inserting slots and deciding their proper position went through several stages before arriving at the final measurements. The shape of slots and its dimensions for first proposed design have illustrated in figure 3.6.

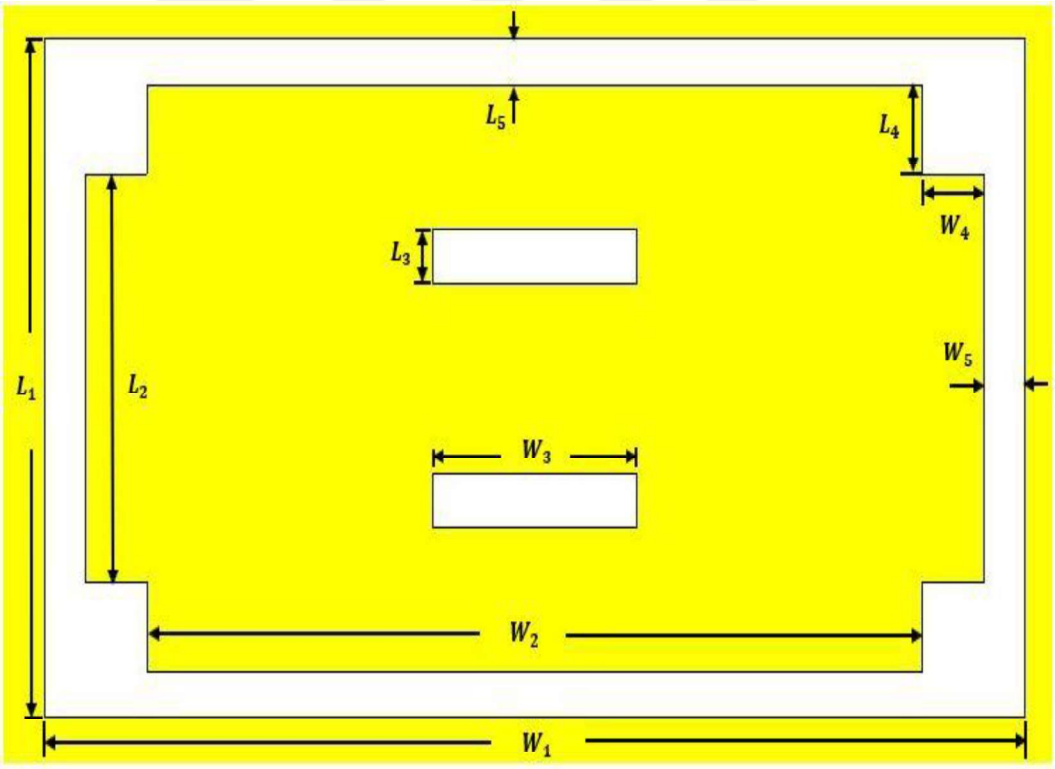

Figure 3.6 Illustrates final dimensions of slots for first proposed design to generate dual-band resonance frequency

This primary slot comprises a rectangle ring separated with small squares in the corners and two small rectangles in the center, as shown in figure 3.6. The object of etching slots within a patch antenna is to establish a dual-band desired frequency.

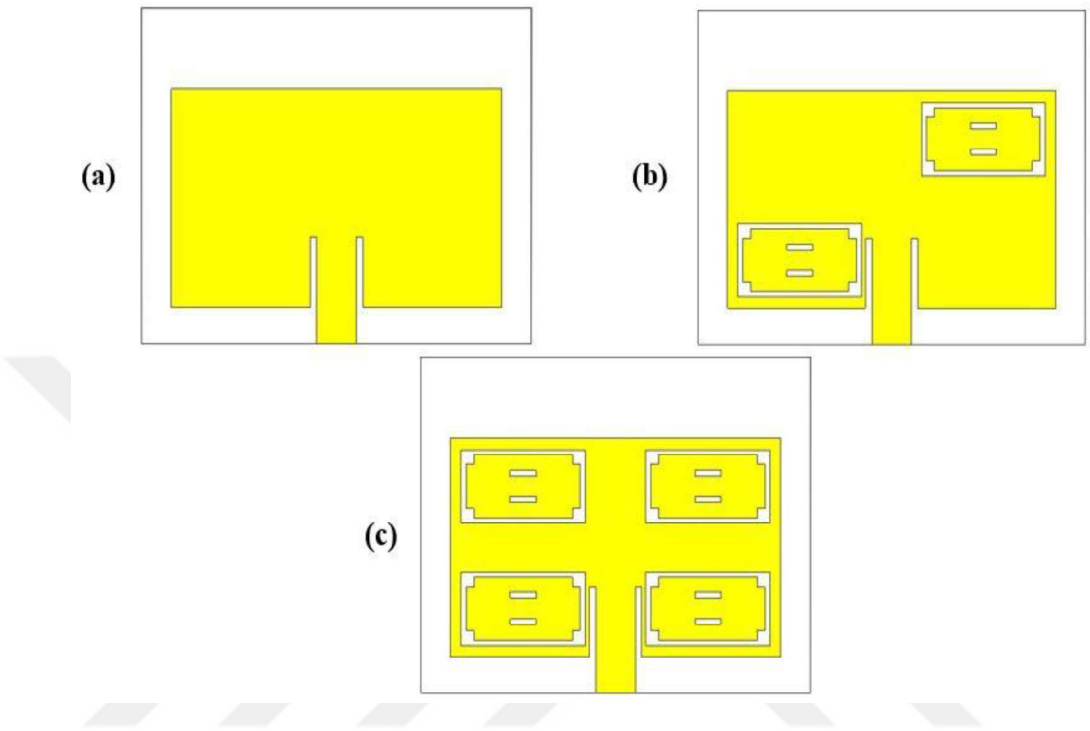

Figure 3.7 Depicts the advancement steps of dual-band proposed first design

After modifying a reference antenna and reducing its size as much as possible, the final traditional version without slots is depicted in figure (3.7(a)). This traditional antenna does not meet the specifications needed to work at future 5G devices because it lacks sufficient gain, has a high VSWR, and has less than 65 percent efficiency. Furthermore, unwanted frequencies have appeared at 21.55 GHz and another at 29.25 GHz that need to shift up, and the first resonance frequency is not appearing.

Slots have been inserted to cancel unwanted frequencies, obtain resonance frequencies, and improve other parameters, as shown in figure 3.6, and positioned diagonally in the upper right and lower left edges of the conductor patch as shown in figure (3.7(b)).

However, at 20.51 GHz, an unwanted frequency reappeared, and other frequencies needed to be shifted down or up at 10.45 GHz and 27.79 GHz, respectively.

The final addition was depicted by positioning the slots near each edge of the radiated portion, as shown in figure (3.7(c)). To clarify what was mentioned previously, figure 3.8 describes return losses for each stage, as seen in figure 3.7.

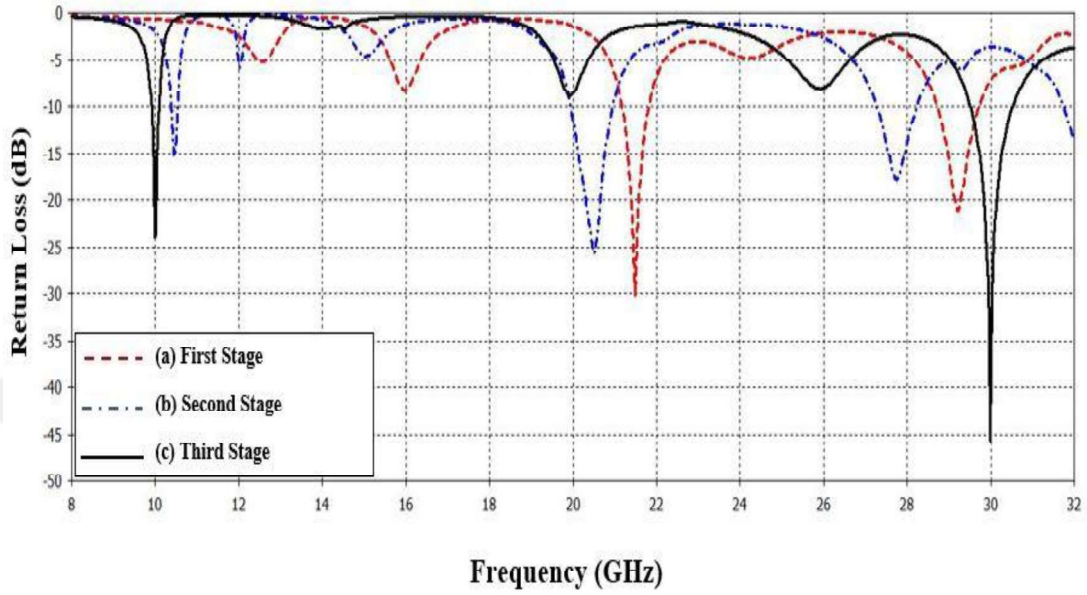

Figure 3.8 Depicts reflection coefficients for each stage of first proposed antenna

The first proposed dual-band microstrip antenna's final design was derived from a reference antenna. This proposed patch's size has been reduced, and various slots shapes have been inscribed inside it. The dimensions of the final design for the first proposed patch antenna are depicted in figure 3.9.

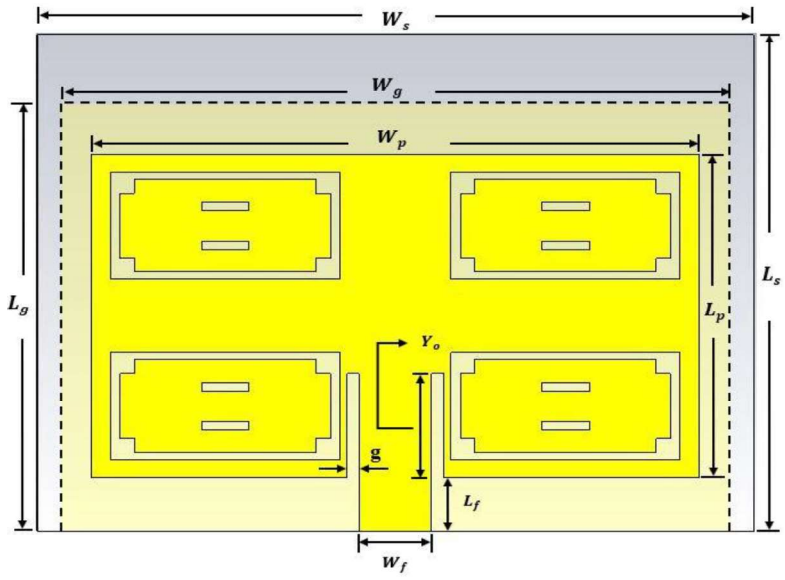

Figure 3.9 Shows final measurements of first proposed multi-band compact patch antenna

The first proposed multi-band microstrip antenna designed consist of copper plate modified after has been minimized that have measurements of 12.72×7.475×0.035 mm^3 placed on the substrate made of Roger RT-5880 Duroid with dimensions of 15 × 11.5×0.508 mm^3 used for high frequencies applications because it has a low value of dielectric constant with 2.2. Substrate material and conductor patch have been printed on the partial copper ground with 14×9.9×0.035 mm^3. Total new slots have been placed near the patch's edges to produce microstrip antenna work at X and Ka-band. Table 3.3 describes the overall measurements of the first dual-band microstrip patch antenna.

Table 3.3 Depicts final dimensions of first multi-band microstrip patch antenna

Parameter	Value (mm)	Description
W_g	14	Width of copper ground plate
L_g	9.9	Length of copper ground plate
W_s	15	Width of Roger RT5880 substrate
L_s	11.5	Length of Roger RT5880 substrate
W_p	12.72	Width of copper patch
L_p	7.475	Length of copper patch
h	0.508	Thickness of substrate
t	0.035	Thickness of copper
W_1	4.8	Width of 1st slot
L_1	2.5	Length of 1st slot
W_2	3.8	Width of 2nd slot
L_2	1.5	Length of 2nd slot
W_3	1	Width of 3rd slot
L_3	0.2	Length of 3rd slot
W_4	0.3	Width of 4th slot
L_4	0.33	Length of 4th slot
W_5	0.2	Width of 5th slot
L_5	0.17	Length of 5th slot
W_f	1.52	Width of microstrip feed line
L_f	1.24	Length of microstrip feed line
Y_o	2.4	Length of gap inside patch
g	0.253	Width of gap inside patch

The first proposed patch antenna was simulated on the CST software version of 2018. Return losses have been measured for each desired frequency less than -10 dB to ensure that the most significant amount of power is transferred in free space with limited power reflected in the source. As shown in figure 3.10, the return loss value of -23.82 dB with a bandwidth of 176.7 MHz and -43.3 dB with a bandwidth of 1.015 GHz at 10 GHz and 30 GHz, respectively. These reflection coefficients with their bandwidths at each resonance frequency consider relevant results for future 5G devices.

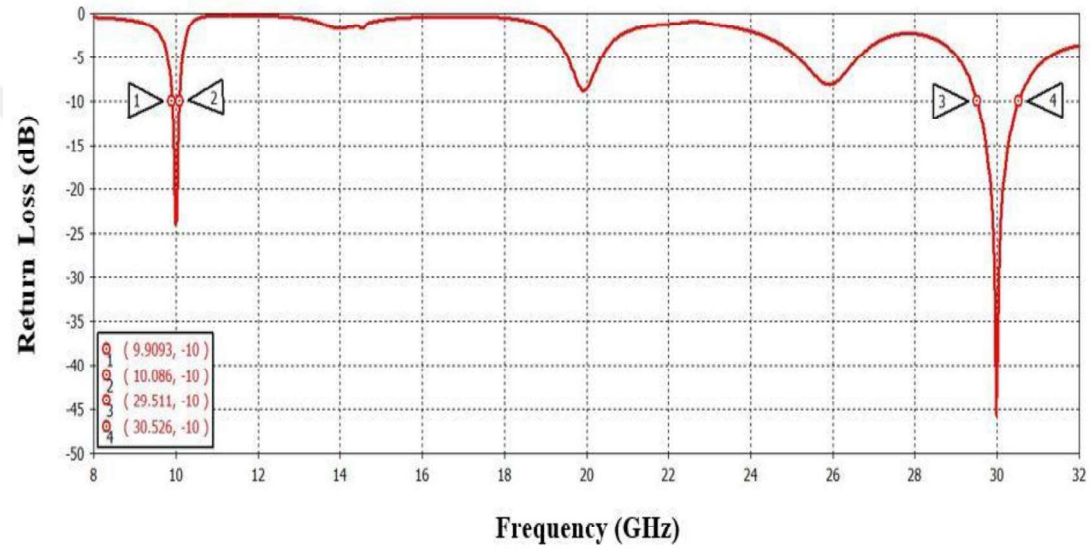

Figure 3.10 Depicts return losses and bandwidth of first proposed microstrip patch antenna

The antenna, which has 100 percent efficiency, means that the total power supplied by the source to the antenna will send all by it without losses. In practical life, there is no perfect antenna. An antenna with an efficiency ranging from (50 to 60) percent is considered a well-functioning antenna.

As shown in figure 3.11, the first proposed microstrip antenna has an adequate and suitable radiation efficiency at each desired frequency of about 72.7 percent and 82.8 percent at 10 GHz and 30 GHz, respectively. Furthermore, the radiation efficiency for each bandwidth at each center frequency is greater than 71 percent at 10 GHz and greater than 82 percent at 30 GHz.

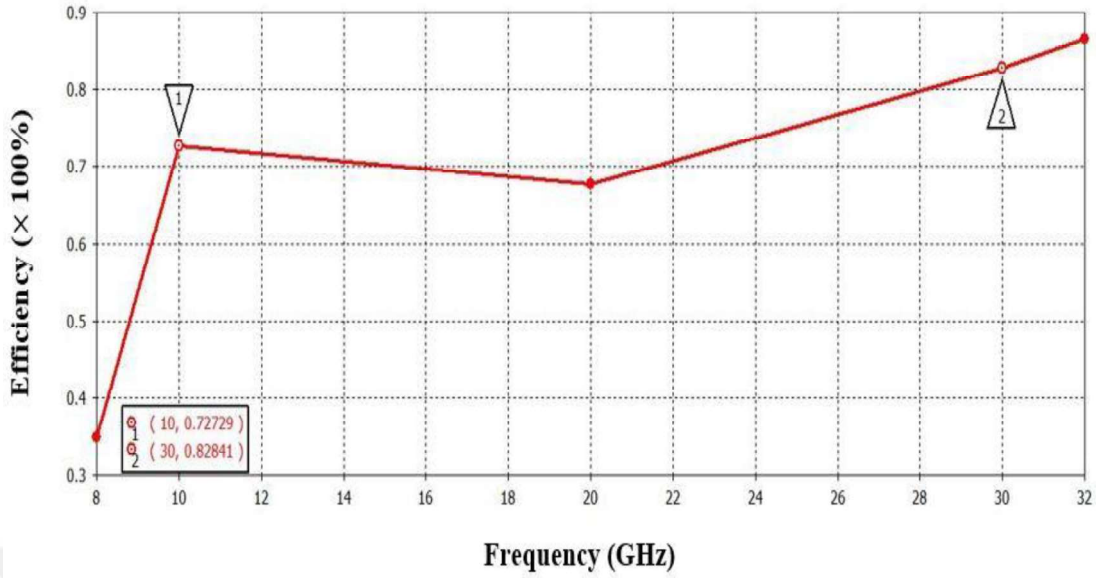

Figure 3.11 Illustrates radiation efficiency of first proposed microstrip patch antenna

In Super High-Frequency bands must be a high gain antenna used. This proposed antenna has achieved a gain of 4.85 dB at 10 GHz and a gain of 8.86 dB at 30 GHz. The high gain antenna refers to be more directional and makes it run more efficiently in receiving mode because of less received noise. These results have been registered as a suitable value for use in future 5G wireless systems. Figure 3.12 illustrates the positive gain at each resonance frequency required.

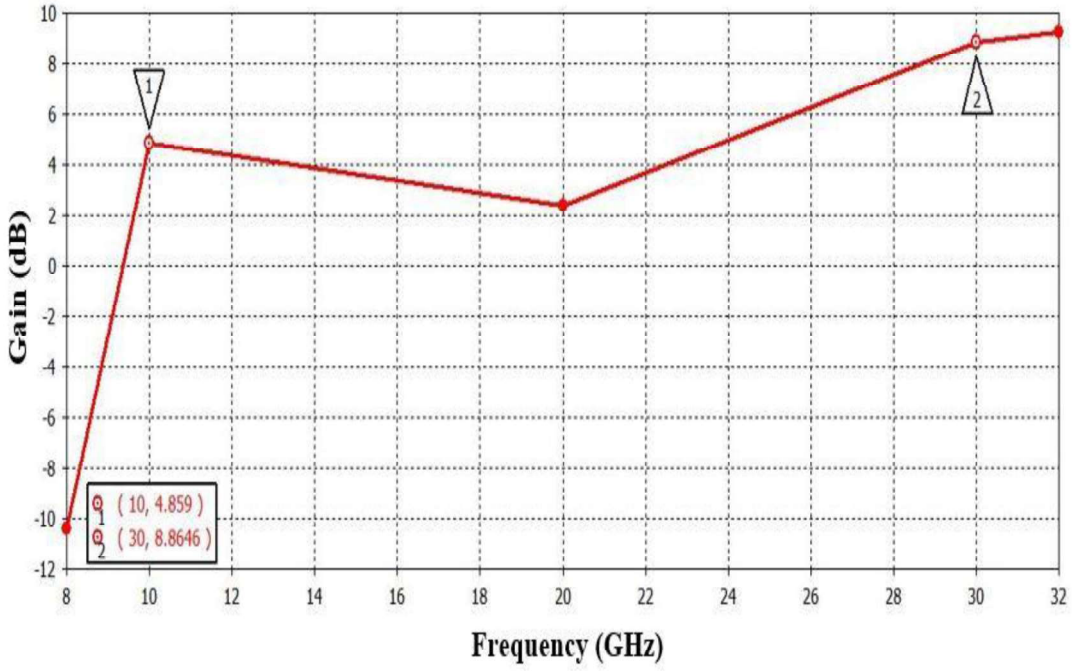

Figure 3.12 Shows gain results of first proposed microstrip patch antenna

Figure 3.13(a) shows the radiation pattern at 10 GHz in the E-plane (phi=0º), with the magnitude and orientation of the main lobe being 6.22 dBi and 0º, respectively, and the angular beamwidth (3 dB) being 87.6º.

Furthermore, figure 3.13(b) at 10 GHz in H-plane (phi=90º) discovered that the magnitude and orientation of the main lobe were 6.26 dBi and 5º, respectively, angular beamwidth (3 dB) being 95º.

The radiation pattern in figure 3.13(c) at 30 GHz, in E-plane (phi=0º), found that the magnitude and direction of the main lobe are 9.68 dBi and 0º, respectively as well as the angular beamwidth (3 dB) is 39.5º.

Besides that, figure 3.13(d) at 30 GHz also, in H-plane (phi=90º), found that the magnitude and direction of the main lobe are 9.68 dBi and 0º, respectively as well as the angular beamwidth (3 dB) is 93.7º.

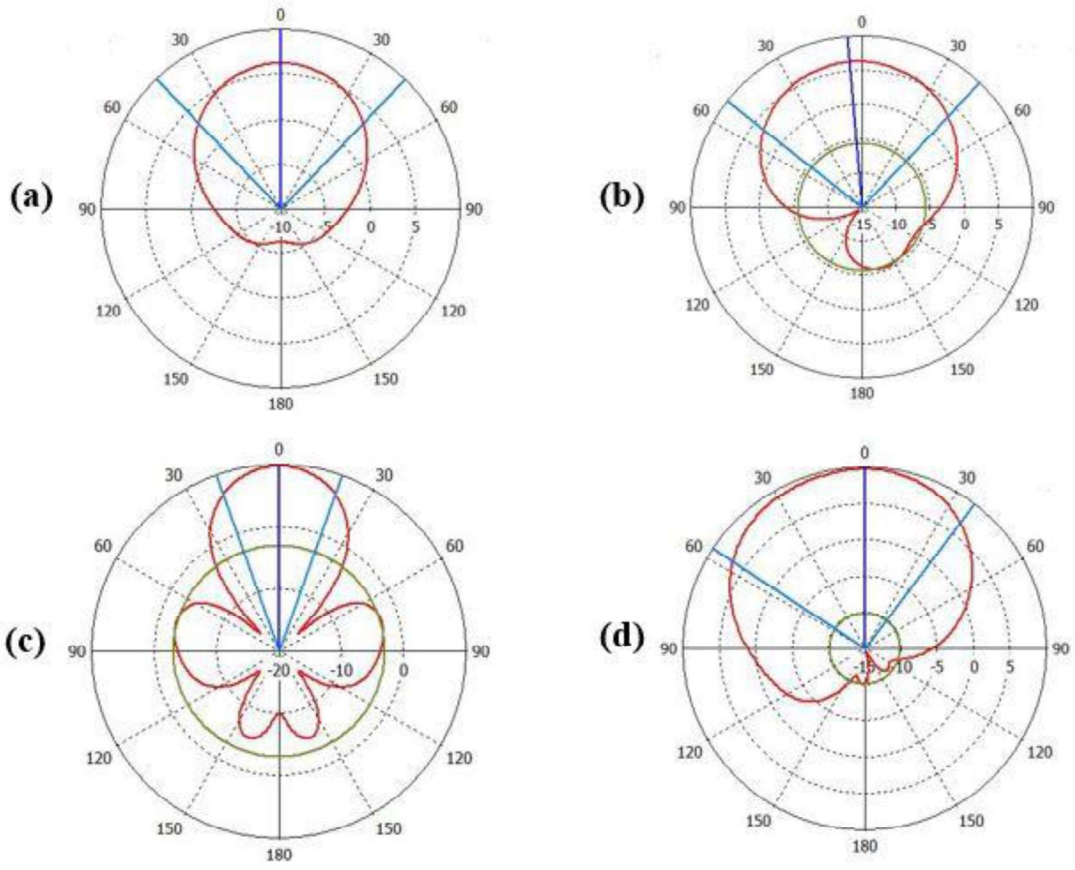

Figure 3.13 Depicts 2D-radiation pattern of first proposed multi-band microstrip antenna for (a-b) at 10 GHz and (c-d) at 30 GHz

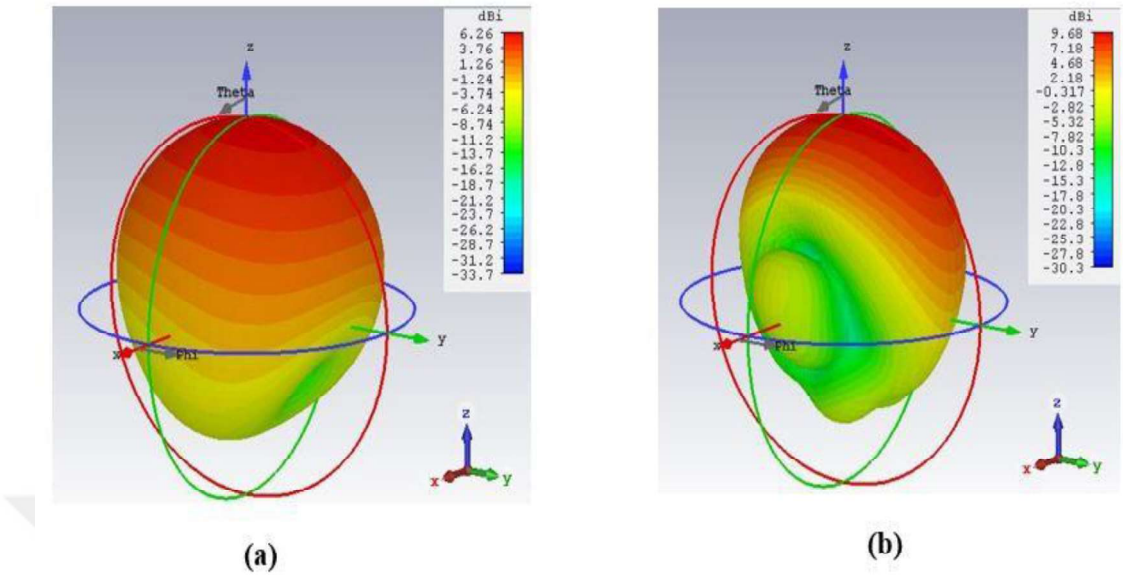

Figure 3.14 Illustrated 3D radiation pattern at (a) 10 GHz and at (b) 30 GHz

The three-dimensional far-field radiation pattern of directivity describes in figure (3.14) for the first proposed dual-band microstrip patch antenna. The directivity value of the first resonance frequency is 6.26 dBi at 10 GHz, as shown in figure 3.14(a), and the second resonance frequency is 9.68 dBi at 30 GHz, as shown in figure 3.14(b). The radiation emits in direction of the Z-axis, which means this antenna has directional radiation.

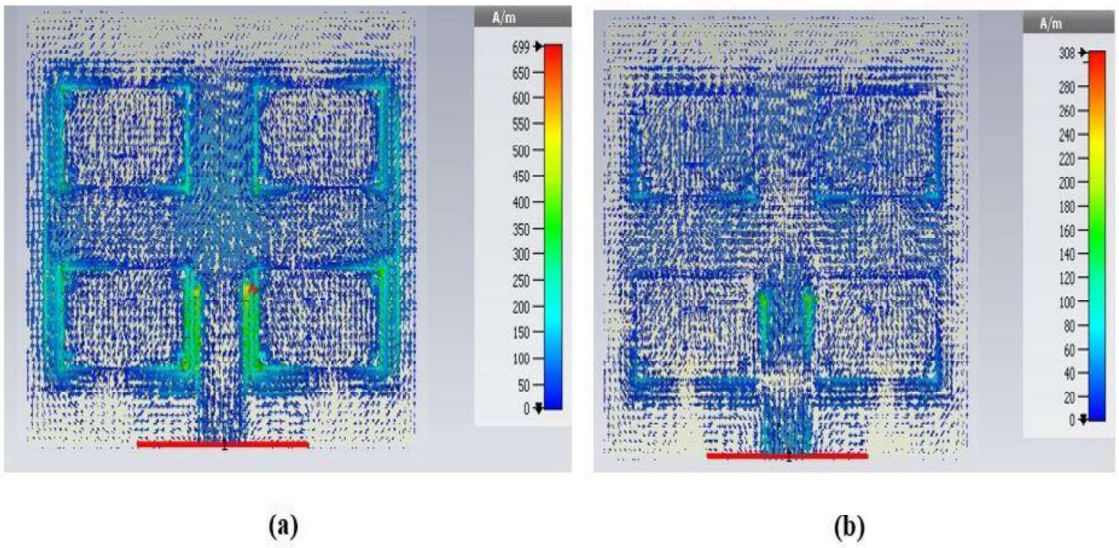

Figure 3.15 Demonstrates current distributions of dual-band first proposed microstrip patch antenna for each resonance frequency at (a) 10 GHz and (b) 30 GHz

Figure 3.15 shows the electrical current behavior on the surface of the compact patch antenna at each wanted frequency. The current at first resonance frequency 10 GHz will be increased at the fringes of rectangle ring slots, and that led to an increase in the electrical length as shown in figure 3.15(a), while the less quantity of current at the second resonance frequency of 30 GHz as shown in figure 3.15(b).

3.4 Second Proposed of Multi-Band Compact Antenna Design

This section would present the second proposal for developing a multiband microstrip patch antenna. This antenna comprises of a conductor copper patch with T-shaped slots horizontally and two slots in the form of a small rectangle, one below its base and the other on one of its sides.

Furthermore, this radiated element has been designed to operate at 10 GHz and 30 GHz after modified reference antenna size to be appropriate for future 5G wireless communication.

3.4.1 Antenna Size Modification

Size reduction is considered a critical method for patch antenna miniaturization and makes it work at different frequencies bands. At first, the patch of a reference antenna must be taken and adjusted in size, and all of its slots deleted to create a traditional patch antenna. Finally, the first change will be to the dimensions $W_p \times L_p$ mm^2 of a reference patch, while all other measurements remain unchanged. The simulation of the modified patch antenna showed different values in return losses near to resonance frequencies of 10 GHz and 30 GHz that need to be shifted up and down. Also, the undesired frequencies have appeared in the curve center between 16.8 GHz and 23.1 GHz that require removal to achieve the necessary results for this second proposed design. After modifying a reference patch antenna, it was discovered that all of the parameters, such as insufficient gain and directivity with high VSWR, and input impedance for matching between the radiated element and the microstrip feeder, were extremely poor. Figure 3.16 shows the different return loss values for all steps of the patch-modified antenna in (mm).

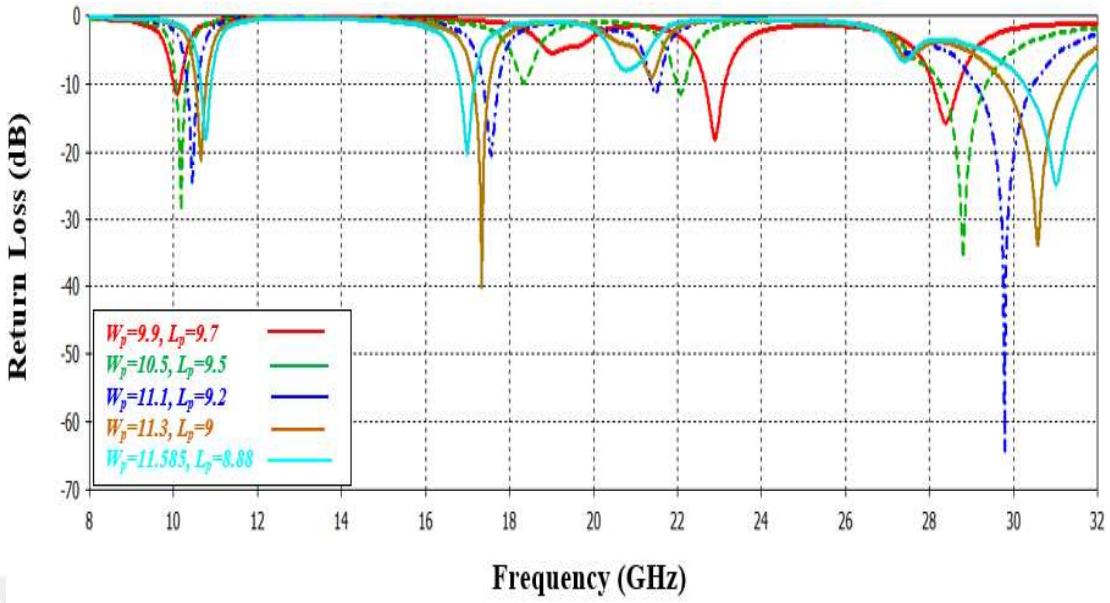

Figure 3.16 Illustrates different results for all steps of modified patch antenna

The measurements of Roger RT-5880 have low permittivity with copper ground plate must be changed after the size of a reference patch antenna is reduced. These materials will be the same size, and a complete ground plate will be used to cover the entire patch from the bottom to increase the gain for each resonance frequency. Figure 3.17 will depict all values of return losses for each step of substrate and ground modification with constant 11.585×8.88 mm2 dimensions of the patch.

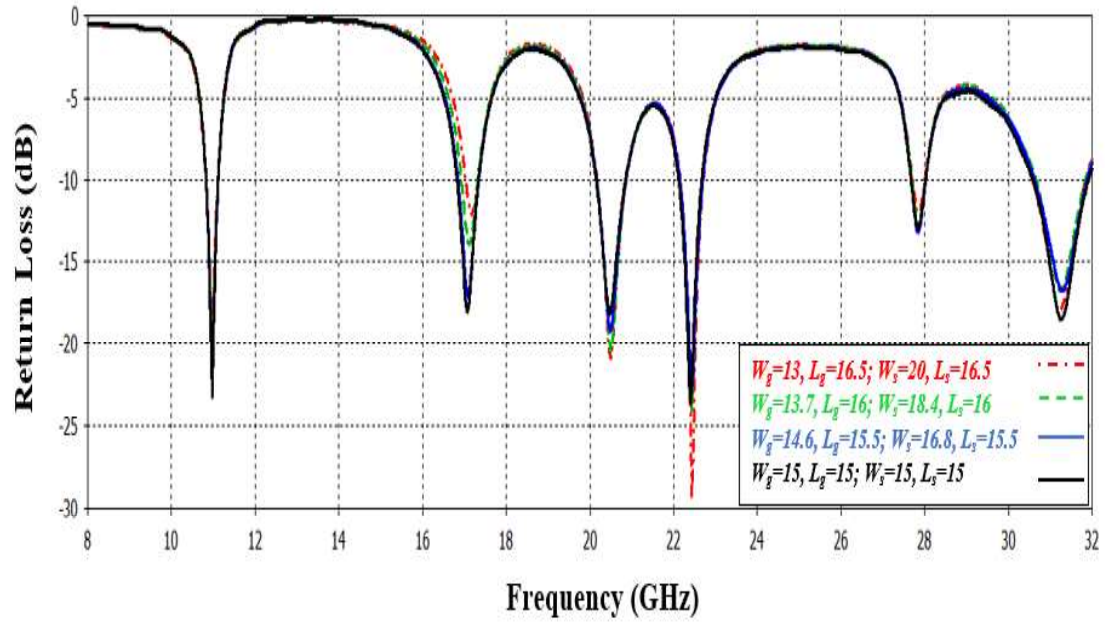

Figure 3.17 Shows return loss values after modified of ground plate and substrate Roger RT-5880

The dielectric material and conductor ground plate were modified in four stages, beginning with increasing the length W_g to 15 mm and decreasing other lengths such as L_g, L_s, and W_s to 15 mm, so their dimensions were equal.

In addition, the feed line sizes for W_f and L_f have been modified to 1.52 mm and 3.06 mm, respectively, to ensure optimum power transmission from the microstrip line feeder to the patch. Figure 3.17 shows the final updated overall antenna measurements without slots, revealing that some unwanted frequencies existed at 17.09 GHz, 20.45 GHz, 22.42 GHz, and 27.81 GHz, with different return losses in each band.

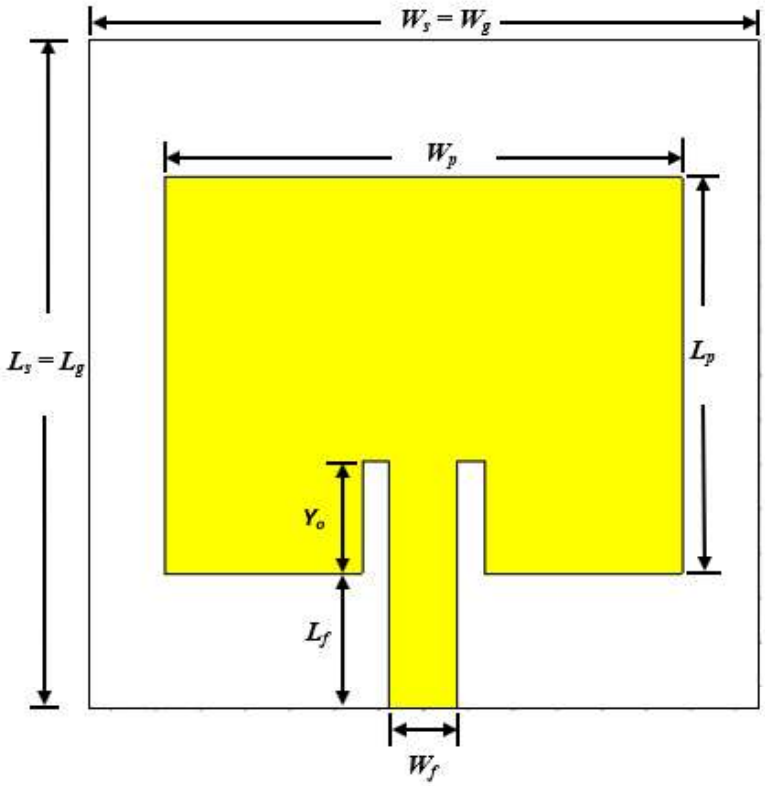

Figure 3.18 Describes the final dimensions of a reference antenna modified without slots

The previously described changes only had an impact on the values of reflection coefficients in the final results. Figure 3.18 illustrated the dimensions modified of patch and substrate with the ground plate to make antenna radiation more direction and thus raise the gain at each band.

The contrast between the measurements modified in the second proposed antenna and a reference antenna with removed its initial slots have been illustrated in table 3.4.

Table 3.4 The comparison between values of second modified and a reference antenna

Parameter	Reference Antenna Value (mm)	Modified Antenna Value (mm)	Description
W_g	13	15	Width of ground plate
L_g	16.5	15	Length of ground plate
W_S	20	15	Width of Roger RT5880 substrate
L_S	16.5	15	Length of Roger RT5880 substrate
W_P	9.9	11.585	Width of copper patch
L_P	9.7	8.88	Length of copper patch
W_f	0.7	1.52	Width of feeder
L_f	4.75	3.06	Length of feeder
W_1	0.5	Removed	Width of slot 1
L_1	5.3	Removed	Length of slot 1
W_2	1.5	Removed	Width of slot 2
L_2	0.5	Removed	Length of slot 2
Y_o	2.4	2.5	Length of gap inside patch

3.4.2 Inserting Slots within Patch Element

To generate dual-band frequency in the modified compact antenna working at 10 GHz and 30 GHz. In the second proposed antenna, different slots have been inscribed with T-shaped slots horizontally, and two slots in the form of a small rectangle, one below its base and the other on one of its sides etched in the radiated element. These slots will lead to an increase in the electrical current path within the patch.

Until arriving at the final dimensions, the process of adding slots and determining their proper location went through several steps. The measurements of slots for the proposed second design have demonstrated in figure 3.19.

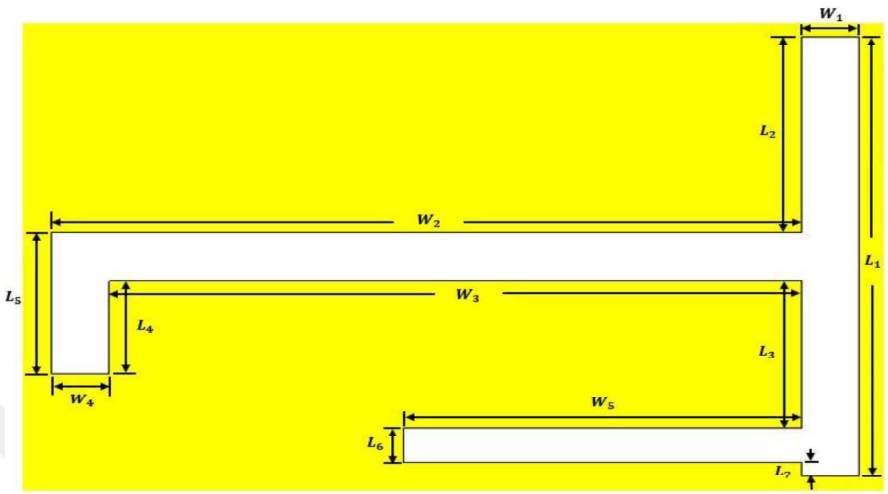

Figure 3.19 Illustrates final dimensions of slots for second proposed design to generate dual-band resonance frequency

The slot consists of two rectangles that form as a shape of T positioned horizontally and other small rectangles, one located below the base and another located near the edge of one of T slot's sides, as shown in figure 3.19. The primary purpose of making slots into the conductor patch is to create a multi-band resonance frequency for upcoming 5G devices.

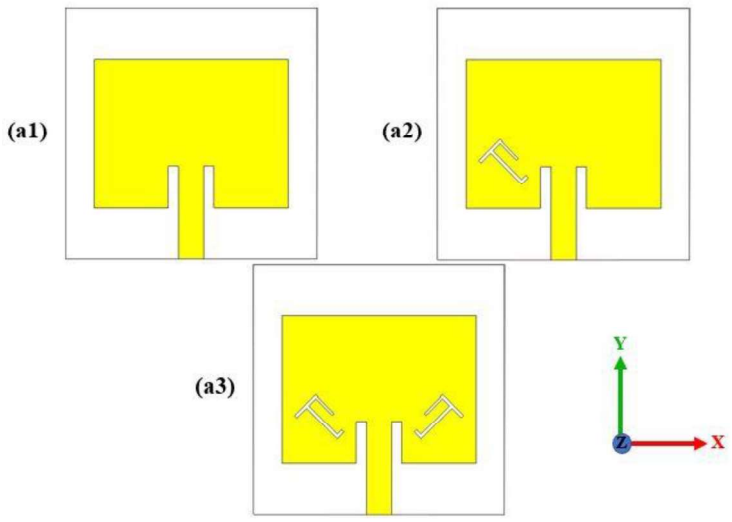

Figure 3.20(a) Shows first three-stages of dual-band second proposed design

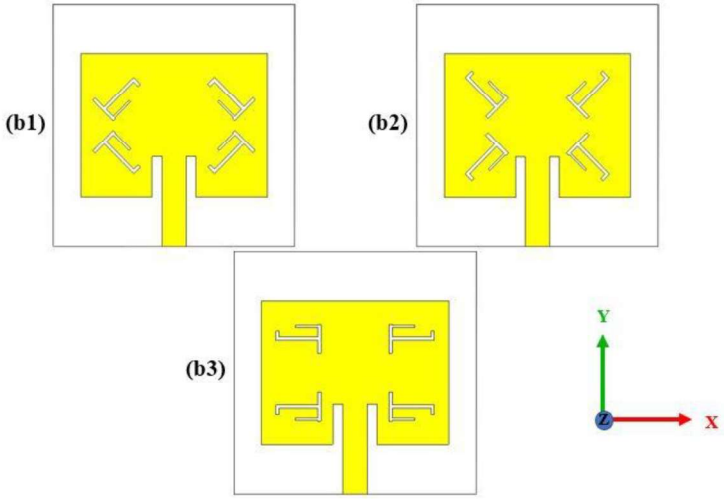

Figure 3.20(b) Shows final three-stages of dual-band second proposed design

Figure 3.20(a1) shows a main microstrip compact antenna that has been reduced in size to the smallest possible size from a reference antenna. This traditional antenna is deemed unsatisfactory and does not satisfy the ambitions needed to build a 5G antenna, such as low input impedance, gain, poor radiation efficiency, and undesired frequencies band, emerged between 17.09 GHz and 27.81 GHz.

For this reason, slot as a figure 3.19 has been placed in the left-bottom of the patch corner with 135 degrees relative to X-axis to remove unwanted bands and generate resonance frequencies required, as shown in figure 3.20(a2).

However, these undesired bands continue to appear in inconvenient locations with high reflection coefficient values. Even though the slot in figure 3.19 has been placed symmetrically around the inset feed line, as shown in figure 3.20(a3), nothing has improved except that appearing band near 10 GHz with high return loss.

These slots were placed next to each one of the patch's edges as shown in figure 3.20(b1), the first resonance frequency and the second one appeared near to 10.19 GHz and 26.4 GHz, respectively that need to move up and down as well as high VSWR values appeared at each band required.

Before the latter stage, the slots at each edge have been rotated with 45 degrees relative to the X-axis to improve the gain and radiation efficiency and place the frequencies

required in their suitable locations, as seen in figure 3.20(b2). However, most ripples were removed except at 18.67 GHz, 25.6 GHz, and 26.98 GHz.

As depicted in figure 3.20(b3), the final stage fixed all problems related to low gain, efficiency, directivity, and appearing undesired frequencies and generated a multi-band microstrip antenna at necessary bands.

Figures 3.20 (a and b) show all stages of transformation of the modified reference antenna and make it work as a multi-band patch antenna for future 5G devices.

To further explain what was previously said, figure 3.21 depicts the return losses at each stage as depicted in Figure 3.20(a, and b). The position, shapes and numbers of slots affected on return losses values as well as on impedance matching values.

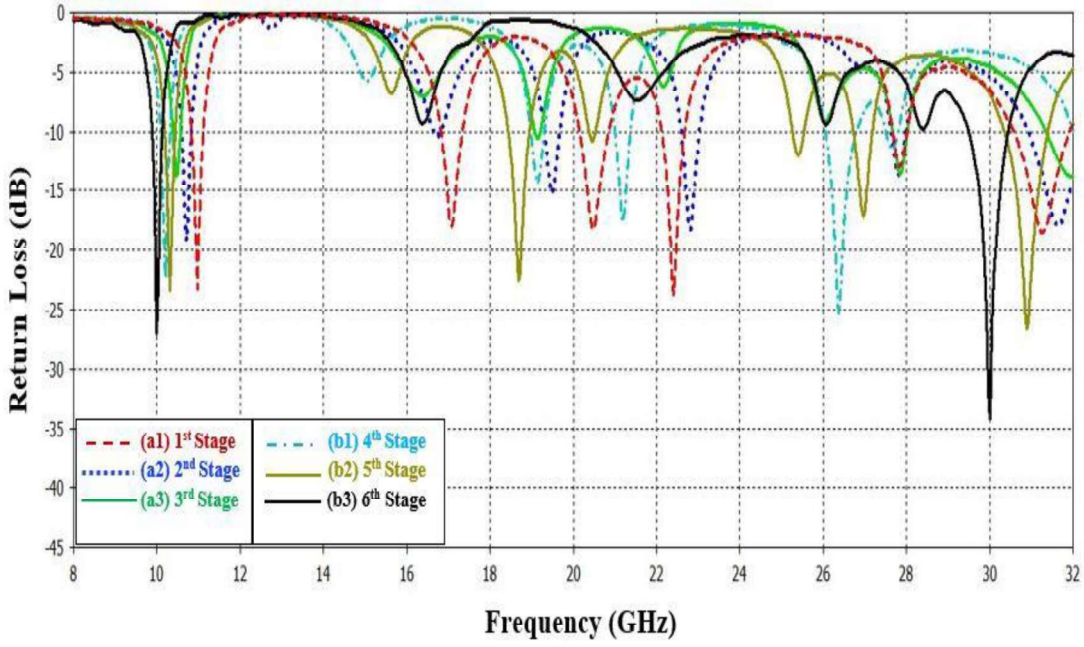

Figure 3.21 Describes reflection coefficients for each stage of second proposed antenna

The second proposed dual-band microstrip patch antenna's final design was obtained after modifying the overall structure of a reference antenna, and then slots were placed next to each corner of the patch. The measurements of the final design of the second proposed patch antenna are illustrated in figure 3.22.

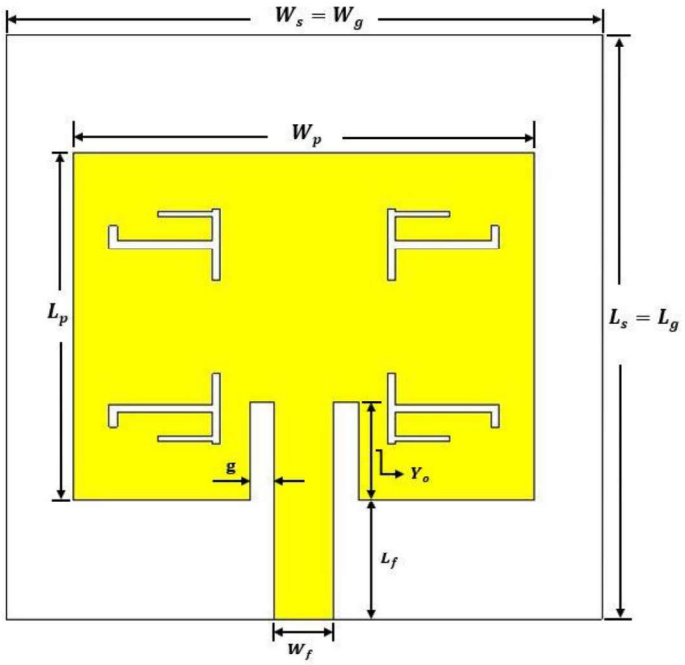

Figure 3.22 Shows final dimensions of second proposed multi-band compact patch antenna

The second suggestion of a multi-band compact patch antenna comprises a conductor copper plane adapted from a reference antenna with dimensions of 11.585×8.88×0.035 mm^3 and connected with a microstrip inset feed line that has measurements for supplying patch with enough amount of power.

The substrate material with the low dielectric constant of 2.2 was used, fabricated from Roger RT5880 Duroid with 15×15×0.508 mm^3 measurements, to obtain multiple high bands, and it has positioned below the copper radiated element.

The whole plate of copper was placed into the bottom of the substrate with 15×15×0.035 mm^3 dimensions to cover most of the patch, and Roger RT5880 to get high gain values resulting in radiation having high directivity.

Finally, slots in the shape of T that positioned horizontally as well as other small rectangles, one located below the base and another also located near the edge of one of T slot's sides, distributed on every corner of the radiator, to create a microstrip patch antenna operates at X and Ka-band. Table 3.5 shows the whole measurements in (mm) of the second dual-band compact patch antenna.

Table 3.5 Depicts final dimensions of second multi-band microstrip patch antenna

Parameter	Value (mm)	Description
W_g	15	Width of copper ground plate
L_g	15	Length of copper ground plate
W_s	15	Width of Roger RT5880 substrate
L_s	15	Length of Roger RT5880 substrate
W_p	11.585	Width of copper patch
L_p	8.88	Length of copper patch
h	0.508	Thickness of substrate
t	0.035	Thickness of copper
W_1	0.2	Width of 1st slot
L_1	1.8	Length of 1st slot
W_2	2.6	Width of 2nd slot
L_2	0.8	Length of 2nd slot
W_3	2.4	Width of 3rd slot
L_3	0.6	Length of 3rd slot
W_4	0.2	Width of 4th slot
L_4	0.38	Length of 4th slot
W_5	1.38	Width of 5th slot
L_5	0.58	Length of 5th slot
L_6	0.14	Length of 6th slot
L_7	0.06	Length of 7th slot
W_f	1.52	Width of microstrip feed line
L_f	3.06	Length of microstrip feed line
Y_o	2.5	Length of gap inside patch
g	0.605	Width of gap inside patch

The second proposed antenna design was created and tested using the 2018 CST Studio Suite version. This microstrip patch antenna is operating in the SHF band at 10 GHz and 30 GHz.

Using reflection coefficient parameters to measure average supplied power sent from the antenna was compared to the sum of power returned to the source. Return loss value equals -26.04 dB with a bandwidth of 253 MHz and -33.35 dB with 948 MHz at 10 GHz and 30 GHz, respectively.

These results with their bandwidths at each resonance frequency have been illustrated in figure 3.23 and become suitable for future 5G wireless communication.

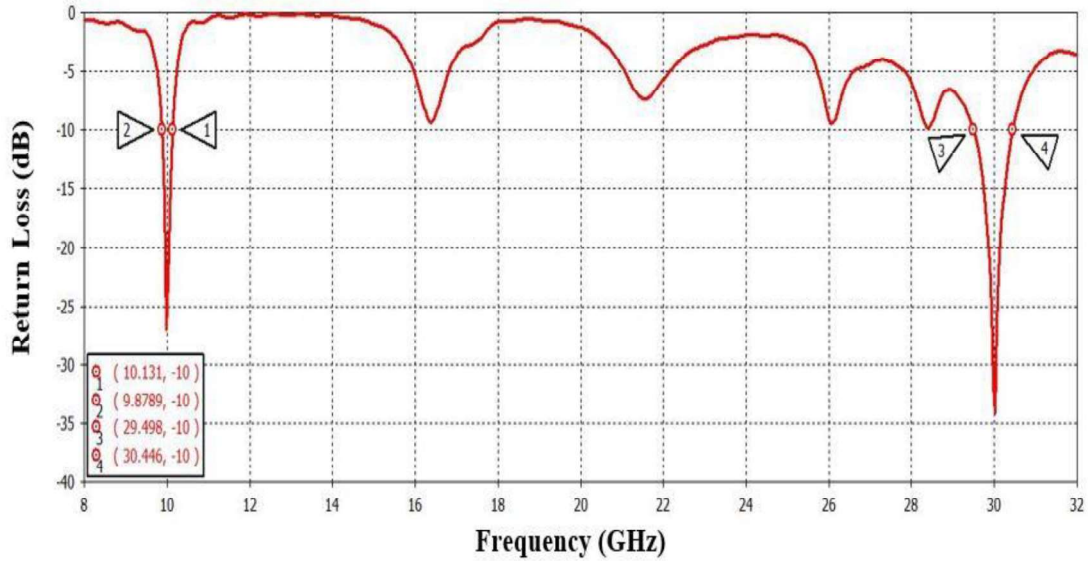

Figure 3.23 Shows return losses and bandwidth of second proposed compact patch antenna

The second suggested microstrip antenna has an appropriate and efficient radiation efficiency of around 79.96 percent and 82.94 percent at 10 GHz and 30 GHz, respectively, shown in figure 3.24. In addition, the radiation efficiency for each bandwidth at each center frequency is greater than 79.6 percent at 10 GHz and greater than 82.7 percent at 30 GHz.

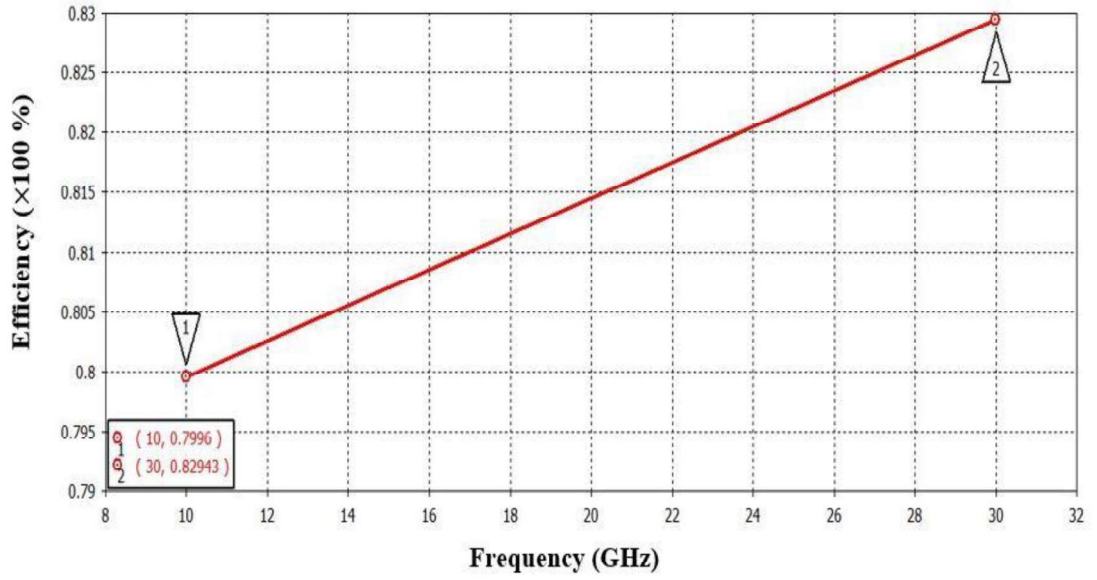

Figure 3.24 Illustrates radiation efficiency of second proposed microstrip patch antenna

At 10 GHz, this suggested antenna has a gain of 6.16 dB, and at 30 GHz, it gains 8.02 dB. Since there is less received noise, the high gain antenna is more directional and runs more effectively in receiving mode. These findings have been accepted as a valid value for prospective 5G systems. Figure 3.25 illustrates the positive value of gain at each desired frequency required.

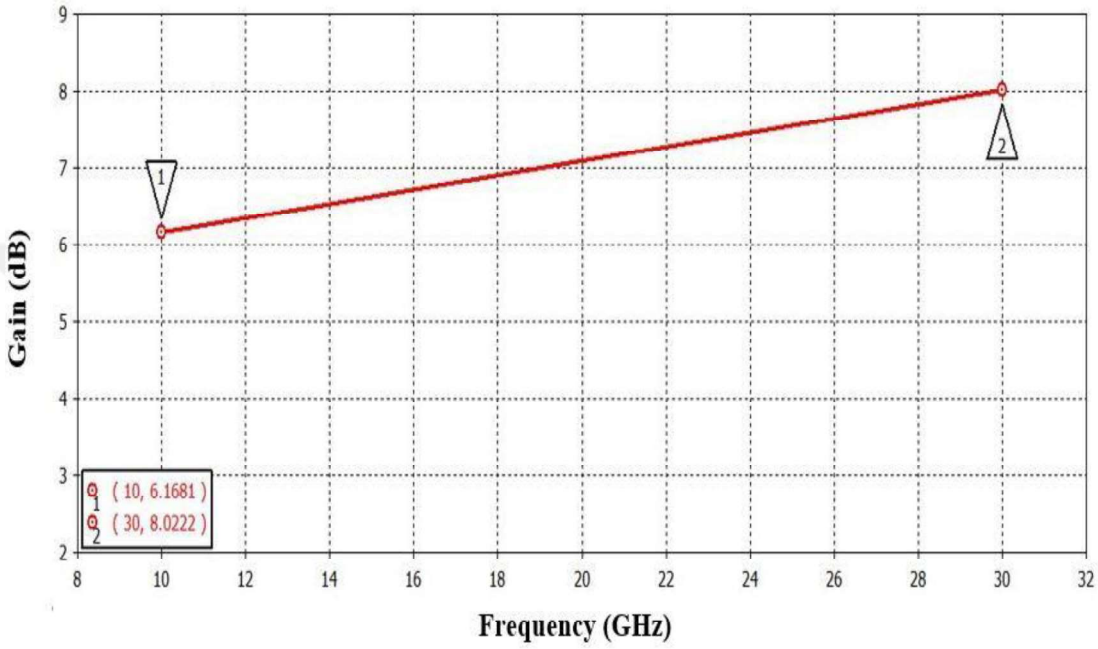

Figure 3.25 Shows gain results of second proposed microstrip patch antenna

The radiation pattern at 10 GHz in the E-plane (phi=0º) as seen in figure 3.26(a), with the main lobe magnitude and orientation of 7.14 dBi and 0º, respectively, and the angular beamwidth (3 dB) of 85.7º.

Furthermore, figure 3.26(b) revealed that the main lobe's magnitude and orientation were 7.14 dBi and 2º, respectively, at 10 GHz in H-plane (phi=90º), angular beamwidth (3 dB) being 84.6º.

Figure 3.26(c) shows the radiation pattern at 30 GHz in the E-plane (phi=0º), with the magnitude and orientation of the main lobe being 8.83 dBi and 0º, respectively, and the angular beamwidth (3 dB) being 32.3º.

In addition, figure 3.26(d) at 30 GHz found that the magnitude and orientation of the main lobe are 8.89 dBi and 2º, respectively, in H-plane (phi=90º) as well as the angular beamwidth (3 dB) is 25.7º.

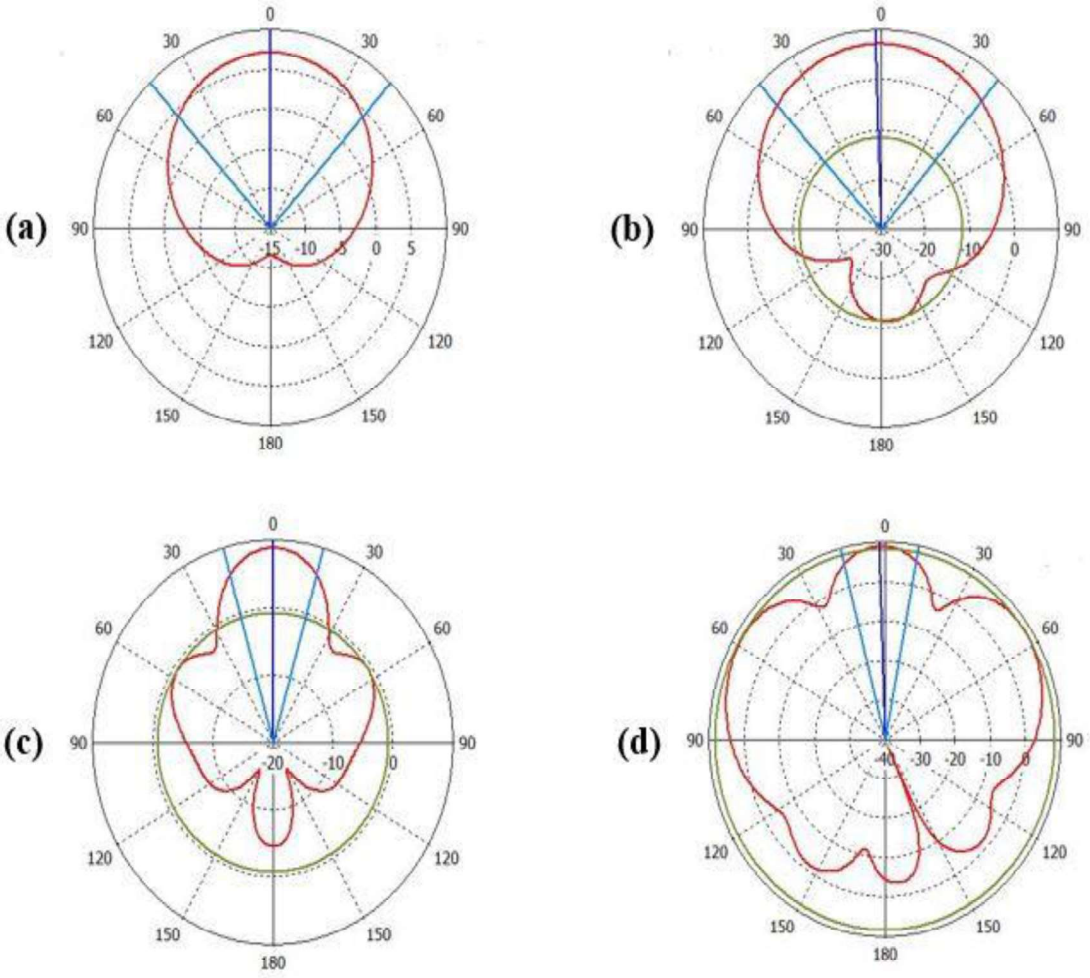

Figure 3.26 Depicts 2D-radiation pattern of second proposed multi-band microstrip antenna for (a-b) at 10 GHz and (c-d) at 30 GHz

Figure (3.27) depicts the 3D far-field radiation directivity pattern for the second proposed dual-band microstrip patch antenna. Figure 3.27(a) displays the directivity value for the lowest resonance frequency of 7.14 dBi at 10 GHz, and figure 3.27(b) displays the directivity value for the highest resonance frequency of 8.83 dBi at 30 GHz. The radiation is emitted in the z-axis direction, which means this antenna has directional radiation.

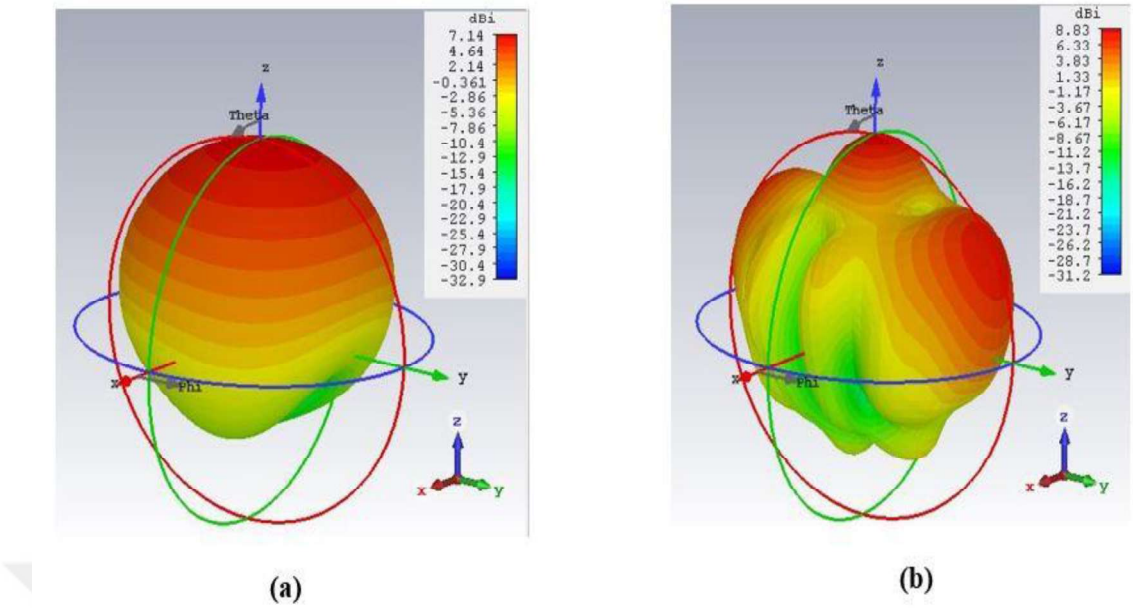

Figure 3.27 Illustrated 3D radiation pattern at (a) 10 GHz and at (b) 30 GHz

The electrical current behavior on the surface of the patch antenna can be described in Figure 3.28 at each wanted frequency. The current field at first frequency 10 GHz will be increased at the small rectangle located below the T-slot and also near at both sides along the patch length as shown in figure 3.28(a), while a small amount of current at second resonance frequency 30 GHz, will be concentrated at the small rectangle, which is also located near the edge of one of T slot's sides as shown in figure 3.28(b).

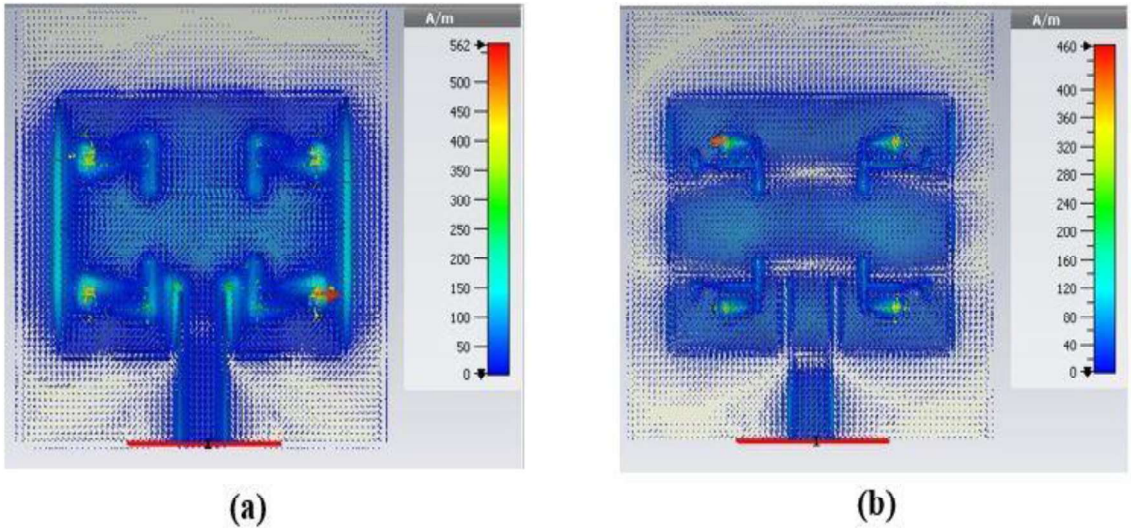

Figure 3.28 Demonstrates current distributions of dual-band second proposed microstrip patch antenna for each resonance frequency at (a) 10 GHz and (b) 30 GHz

3.5 Final Proposed of Multi-Band Compact Antenna Design

This proposed design introduces the final microstrip patch antenna design, which is based on the basic dimensions of the previous structure, such as the ground plate and substrate, but differs in feed line dimensions to pass the maximum power between the feeding and the patch. This antenna is composed of a copper-radiated element with slots as a shape of Fork and small squares. This suggestion has been designed to work at 10 GHz and 30 GHz after removing the slots from the second design and replacing them with new ones. The final design aimed to achieve as high gains as possible at each resonance frequency while retaining acceptable values for the other parameters.

3.5.1 Modification of Inset Feed Line and Patch Length

The first modification includes changing the patch and feed line's length and the width g of the inset feed for impedance matching. The radiated element of the proposed second design must be taken and remove all of its slots, to produce a conventional antenna.

The parametric study was done, where the length of the feed line has been reduced from 3.06 mm to 2 mm and increase the width of the inset feed from 0.605 mm to 0.61 mm, as well as the length of a patch from 8.88 mm to 8.98 mm while other measurements of second design, will remain fixed.

After simulation of patch and feed line in CST software, undesired frequencies appeared at 17.09 GHz, 20.38 GHz, and 22.44 GHz with different return losses that require to cancel them to get the necessary results for the last proposed design, as well as some bands, emerged near each resonance frequency that needs to be shifted down. Simulation of modified antenna showed poor values of all parameters, such as gain, directivity, return loss and high VSWR value.

The change in patch length L_p had an impact on the return loss for each desired and undesired frequency and shifting each band down. Figure 3.29 shows the different return loss values for all modification steps of patch length and feed line in (mm).

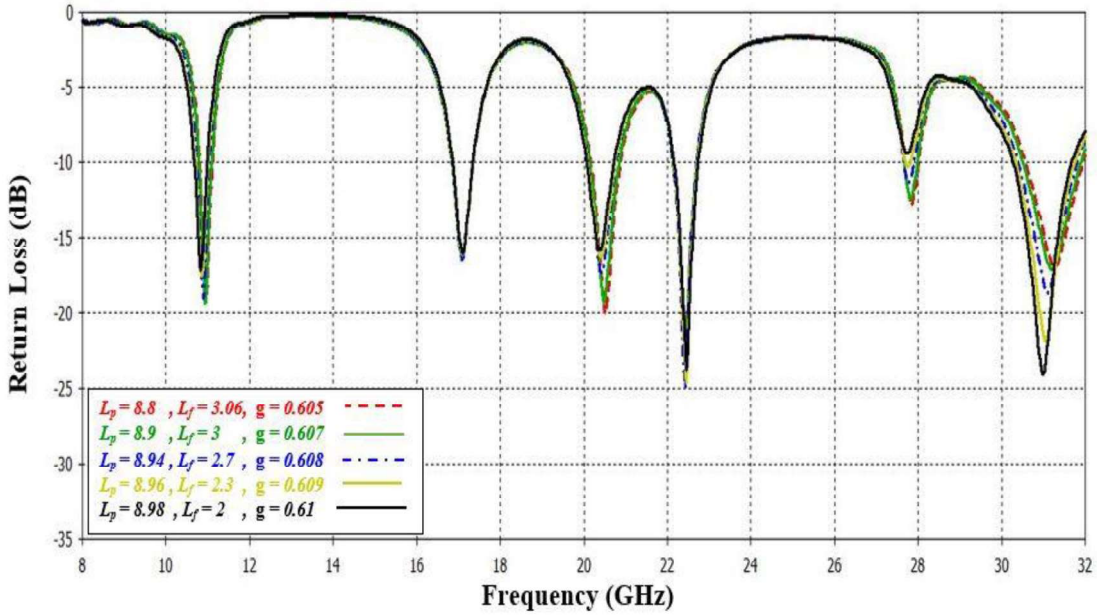

Figure 3.29 Illustrates return loss values of all modification steps of patch length and feed line

The third proposed traditional patch antenna without slots was created by simply changing the previous design's patch length and feed line measurements. Figure 3.30 depicts the third proposed antenna without inserted slots.

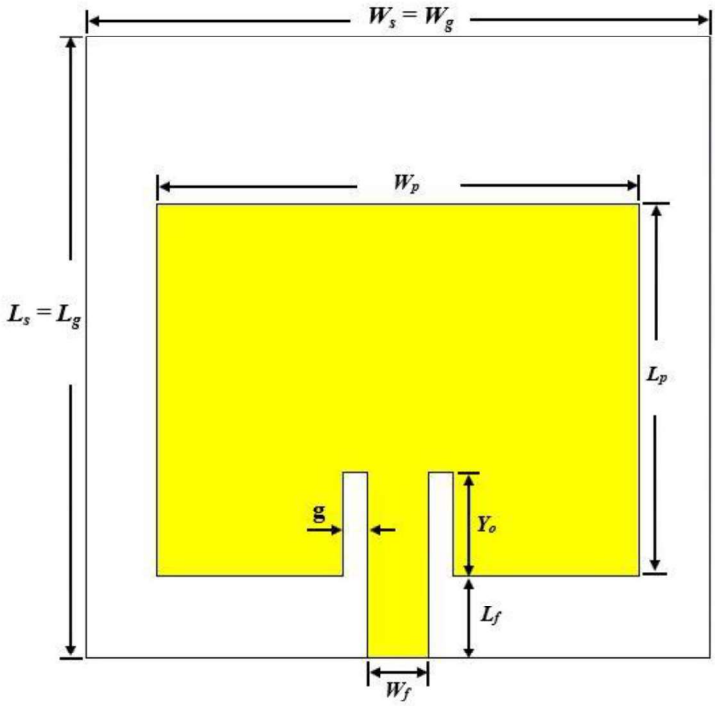

Figure 3.30 Shows the conventional third proposed antenna design dimensions

The contrast between the measurements modified in the previously proposed antenna and a present proposed antenna with removed initial slots has been illustrated in table 3.6.

Table 3.6 The comparison between measurements of present modified and previous proposed antenna

Parameter	Previous proposed Antenna Value (mm)	Modified Antenna Value (mm)	Description
W_g	15	15	Width of ground plate
L_g	15	15	Length of ground plate
W_S	15	15	Width of Roger RT5880 substrate
L_S	15	15	Length of Roger RT5880 substrate
W_P	11.585	11.585	Width of copper patch
L_P	8.88	8.98	Length of copper patch
W_f	1.52	1.52	Width of feeder
L_f	3.06	2	Length of feeder
Y_o	2.5	2.5	Length of gap inside patch
g	0.605	0.61	Width of gap inside patch

3.5.2 Inserting Slots within Patch Element

After used the main structure of the second proposed design and just modified its patch length with the feed line, the modified patch became ready to create slots within, to produce multi-band resonance frequency at 10 GHz and 30 GHz, and also to cancel unwanted bands. Furthermore, slots were attached to the patch antenna to solve input impedance and reflection coefficient problems and maximize bandwidth. These slots will lengthen the electrical current direction within the radiated element. There were several steps involved in determining the correct placement of slots and their dimensions. The final dimensions of slots of the proposed third design have described in figure 3.31.

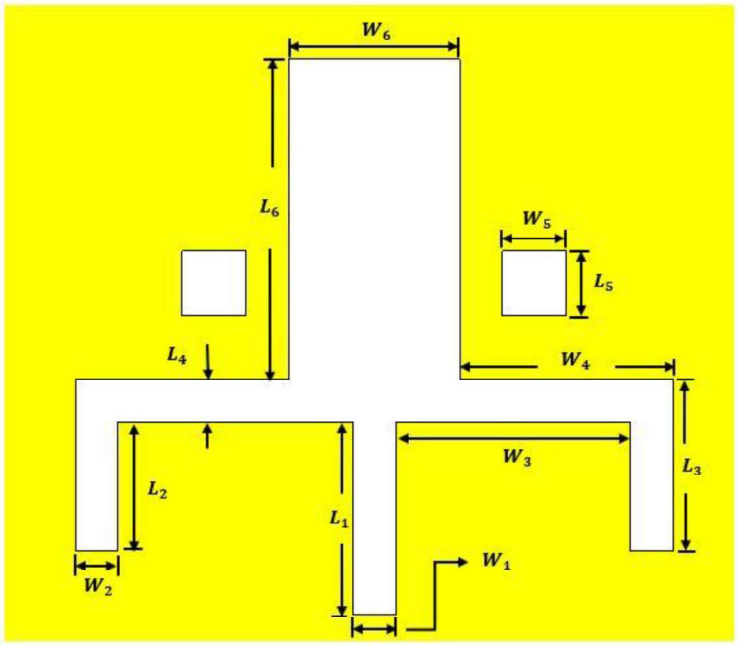

Figure 3.31 Demonstrates final measurements of slots for third proposed design to generate dual-band resonance frequency

Slots will be as shape of Fork and two small slots of squares placed symmetrically around the main arm of each Fork.

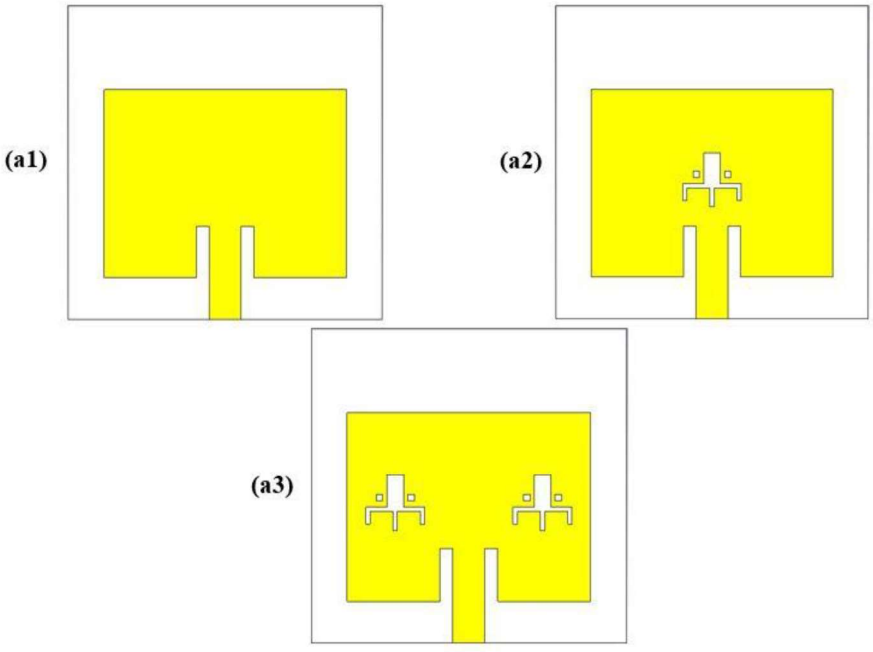

Figure 3.32(a) Shows first three-stages of dual-band third proposed antenna design

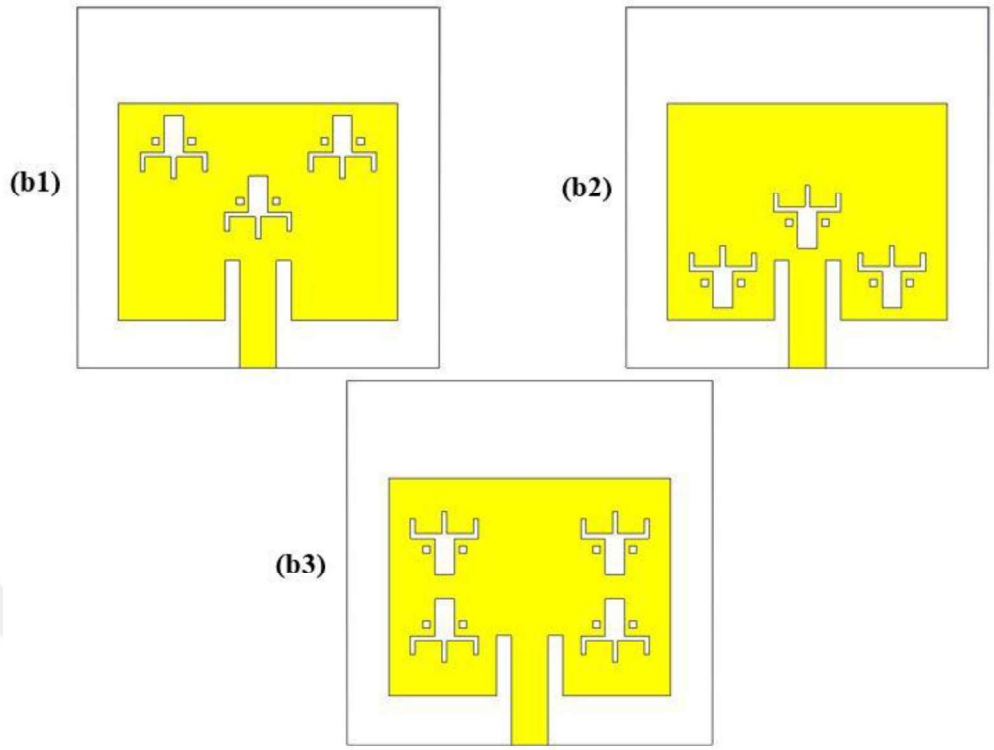

Figure 3.32(b) Shows final three-stages of dual-band third proposed antenna design

Figure 3.32(a1) depicts a traditional patch antenna without slots with patch length and feed line dimensions modified depending on the second proposed antenna. This stage did not provide the required effects, and specific undesirable frequencies were detected at 17.12 GHz, 20.45 GHz, and 22.5 GHz; these bands can only be eliminated by inserting slots to the radiating portion.

As a result, as seen in figure 3.31, a slot has been put in the middle of the patch to study the variation that would occur in parameters, as seen in figure 3.32. (a2). However, these undesirable bands continue to occur in unfavorable locations with high reflection coefficient values.

Although the slot in figure 3.31 was placed symmetrically around the inserted feed, as shown in figure 3.32 (a3), no resonance frequency near 30 GHz appeared, but the lowest resonance frequency was very close to 10 GHz. and unwanted bands occurred at 20.53 GHz and 22.42 GHz. For this purpose, these slots were placed in the upper half of the patch, and the middle one was returned (see figure 3.32 (b1)).

It was observed that the frequency of the first resonance shifted slightly forward than in the previous stage, and the positions of the unwanted frequencies at 15.85 GHz and 19.28 GHz changed, as well as the high VSWR at the frequency of lower resonance.

Before the final stage, the slots from the previous stage to the bottom half of the patch were placed upside down to get the required frequencies in the right places, as shown in figure 3.32 (b2). However, ripples appeared near the highest resonance frequency and some undesired frequencies at 18.82 GHz and 20.24 GHz that need to be removed.

As shown in figure 3.32 (b3), the final stage solved all problems related to low gain, efficiency, directivity, and the appearance of unwanted frequencies and created a multiband microstrip patch antenna in the required bands.

Figures (a and b) show all stages of the traditional antenna that have been modified to function as a multiband patch antenna for future 5G devices. To explain in more detail what was said above, figure 3.33 shows the return losses at each stage, as shown in figure 3.32 (a and b).

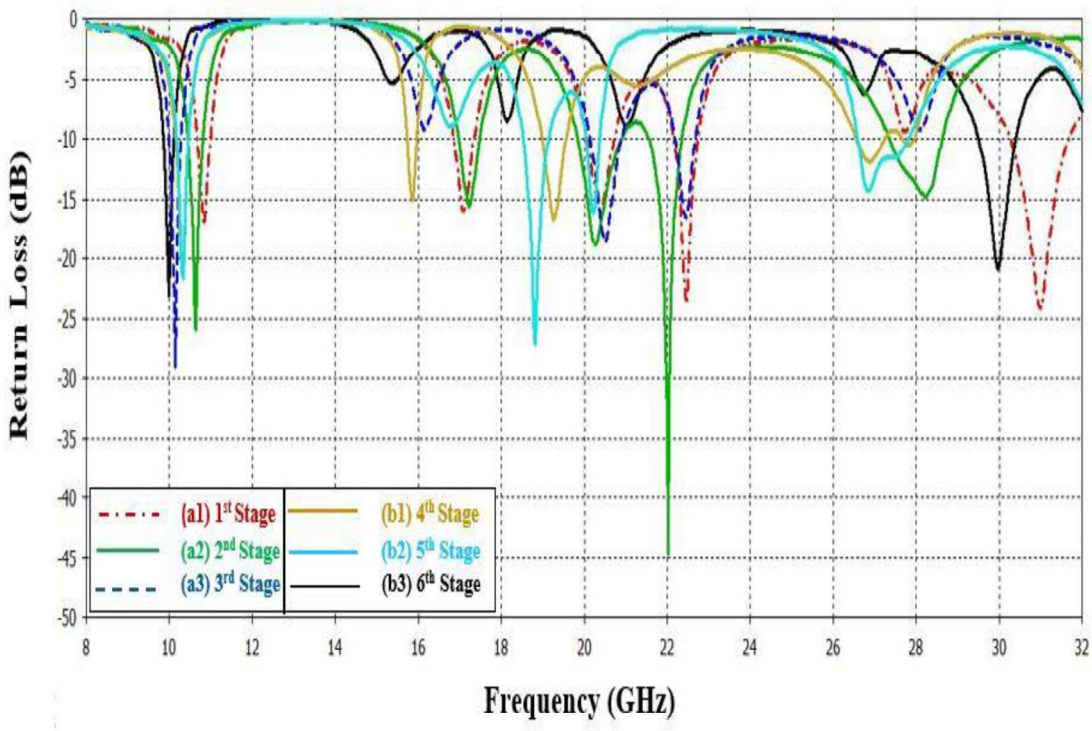

Figure 3.33 Describes reflection coefficients for each stage of third proposed antenna

The third proposed final design of dual-band micro-strip patch antennas was obtained after changing dimensions, the length of the patch, and the feed line of the second proposed antenna, and the slots placed in the top and bottom halves of the patch near to its edges. The final design dimensions of the proposed third antenna are shown in figure 3.34.

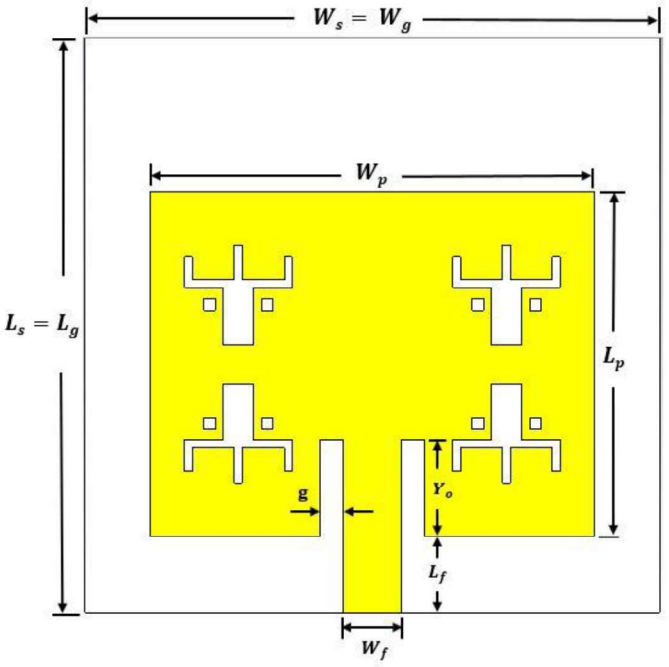

Figure 3.34 Shows final dimensions of third proposed multi-band compact patch antenna

The third proposed multiband patch antenna consists of a copper plane taken from the second proposed antenna after the reference antenna has been modified with dimensions of 11.585×8.98×0.035 mm^3 and connected to an inserted microstrip power line, the dimensions of which are to supply the patch with enough power. Substrate material with a low dielectric constant of 2.2, made from Roger RT5880 Duroid measuring 15×15×0.508 mm^3, was used to obtain multiple high bands and positioned below the copper radiated element. The full copper plate was placed at the bottom of the substrate, measuring 15×15×0.035 mm^3 to cover most of the patch and the Roger RT5880 to obtain high gain values resulting in radiation with high directivity. Finally, as in figure 3.31, four slots have been placed close to each corner of the patch at the upper and lower half to make the antenna operate at X and Ka-band and remove unwanted bands.

Table 3.7 shows the whole measurements in (mm) of the third dual-band compact patch antenna.

Table 3.7 Depicts final dimensions of third multi-band microstrip patch antenna

Parameter	Value (mm)	Description
W_g	15	Width of copper ground plate
L_g	15	Length of copper ground plate
W_s	15	Width of Roger RT5880 substrate
L_s	15	Length of Roger RT5880 substrate
W_p	11.585	Width of copper patch
L_p	8.98	Length of copper patch
h	0.508	Thickness of substrate
t	0.035	Thickness of copper
W_1	0.2	Width of 1st slot
L_1	0.9	Length of 1st slot
W_2	0.2	Width of 2nd slot
L_2	0.6	Length of 2nd slot
W_3	1.1	Width of 3rd slot
L_3	0.8	Length of 3rd slot
W_4	1	Width of 4th slot
L_4	0.2	Length of 4th slot
W_5	0.3	Width of 5th slot
L_5	0.3	Length of 5th slot
W_6	0.8	Width of 6th slot
L_6	1.5	Length of 6th slot
W_f	1.52	Width of microstrip feed line
L_f	2	Length of microstrip feed line
Y_o	2.5	Length of gap inside patch
g	0.61	Width of gap inside patch

The third proposed microstrip antenna was designed and tested using the 2018 version of CST. It found that this antenna operates with the lowest resonance frequency at 10 GHz and the highest resonance frequency at 30 GHz. Using reflection coefficient parameters to calculate the average supplied power sent from the antenna compared to the sum returned to the source.

The return loss equals -22.77 dB with the bandwidth of 263 MHz and -19.27 dB with 901 MHz at 10 GHz and 30 GHz, respectively. Figure 3.35 will demonstrate reflection coefficients at each resonance frequency with their bandwidths, which is suitable for future 5G devices.

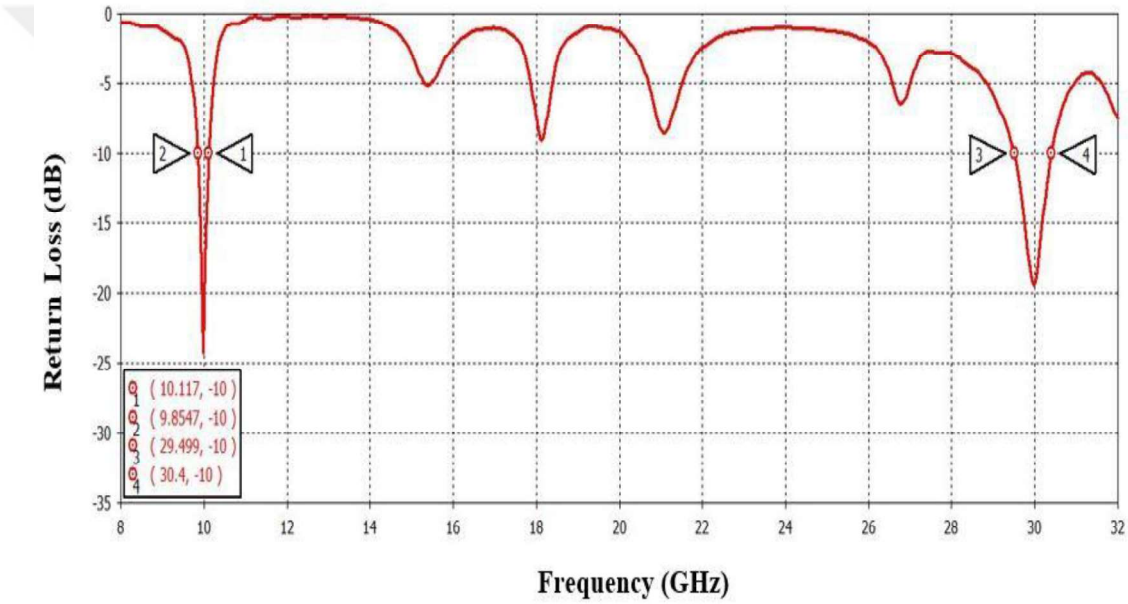

Figure 3.35 Shows return losses and bandwidth of third proposed compact patch antenna

The radiation efficiency is the ratio amount of power emitted into space to the power supplied by the source to the antenna. As mentioned before, an antenna with an efficiency ranging from (50 to 60) % is considered a well-functioning antenna. The third proposed compact antenna achieved high radiation efficiency at each desired frequency. Radiation efficiency was 82.18 percent at 10 GHz and 84.95 percent at 30 GHz, as shown in figure 3.36. Furthermore, the radiation efficiency for each bandwidth at each center frequency is greater than 82.1 percent at 10 GHz and greater than 84.8 percent at 30 GHz.

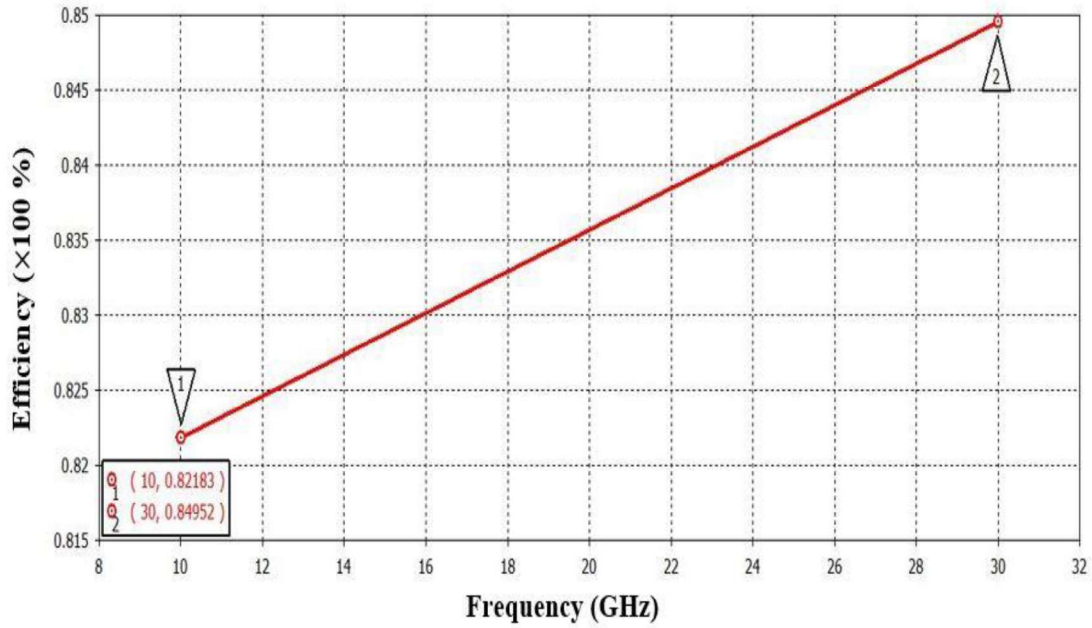

Figure 3.36 Illustrates radiation efficiency of third proposed microstrip patch antenna

The high gain indicates that the antenna can concentrate its radiation in one direction rather than another, making it more efficient, especially in receiving mode. At 10 GHz and 30 GHz, this antenna achieved gains of 6.14 dB and 10.66 dB, respectively. Figure 3.37 depicts the positive gain value at each wanted frequency.

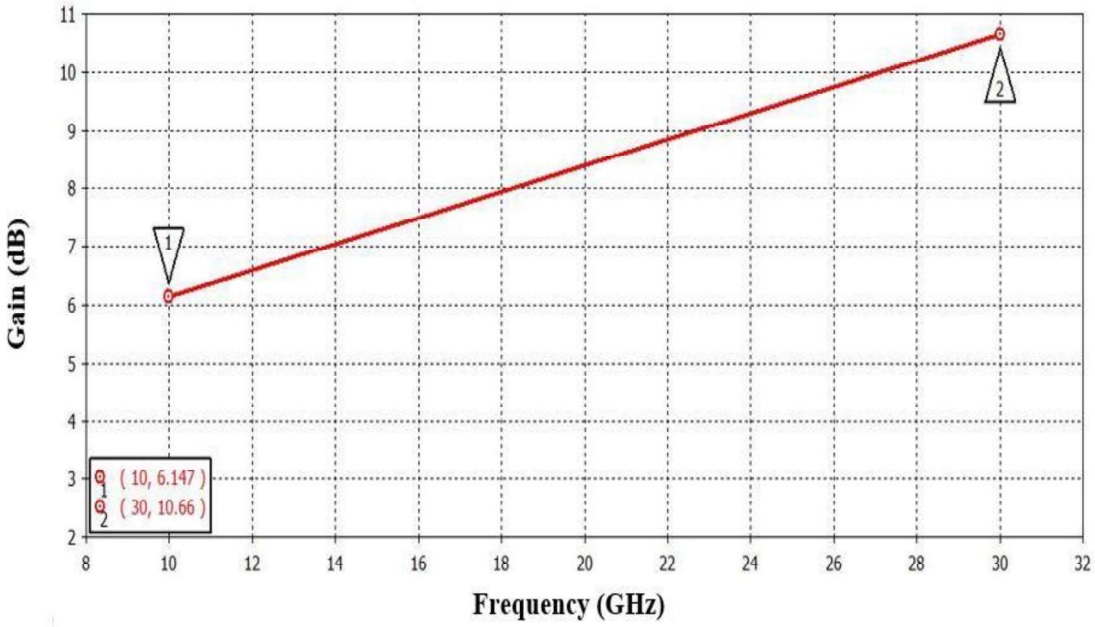

Figure 3.37 Shows gain results of third proposed microstrip patch antenna

The radiation pattern at 10 GHz in the E-plane (phi=0º) as seen in figure 3.38(a), with the main lobe magnitude and orientation of 6.99 dBi and 0º, respectively, and the angular beamwidth (3 dB) of 86.3º.

Furthermore, figure 3.38(b) revealed that the main lobe's magnitude and orientation were 7 dBi and 3º, respectively, at 10 GHz in H-plane (phi=90º), angular beamwidth (3 dB) being 86.7º.

Figure 3.38(c) depicts the radiation pattern at 30 GHz in the E-plane (phi=0º), with the magnitude and orientation of the main lobe being 1.72 dBi and 0º, respectively, and the angular beamwidth (3 dB) being 43.1º.

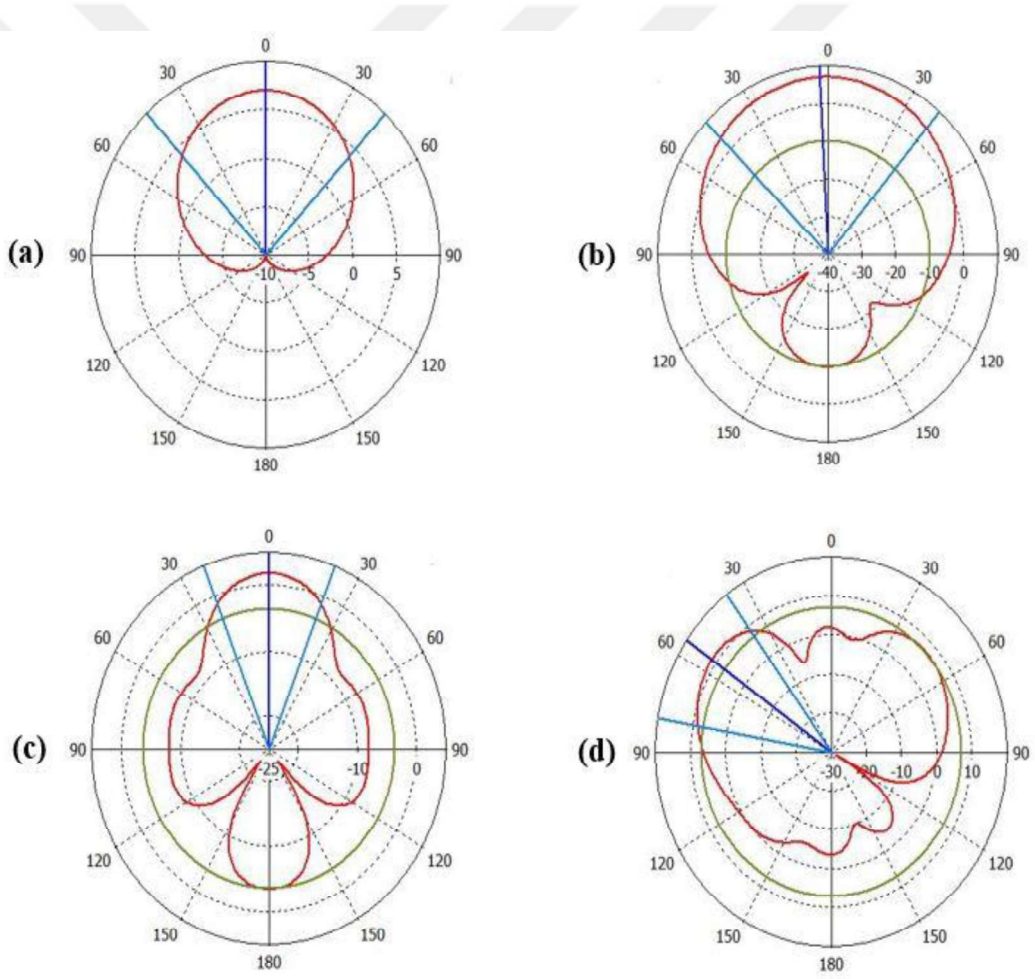

Figure 3.38 Depicts 2D-radiation pattern of third proposed multi-band microstrip antenna for (a-b) at 10 GHz and (c-d) at 30 GHz

Finally, figure 3.38(d) at 30 GHz found that the magnitude and orientation of the main lobe are 11.4 dBi and 55°, respectively, in H-plane (phi=90°) as well as the angular beamwidth (3 dB) is 43.4°

The third proposed microstrip antenna radiates a three-dimensional far-field pattern of directivity, as seen in figure 3.39. It found that the directivity value at each resonance frequency required equal 7 dBi at 10 GHz, as seen in figure 3.39 (a), and 11.4 dBi at 30 GHz, as shown in figure 3.39 (b).

The High results of directivity refer to the ability of this proposed antenna to concentrate radiation in a specific direction comparing with an isotropic antenna; The radiation emits in the z-axis direction, which means this antenna has directional radiation.

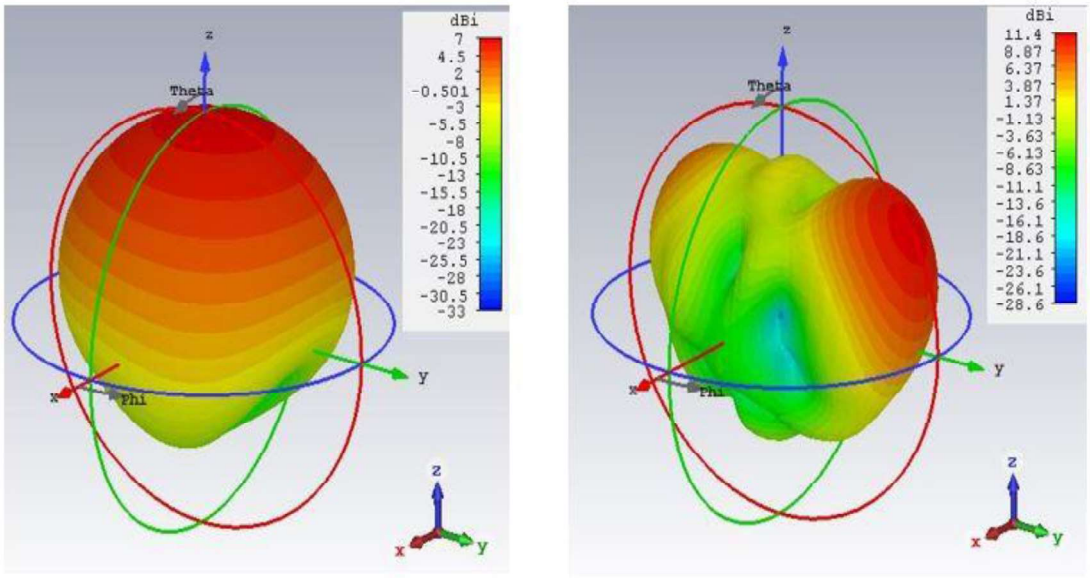

Figure 3.39 Illustrates 3D-radiation pattern at (a) 10 GHz and at (b) 30 GHz

The electrical current behavior on the surface of the patch antenna has described in figure 3.40 at each wanted frequency. The electric current field will concentrate on forks' side tines etched lower half of the patch as well as at the end of the inset feeding at 10 GHz as described in figure 3.40 (a), while at 30 GHz, the current field will concentrate at the side tines of all forks etched of the patch as well as at the main arm of the Forks as shown in figure 3.40 (b).

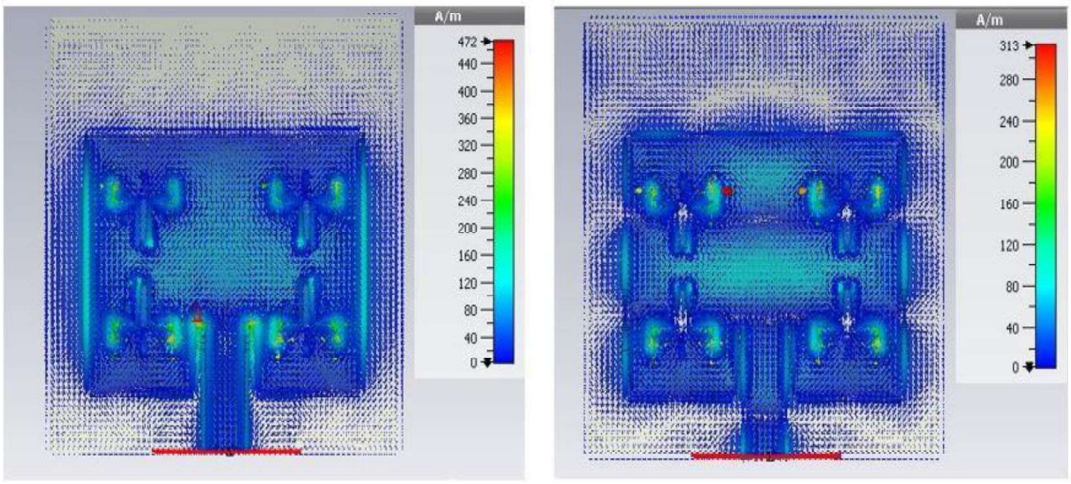

Figure 3.40 Demonstrates current distributions of dual-band third proposed microstrip patch antenna for each resonance frequency at (a) 10 GHz and (b) 30 GHz

3.6 Comparison Between Proposed Antennas with Other Designs

During the past ten years, the researchers have done many works about dual-band 5G micro-strip patch antenna, with different shapes, dimensions, slots, resonance frequency, parameters values, and feed techniques.

The antennas suggested in this thesis will be compared to other works regarding resonant frequency and antenna dimensions and the acceptable values of gain, return loss and bandwidth, to check suitability for future 5G wireless communication. Table 3.8 displays the variance of results between researchers work and proposed antennas in this study.

Table 3.8 Depicts comparison between proposed antennas and former works

Antenna	Freq. (GHz)	Dim. (mm^3)	R.L (dB)	Gain (dB)	B.W (GHz)	App.
Patch antenna as spanar [28]	10	31.7×18.5×1.6	-30.5	4.123	2.25	Bio-Medical and Radar systems

Small microstrip antenna [34]	10.15	20×20×1.6	-18.27	4.46	0.38	Smart grids and cities, handheld devices and Tele-medical
Dual-band monopole antenna [29]	28 38	4×8×0.254	-18.2 -20.5	4.73 4.73	6.35 8.4	Future 5G Mobile phones
Dual-band MIMO antenna [30]	28 38	55×110×0.508	-27.84 -18.35	7.18 9.24	1.2 1.3	5G mobile and Smartpho-nes
Dual-band Slotted patch antenna [32]	28 38	10×10×0.245	-27 -22.5	4.73 5.13	0.4 1.5	Smart transpor-tion, 5G mobile network
Dual-band CPW slot antenna [33]	28 38	10×10×0.245	-40.7 -48.2	6.6 5.6	0.58 0.67	Short range communi-cation, sensor systems

Reference antenna [31]	10 28 38	20 ×16.5×0.508	-25.8 -24.9 -32.9	5.67 9.33 9.57	0.343 0.761 1.5	Point to point wireless comm. and devices with space constrians
First proposed antenna	10 30	15 ×11.5×0.508	-23.82 -43.3	4.85 8.86	0.176 1.015	Radar, TV, Satellite links, Micro-wave radio relay links, Voice multi-media-LEOs/ GEOs, WIFI, 5G mobile,
Second Proposed antenna	10 30	15 ×15×0.508	-26.04 -33.35	6.16 8.02	0.253 0.948	

Third Proposed antenna	10 30	15 ×15×0.508	-22.77 -19.27	6.14 10.66	0.263 0.901	Aircraft Naviga-tion, Subscriber radio, Medical diathermy and Micro-wave hyper-thermy

We observed that the three compact designs in this thesis had achieved different results that outperformed previous works and surpass their performance in terms of antenna size dimensions and other parameters such as gain, return losses and bandwidth values in comparison with a reference antenna and former designs as seen in table 3.8 above.

In general, a microstrip patch antenna suffers from some drawbacks; it is a narrow band antenna that needs to use a unique feeding technique, mentioned in the future work section.

CHAPTER 4

CONCLUSIONS AND FUTURE WORK

4.1 Conclusions

The design of the compact antenna working at Super High Frequency (SHF) bands for future 5G applications represents one of the most significant challenges that researchers face in designing a small-size patch antenna with optimal performance. This thesis introduces three miniaturized microstrip patch antennas design by using the CST software version of 2018. According to their results and after checking all parameters, the dual-band resonance frequency behavior obtains successfully. The following are some of the conclusions observed and analyzed from these findings:

1. The dimensions of the three proposed antennas were smaller than designers' ex-works and the reference antenna that depended upon this study.
2. The electrical current behavior study on the surface of the suggested patch antenna at various desired frequencies plays an essential role to reach the suitable final design for dual-band resonance frequency.
3. Microstrip patch antenna considers a completely independent structure in its own right, so any adjustment process on the primary antenna structure by addition or removal parts on its body will affect on appearing of desired and undesired frequencies, making it possible to control the electrical current path on the antenna structure and enhance the ability to find resonance frequencies required.
4. Using partially or fully ground plate and changing the feedline dimensions and etching slots within the patch, all mentioned before, will reduce antenna size and make it operate in another band.
5. Modifications on the ground plane will affect some of the antenna's parameters, such as the bandwidth range and the directivity and gain values of radiation that determine whether the antenna has a directional or Omnidirectional radiation pattern.

6. The inset feed technique is used for maximum power transfer to the patch, but changing the shapes and dimensions of the slots used inside the patch will also directly affect impedance matching.
7. The three suggested antennas have printed on Roger RT5880 Duroid substrate rather than another dielectric material such as FR-4 because of its low permittivity of 2.2 used for high-frequencies applications.
8. Directional radiation for dual-band patch antenna attained in this thesis for future 5G wireless communication systems.
9. This work achieved overall good radiation efficiencies greater than 72% at the first resonance frequency of 10 GHz and greater than 82% at the second resonance frequency of 30 GHz for each proposed patch antenna in this thesis.
10. High directivity and gain achieved for each of the resonance frequencies suggested in this thesis.

4.2 Future Work

The designs of this thesis may be updated and developed in the future by working on the following topics:

1. Using more than one substrate with a different dielectric constant in microstrip antenna design, and this technique is known as aperture coupled or proximity coupled according to the positioning of the feed line and ground plane thus the thickness of the antenna will be increased and lead to improving return losses and broader bandwidth.
2. many miniaturization techniques can be used on time to increase the reduction level of antenna size as much as possible.
3. Improving the gain value of the first resonant frequency band and make it the same as the gain level of the second resonant frequency of the three proposed antennas by invented a suitable method to attain the purpose of gain improvement such as using a group of radiated elements simultaneously, and make them work as an array antenna.
4. Design of a single band patch antenna working at 60 GHz, with the ability to control beam direction by using different shapes of metamaterial structures.

REFERENCES

[1] Bhandari, Nikhil, Shivinder Devra, and Karamdeep Singh. "Evolution of cellular network: from 1G to 5G." International Journal of Engineering and Techniques 3.5, 2017.

[2] Kachhavay, Meenal G., and Ajay P. Thakare. "5G technology-evolution and revolution." International Journal of Computer Science and Mobile Computing 3.3, 2014.

[3] Salih, Azar Abid, et al. "Evolution of Mobile Wireless Communication to 5G Revolution." Technology Reports of Kansai University 62.5 (2020): 2139-2151.

[4] Pisarov, Jelena, and Gyula Mester. "The Impact of 5G Technology on Life in 21st Century." IPSI BgD Transactions on Advanced Research (TAR) 16.2, 2020.

[5] Vora, Lopa J. "Evolution of mobile generation technology: 1G to 5G and review of upcoming wireless technology 5G." International journal of modern trends in engineering and research 2.10, 2015.

[6] Wang, Haiming, et al. "Radio propagation and wireless coverage of LSAA-based 5G millimeter-wave mobile communication systems." China Communications 16.5, 2019.

[7] Khan, Muhammad Umar, Mohammad Said Sharawi, and Raj Mittra. "Microstrip patch antenna miniaturisation techniques: a review." IET Microwaves, Antennas & Propagation 9.9, 2015.

[8] Aijaz, Zarreen, and S. C. Shrivastava. "An introduction of aperture coupled microstrip slot antenna." International Journal of Engineering Science and Technology 2.1, 2010.

[9] Ahmed, Kazi Tofayel, Md Bellal Hossain, and Md Javed Hossain. "Designing a high bandwidth Patch Antenna and comparison with the former Patch Antennas." Canadian Journal on Multimedia and Wireless Networks 2.2, 2011.

[10] Yaseen, Mahmoud Taha. Design of Dual-Band Antenna for Wireless Communication Applications. Diss. Doctoral dissertation, University of Technology, 2013.

[11] Zhao, Gang, et al. "Compact ring monopole antenna with double meander lines for 2.4/5 GHz dual-band operation." Progress In Electromagnetics Research 72, 2007.

[12] Bharathi, Anantha, Merugu Lakshminarayana, and PVD Somasekhar Rao. "A quad-polarization and frequency reconfigurable square ring slot loaded microstrip patch antenna for WLAN applications." AEU-International Journal of Electronics and Communications 78, 2017.

[13] Yadav, Shekhar, et al. "Notch-Loaded Patch Antenna with Multiple Shorting for X and Ku Band Applications." Recent Trends in Communication, Computing, and Electronics. Springer, Singapore, 2019.

[14] Romputtal, Adisak, and Chuwong Phongcharoenpanich."Frequency reconfigurable multiband antenna with embedded biasing network." IET Microwaves, Antennas & Propagation 11.10, 2017.

[15] Jing, Jianwei, et al. "A Multiband Compact Low-Profile Planar Antenna Based on Multiple Resonant Stubs." Progress In Electromagnetics Research 94, 2020.

[16] Yassen, Mahmood T., et al. Extraction of dual-band antenna response from UWB based on current distribution analysis. Technical Report, MRG 6–2016, Microwave Research Group, Department of Electrical Engineering, University of Technology, Iraq, 2016.

[17] Amin, MK Mohamed, et al. "28/38GHz dual band slotted patch antenna with proximity-coupled feed for 5G communication." 2017 International Symposium on Antennas and Propagation (ISAP). IEEE, 2017.

[18] Hassan, Nornikman, et al. "Design of dual-band microstrip patch antenna with right-angle triangular aperture slot for energy transfer application." International Journal of RF and Microwave Computer-Aided Engineering 29.1, 2019.

[19] Liu, Pengfei, et al. "Patch Antenna Loaded With Paired Shorting Pins and H-Shaped Slot for 28/38 GHz Dual-Band MIMO Applications." IEEE Access 8, 2020.

[20] Ata, Osama W., Mohammad Salamin, and Khaleel Abusabha. "Double U-slot rectangular patch antenna for multiband applications." Computers & Electrical Engineering 84, 2020.

[21] Wa'il, A., Raed M. Shaaban, and Akeel Tahir. "Design, simulation and measurement of triple band annular ring microstrip antenna based on shape of crescent moon." AEU-International Journal of Electronics and Communications 117, 2020.

[22] Mishra, Brijesh, Vivek Singh, and Singh Rajeev."Gap-coupled H-shaped antenna for wireless applications." Proceedings of the National Academy of Sciences, India Section A: Physical Sciences, 2019.

[23] Surjati, Indra, Yuli Kurnia Ningsih, and Syah Alam. "Stacked rectangular ring slot microstrip antenna with parasitic load for UMTS, LTE and WiFi applications." 2017 International Conference on Radar, Antenna, Microwave, Electronics, and Telecommunications (ICRAMET). IEEE, 2017.

[24] Villano, Michelangelo, Gerhard Krieger, and Alberto Moreira. "Nadir echo removal in synthetic aperture radar via waveform diversity and dual-focus postprocessing." IEEE Geoscience and Remote Sensing Letters 15.5, 2018.

[25] Yurovsky, Yury Yu, et al. "Validation of Doppler Scatterometer Concepts using Measurements from the Black Sea Research Platform." 2018 Doppler Oceanography from Space (DOfS). IEEE, 2018.

[26] Tiwari, Devesh, et al. "Analysis of a Miniaturized Hexagonal Sierpinski Gasket fractal microstrip antenna for modern wireless communications." AEU-International Journal of Electronics and Communications 123, 2020.

[27] Rian, Iasef Md, Mario Sassone, and Shuichi Asayama. "From fractal geometry to architecture: Designing a grid-shell-like structure using the Takagi–Landsberg surface." Computer-Aided Design 98, 2018.

[28] Othman, Mohd Azlishah, et al. "10 GHz microstrip spanar antennas: an experimental analysis." Journal of Physics: Conference Series. Vol. 495. No. 1. IOP Publishing, 2014.

[29] Ullah, Hidayat, Farooq A. Tahir, and Muhammad U. Khan. "Dual-band planar spiral monopole antenna for 28/38 GHz frequency bands." 2017 IEEE International Symposium on Antennas and Propagation & USNC/URSI National Radio Science Meeting. IEEE, 2017.

[30] Marzouk, H. M., M. I. Ahmed, and A. A. Shaalan. "A Novel Dual-band 28/38 GHz Slotted Microstip MIMO Antenna for 5G Mobile Applications." 2019 IEEE International Symposium on Antennas and Propagation and USNC-URSI Radio Science Meeting. IEEE, 2019.

[31] Abdelaziz, Ahmed, and Ehab KI Hamad. "Design of a compact high gain microstrip patch antenna for tri-band 5 G wireless communication." Frequenz 73.1-2, 2019.

[32] Almashhdany, Mohammad B., et al. "Design of Multi-band Slotted mmWave Antenna for 5G Mobile Applications." IOP Conference Series: Materials Science and Engineering. Vol. 881. No. 1. IOP Publishing, 2020.

[33] Ali, Mohamed Mamdouh M., and Abdel-Razik Sebak. "Dual band (28/38 GHz) CPW slot directive antenna for future 5G cellular applications." 2016 IEEE International Symposium on Antennas and Propagation (APSURSI). IEEE, 2016.

[34] Verma, Shivangi, et al. "A small microstrip patch antenna for future 5G applications." 2016 5th International Conference on Reliability, Infocom Technologies and Optimization (trends and future directions) (ICRITO). IEEE, 2016.

[35] Balanis, Constantine A. Antenna theory: analysis and design. John wiley & sons, 2015.

[36] Fang, Da-Gang. Antenna theory and microstrip antennas. CRC Press, 2017.

[37] Mao, Chun Xu, et al. "Compact Patch Antenna with Vertical Polarization and Omni-Directional Radiation Characteristics." IEEE Transactions on Antennas and Propagation, 2020.

[38] Dutta Chaudhury, Nandan. "An investigation on the possibility for bandwidth improvement of dielectric antennas via modification of their geometry.", 2020.

[39] Pozar, David M. Microwave engineering. John wiley & sons, 2011.

[40] M. Z. Hadi, J.S.Aziz. “Design and Analysis of Reduced Size UWB Antenna for EM Radiation Monitoring”, M.Sc. thesis in Electronic and Communications Engineering, Al-Nahrain University. October 2019.

[41] Slovick, Brian Alan. "Infrared phased-array antenna-coupled tunnel diodes.", 2011.

[42] Aragon-Zavala, Alejandro. Antennas and propagation for wireless communication systems. John Wiley & Sons, 2008.

[43] Davis, William A., and Warren L. Stutzman. "Antenna Theory." Encyclopedia of RF and Microwave Engineering, 2005.

[44] Chen, Wai Kai. The electrical engineering handbook. Elsevier, 2004.

[45] Rozi, Fakhru, and Umar Khayam. "Design, implementation and testing of triangle, circle, and square shaped loop antennas as partial discharge sensor." The 2nd IEEE Conference on Power Engineering and Renewable Energy (ICPERE) 2014. IEEE, 2014.

[46] Djordfevic, Antonije R., et al. "Optimization of helical antennas [antenna designer's notebook]." IEEE Antennas and Propagation Magazine 48.6, 2006.

[47] Jacobs, Ockert Botha, Johann Wilhelm Odendaal, and Johan Joubert. "Elliptically shaped quad-ridge horn antennas as feed for a reflector." IEEE Antennas and Wireless Propagation Letters 10, 2011.

[48] A. A. Marzah, J.S.Aziz. “Design and Analysis of Miniaturized Band Pass Filter Using Fractal Geometry Technique”, M.Sc. thesis in Electronic and Communications Engineering, Al-Nahrain University. January 2019.

[49] Chen, Chia-Mao, et al. "Fabrication of compact microstrip line-based balun-bandpass filter with high common-mode suppression." 2014 Mathematical Problems in Engineering, 2014.

[50] Nesic, Dusan, and Ivana Radnovic. "Parallel-Strip Line Stub Resonator for permittivity Characterization." Facta Universitatis, Series: Electronics and Energetics 33.1, 2019.

[51] R Rahman, Saifur, et al. "Nature inspired MIMO antenna system for future mmWave technologies." Micromachines 11.12, 2020.

[52] Alkhafaji, Mohammed K., et al. "Study on the effect of the substrate material type and thickness on the performance of the filtering antenna design." Telkomnika 18.1, 2020.

[53] Liew, Elaine, et al. "Signal transmission loss due to copper surface roughness in high-frequency region." Proceedings of IPC APEX EXPO 2014 Technical Conference. 2014.

[54] Pandey, Anil. Practical microstrip and printed antenna design. Artech House, 2019.

[55] Mak, Ka Ming, Hua Wah Lai, and Kwai Man Luk. "A 5G wideband patch antenna with antisymmetric L-shaped probe feeds." IEEE Transactions on Antennas and Propagation 66.2, 2017.

[56] Paul, Liton Chandra, et al. "The effect of changing substrate material and thickness on the performance of inset feed microstrip patch antenna." American Journal of Networks and Communications 4.3, 2015.

[57] Nascimento, Daniel C., and JC da S. Lacava. "Probe-fed linearly-polarized electrically-equivalent microstrip antennas on FR4 substrates." Journal of Microwaves, Optoelectronics and Electromagnetic Applications 13.1, 2014.

[58] Gaya, Abinash, et al. "Design of Wideband Dielectric Resonator Antenna with Aperture Coupled technique for 5G Applications." 2018 IEEE International RF and Microwave Conference (RFM). IEEE, 2018.

[59] Jothilakshmi, K., and P. Jothilakshmi. "Design of multilayer microstrip patch antenna for satellite application." International Journal of Innovative Research in Computer and Communication Engineering 5.3, 2017.

[60] Diawuo, Henry Abu, and Young-Bae Jung. "Wideband proximity coupled microstrip linear array design for 5G mobile communication." Microwave and Optical Technology Letters 59.12, 2017.

[61] Lee, Kai Fong, Kwai Man Luk, and Hau Wah Lai. Microstrip patch antennas. World Scientific, 2017.

[62] Peng, Sheng, and Hongxing Zheng. "Design of Coplanar-Waveguide-Feed Antenna." structure 4, 2015

[63] Chen, Zhi Ning, and Michael Yan Wah Chia. Broadband planar antennas. Hoboken^ eNJ NJ: John Wiley & Sons, 2006.

[64] Ahmad, Farhan, and Boutheina Tlili. "Design and analysis of millimeter wave double F slot patch antenna for future 5G wireless communication." 2017 International Conference on Electrical and Computing Technologies and Applications (ICECTA). IEEE, 2017.

[65] Sanmugasundaram, R., D. Dileepan, and S. Natarajan. "Design of CPW antenna for network applications." International Journal of Engineering & Technology 7.4, 2018.

[66] KIŞLAL, Ahmet Oğuz. "Software Defined GMSK Modulator/Demodulator Design for Cube Satellites.", 2016.

[67] dos Santos, T. B., A. T. Fabro, and J. R. F. Arruda. "Stochastic analysis for simple and computationally effi-cient models for tire non-uniformity investigation." 2010.

[68] Mishra, Ranjan. "An overview of microstrip antenna." HCTL Open International Journal of Technology Innovations and Research (IJTIR) 21.2, 2016.

[69] Demir, Oğuz. Analysis of spherical-rectangular printed antennas and antenna arrays using cavity model. MS thesis. 2017.

[70] Upadhyay, Divyanshu, and Ravi Prakash Dwivedi. "Antenna miniaturization techniques for wireless applications." 2014 Eleventh International Conference on Wireless and Optical Communications Networks (WOCN). IEEE, 2014.

[71] Li, Runlong, et al. "Design of a miniaturized antenna based on split ring resonators for 5G wireless communications." 2019 Cross Strait Quad-Regional Radio Science and Wireless Technology Conference (CSQRWC). IEEE, 2019.

[72] Raviteja, G. Viswanadh, et al. "Defected Ground Structured Microstrip Patch Antenna with Quad L–Shaped Slot for Gain Enhancement at 4.8 GHz Frequency." Communications 7, 2018.

[73] R. R. Patil, V. R. M, P.V. Hunagund. “Antenna miniaturization techniques for wireless applications”, International journal of electronics and communication engineering & technology (ijecet), Volume 3, Issue 3, October- December 2012.

[74] Rahman, Md Mahfuzur. "Small size coupling feed and inductive shorting antenna for wide bandwidth, increased gain and efficiency with low specific absorption rate (SAR) operation.", 2016.

[75] Kamal, Shahanawaz, et al. "A novel lumped LC resonator antenna with air-substrate for 5G mobile terminals." Progress In Electromagnetics Research 88, 2020.

[76] DeJean, Gerald R., and Manos M. Tentzeris. "The application of lumped element equivalent circuits approach to the design of single-port microstrip antennas." IEEE Transactions on Antennas and Propagation 55.9, 2007.

[77] Can, Sultan, K. Yavuz Kapusuz, and E. Aydm. "Design & analyzes of dual-frequency circular microstrip patch antenna with a shorting pin." 12th Mediterranean Microwave Symposium (MMS). 2012.

[78] Ahmad, Waleed, and Wasif Tanveer Khan. "Small form factor dual band (28/38 GHz) PIFA antenna for 5G applications." 2017 IEEE MTT-S International Conference on Microwaves for Intelligent Mobility (ICMIM). IEEE, 2017.

[79] Zhang, Xiao, and Lei Zhu. "Patch antennas with loading of a pair of shorting pins toward flexible impedance matching and low cross polarization." IEEE Transactions on Antennas and Propagation 64.4, 2016.

[80] Srivastava, Preeti, and O. P. Singh. "A review paper on fractal antenna and their geometries." Advances in Electrical & Information Communication Technology", AEICT-2015, 2015.

[81] Tuteja, Rinka, and Ashok Kumar. "Study of Fractal Antennas and Characterization." International Journal of Engineering Technology, Management and Applied Sciences 3, 2015.

[82] Nair, Rekha G."Comparative Study of Multiband Antennas With Fractal Geometry." International Journal Of Innovative Research In Electrical, Electronics, Instrumentation And Control Engineering 4.2, 2016.

[83] Sharma, Narinder, Amandeep Kaur, and Vipul Sharma."A novel design of circular fractal antenna using inset line feed for multiband applications." 2016 IEEE 1st International Conference on Power Electronics, Intelligent Control and Energy Systems (ICPEICES). IEEE, 2016.

[84] Anguera, Jaume, et al. "Fractal antennas: An historical perspective." Fractal and Fractional 4.1, 2020.

[85] Olukoya, Oludotun, et al. "Miniaturized quadrature hybrid couplers based on novel U-shaped transmission lines." Microwave and Optical Technology Letters 61.2, 2019.

[86] Karimbu Vallappil, Arshad, et al. "Dual-band Minkowski–Sierpinski fractal antenna for next generation satellite communications and wireless body area networks." Microwave and Optical Technology Letters 60.1, 2018.

[87] Khanna, Ghriti, and Narinder Sharma. "Fractal antenna geometries: A review." International Journal of Computer Applications 153.7, 2016.

[88] Nicolini, Piero, and Benjamin Niedner. "Hausdorff dimension of a particle path in a quantum manifold." Physical Review D 83.2, 2011.

[89] Ni, Shucheng, et al. "A Novel Meander Line Array Antenna for 5G Application." 2020 International Conference on Microwave and Millimeter Wave Technology (ICMMT). IEEE, 2020.

[90] Volakis, John, Chi-Chih Chen, and Kyohei Fujimoto. Small antennas: miniaturization techniques & applications. McGraw Hill Professional, 2009.

[91] Ogherohwo, E. P., S. D. Mado, and M. Y. Eggah. "Design and analysis of meander microstrip antenna at wireless band.", 2015.

[92] Lin, Hwaider, et al. "Future antenna miniaturization mechanism: Magnetoelectric antennas." 2018 IEEE/MTT-S International Microwave Symposium-IMS. IEEE, 2018.

[93] Raviteja, G. Viswanadh. "A Dual-Band Millimeter-Wave Microstrip Antenna Array for 5G Applications." International Journal for Computer Applications 177.15, 2019.

[94] Nahas, Mousaab M., and Mouaaz Nahas. "Bandwidth and efficiency enhancement of rectangular patch antenna for SHF applications." Engineering, Technology & Applied Science Research 9.6, 2019.

[95] CST Studio Suite – EM Simulation Software. [Online]. Available: http://www.Cst.com/Content/Products/CST_S2/Overview.aspx, 2019.

[96] Roslee, Mardeni, Khazaimatol Shima Subari, and Intan Suraya Shahdan. "Design of bow tie antenna in CST studio suite below 2GHz for ground penetrating radar applications." 2011 IEEE International RF & Microwave Conference. IEEE, 2011.

[97] Bukhari, Bisma, and G. M. Rather. "Ground Plane Effects on the Performance of a Rectangular Microstrip Patch Antenna: A Study." 2020 5th IEEE International Conference on Recent Advances and Innovations in Engineering (ICRAIE). IEEE, 2020.